TRANSFORMATION OF POORLY WATER SOLUBLE DRUGS INTO IONIC LIQUIDS USING BIOCOMPATIBLE CATIONS: SOLUBILITY, PERMEATION AND CYTOTOXICITY STUDIES

モハマド, モシクル, ラハマン

https://doi.org/10.15017/2534429

TRANSFORMATION OF POORLY WATER SOLUBLE DRUGS INTO IONIC LIQUIDS USING BIOCOMPATIBLE CATIONS: SOLUBILITY, PERMEATION AND CYTOTOXICITY STUDIES

A Thesis Submitted to Kyushu University for the degree of Doctor of Philosophy

By

MD MOSHIKUR RAHMAN

Faculty of Engineering
Department of Chemical Systems & Engineering
Kyushu University
2019 June

IN THE MIDDLE OF DIFFICULTY LIES OPPORTUNITY.

Albert Einstein

ABSTRACT

Most pharmaceutical industries are facing unprecedented challenges for designing the smart drug delivery systems of poorly water-soluble drugs over the years because of their limited solubility, permeability and bioavailability. Recently, the pharmacological properties of active pharmaceutical ingredients (APIs) are greatly enhanced when they are transferred into ionic liquids (ILs) form. API-ILs provide generally better solubility, permeability and thermal stability than that of solid-state salts or crystalline drugs. However, the toxicological aspect of API-ILs is the main concern for their effective applications in a drug delivery. Even though, many of API-ILs are based on unlike cations, including imidazolium, pyridinium, pyrrolidinium, and morpholinium, which are not biocompatible because of their high toxicity and non-biodegradable nature. To address this issue, it is therefore desirable to synthesize API-ILs with cations that are not only effective in delivery systems (oral, topical and transdermal), but are also biocompatible, to further increase the potential applications of API-ILs.

Here, three series of poorly water-soluble model APIs; salicylic acid (Sal) as a keratolytic agent, methotrexate (MTX) as an anticancer drugs and ibuprofen (Ibu) as a painkiller were selected to formulate ionic liquefied drugs by combining with a series of potent biocompatible counters such as amino acid esters (AAEs), choline, *N*-methyl-2-pyrrolidone (NMP), etc. The physico-thermal or biological properties of API-ILs such as solubility, bioavailability, permeability and cytotoxicity were evaluated for envisaging their biomedical applications, which are mainly depended on the presence of cations. The solubility of Sal-ILs or MTX-ILs was significantly increased (> 5000 times higher) than that of free drugs, which were greatly influenced by the hydrophilic nature of cations. Importantly, the MTX-ILs showed significantly higher pharmacokinetic parameters than that of sodium salt of MTX. The bioavailability of [ProEt][MTX] showed at least six times higher than that of sodium MTX. However, cytotoxicities of API-ILs also depended significantly on the structure of cations, especially when cations contained sulfur, aromatic rings and long alkyl chains in side groups. Regarding the permeation studies, the API-ILs showed a significant effect on the penetration through skin as compared to their neutral analogs. Interestingly, the drug accumulation ability of API-ILs in the target tissue was significantly enhanced due to the presence of NMP cation while the permeation rate was slow down through the skin as compared with choline cation at periodic times. The obtained results suggest that AAEs or NMP could be a potent biocompatible counter ion to eliminate the use of traditional toxic solvents for oral/ topical/ transdermal delivery of poorly water-soluble drugs, since they allow an increased solubility or permeability of the studied APIs.

TABLE OF CONTENTS

CHAPTER 1: IONIC LIQUIDS IN DRUG DELIVERY SYSTEMS: CHALLENGES AND OPPORTUNITIES FOR PHARMACEUTICAL INDUSTRY

1.1. Introduction

The development of smart drug delivery systems for various disease management has been a challenging task for pharmaceutical researchers without negotiating on safety and efficacy of drugs. Currently, the pharmaceutical industries mainly depend on solid active pharmaceutical ingredients (APIs) which are approved by the Food and Drug Administration (FDA). These APIs are divided as a single- component APIs (individual component) and multi-component APIs (Salts, solvates/hydrates or co-crystal)[1]. Moreover, pharmaceutical researchers are searching the innovative drugs or improving the existing formulations of drugs so that the unmet medical behavior of drugs could be explored. Innovation of new drugs or dosage forms and modification of existing form of drugs or formulations causes to significantly increase the number of drugs which possess poor biopharmaceutical properties[1–3]. By developing or improving the existing formulations of these insoluble drugs, pharmaceutical companies are trying to take profitable strategies for filing in NDA under 505(b)(2) with faster dissolution and enhanced bioavailability [4]. In 2018, The FDA's Center for Drug Evaluation and Research approved 59 novel drugs; 42 New Chemical Entities and 17 Biologics drugs, which is the highest in last few decades (Figure 1.1)[5].

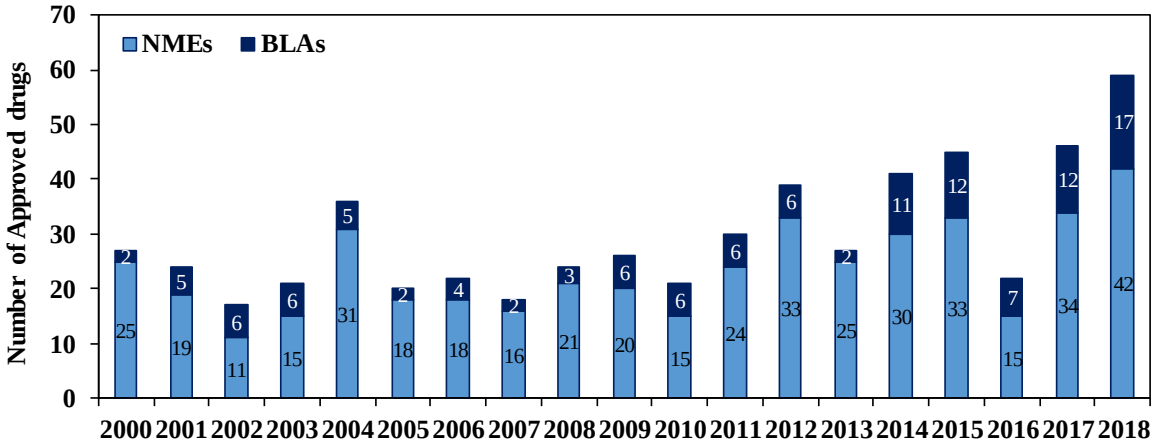

Figure 1.1. Novel FDA approvals since 1993. Annual numbers of new molecular entities (NMEs) and biologics license applications (BLAs) approved by CDER. Figure reproduced with permission from ref.[5]

An estimated 40% of the top 200 oral drugs (marketed in the US and Europe), nearly 90% of the developed pipeline drugs, 75% of compounds under development and 33% of FDA drugs

consist of poorly soluble compounds[1,6,7]. These marketed drugs suffer from poor solubility, low permeability, rapid metabolism and elimination from the body along with poor safety and tolerability[4,8,9]. Therefore, to develop the effective formulations of these marketed drugs, it is necessary to understand the problematic characteristics and properties of drug molecules.

1.2. Problems of conventional drugs: Polymorphism, limited solubility and bioavailability

1.2.1.Limited solubility and bioavailability

Limited aqueous solubility of APIs is the tremendous challenges for improving their pharmacokinetics and pharmacodynamics due to the lower dissolution and absorption rates in body fluids[1,10,11]. The therapeutic efficiency of a drug mainly depends on its bioavailability, which directly interrelated to the drug solubility and permeability[10]. Limited aqueous solubility of an orally administered drug represents the lower dissolution in body liquids with low absorption by the gastrointestinal tract (GIT)[9,12]. Generally, dissolution-limited absorption occurred when the drugs dissolve lower than 100 µg/mL in water or physiological fluids (PBS, SIF, or SFG)[3,13]. In such cases, low permeability (barriers to drug delivery), narrow therapeutic windows and a short half-life limit with systemic side effects are observed in their respective clinical applications[9,12,14]. As a result, higher doses of drugs are required for reaching the therapeutic effect which causes topical toxicity in the GIT upon oral administration[3]. Moreover, formulation development for higher doses is generally difficult because of their poor powder flow ability and higher sticking tendency during granulation and tableting process[3]. In addition, the manufacturing cost would increase since a large amount of API might be consumed to develop and manufacture the drug product[1].

1.2.2.Polymorphism

Polymorphism (derived from the Greek words: ‘polys’ or multiple and ‘morfe´’ or shape) is major complication of solid APIs when one crystalline chemical can exist in more than one crystal form with different properties such as solubility, stability, absorption and bioavailability[1,10,15]. During a product processing, the polymorphic phases may be affected by manufacturing conditions (solvent, temperature and pressure) and coexist into the drug product which could crystallize out/ precipitate in solution/ formulation and varies the bioavailability[10,16]. Even though, the effective dose of polymorphic drugs could be harmful/ lethal when the drugs converts to a much more soluble/ bioavailable form. Ghielmetti et al. reported that the toxicity or LD_{50} value of nystatin antibiotic was significantly varied due to their polymorphic forms[17]. Moreover, pharmaceutical polymorphic and pseudo-

polymorphic (water/ solvent in drug lattice) conversions can occur at any stage of manufacturing or storage, and very difficult to control their formation[10].

1.2.3.Particle size

Particle size is another common problem of solid APIs. The pharmaceutical properties of a drug such as solubility, dissolution rate, uniform distribution, suspendability and penetrability can be significantly affected by increasing or decreasing the particle size[10,18]. Therefore, it is important and requires critical care to manufacture solid APIs with not only controlled polymorphic form, but also with controlled crystal size and product solubility.

1.2.4. Route of administration

Irrespective of the intended route of administration the active substance needs to dissolve or be solubilized in aqueous media for intravenous formulations to become bioavailable or applicable to the patient. Liquid formulations have the advantage of dosing flexibility and a reduced risk of choking. They can also be applied in other populations, such as geriatric patients with swallowing difficulties, or in a palliative setting. Possible disadvantages of liquid formulations are issues with stability and palatability, parameters that need to be considered in the design.

1.3. Strategies for formulating and delivering poorly water soluble APIs

The technological utility is playing a vital role for enhancing the essential properties of API such as, solubility bioavailability, stability and permeability. A variety of pharmaceutical approaches have been considered to overcome the limited water solubility and dissolution rate of poorly soluble drugs in research and development. These techniques are divided into two categories based on the nature of modification of APIs such as the physical and chemical modification, which may be applied in either alone or in combination (Figure 1.2).

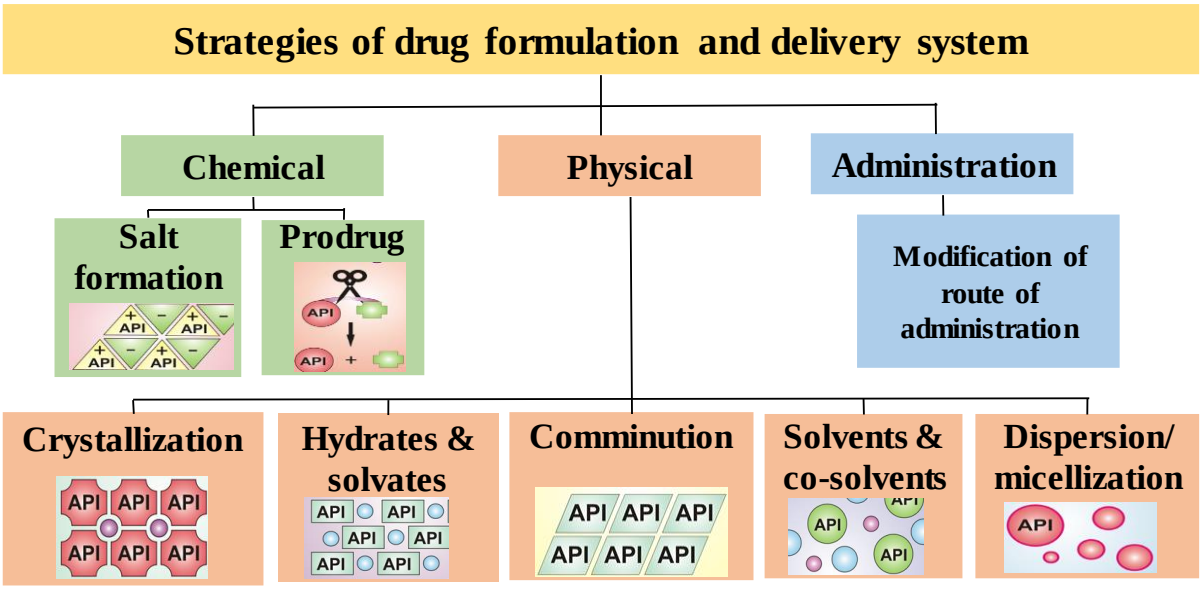

Figure 1.2. A schematic representation of the main approaches used to improve drug solubility as well as drug delivery of poorly water-soluble drugs.

Prodrugs and salt formations are the popular strategies for chemical modification, whereas crystallization and co-crystallization, solid dispersion, commiution (decrease particle size), micellization, hydrates and solvates preparations, and employment of alternative solvents and co-solvents are the common physical approaches for achieving the therapeutic excellence or capturing the market economies [6,10].

1.3.1. Salt formation

In the pharmaceutical industry, salt formation is the widely used techniques for ionizable drugs to the enhance solubility and dissolution rate. When the physico-chemical or biological properties of an ionizable drug molecule are undesirable, the salt form of that drug is the typical solution to improve properties and overcome problems faced within neutral drugs. An estimated about 70% of marketed drugs are ionizable, of which of a majority are weakly acid or base[4]. Currently, 50% of all drugs in the pharma industry are salts. Generally, salts are formed via the proton transfer between an acid and a base when the pKa difference is greater than 3[19]. There are several lists of inorganic or organic salt formers, which are approved by FDA[1]. Sulfate, phosphate, chloride and bromide are widely used as an inorganic anions and sodium as an inorganic cation. The most common organic anions are acetate, citrate, maleate, mesylate and tartrate, while N-methyl glucamine is a common organic cation[1,20,21]. The pharmacological properties of a drug may be strongly affected by the choice of counterions. Even, the solubility or dissolution rate of chloride salts may reduce in the stomach due to the

common-ion effect (presence of chloride ions)[3]. However, salt formation not only improve the solubility and dissolution rate but also affects the physico-chemical stability, manufacturability, impurity and toxicity[1]. Nevertheless, the solubility or dissolution rate of chloride salts may reduce in the stomach due to the common-ion effect (presence of chloride ions)[3].

1.3.2. Prodrugs

Prodrugs are the one of the most promising and versatile strategies to improve the solubility and bioavailability of a drug. Over the past decades, prodrugs strategy has been gaining attention for pharmaceutical companies because of its usefulness in drug formulation. Prodrugs can be solved a large variety of drugs related issues such as solubility, stability, toxicity, absorption, distribution, metabolism, among others[5,10,22]. An estimated about 10% of marketed drugs and 33% of the APIs were approved by FDA in 2008. Recently (2015), FDA approved 45 new drugs of which 7 drugs are clearly identified as prodrugs (Figure 1.3A)[22]. Generally, a prodrug is an inactive and chemically modified drug of a parent drug which possesses improved solubility, stability and permeability[23]. A good prodrug can release the active part at a specific target site of organism and capable to relieve its toxicity (Figure 1.3B)[16].

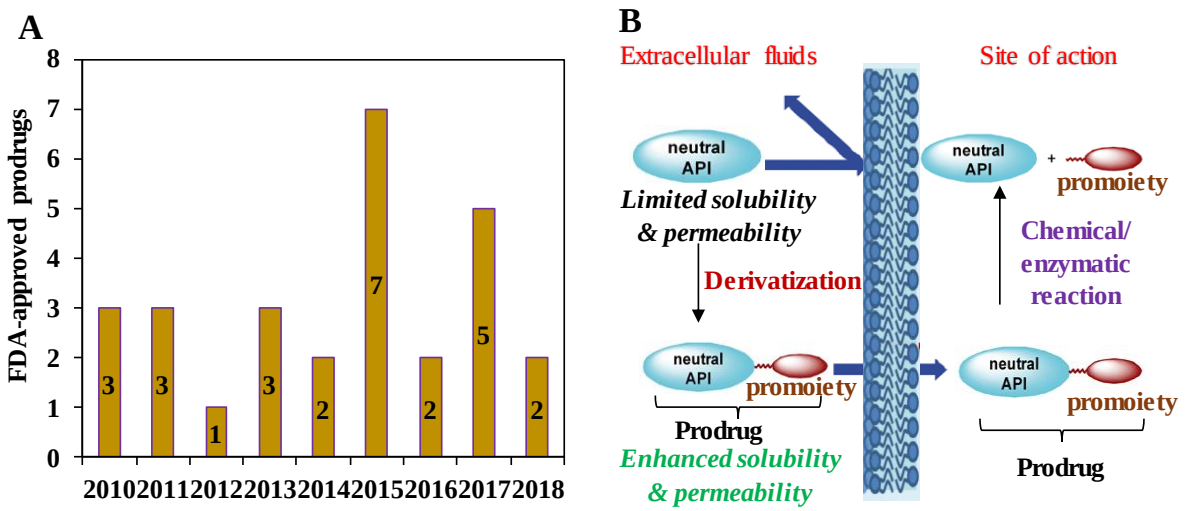

Figure 1.3. General aspect of prodrugs. A) FDA-approved prodrugs during 2010-2018[23]. B) A schematic view of prodrugs concept.

There are two categories of prodrugs: First one is carrier-linked prodrugs where the prodrug moiety is covalently linked with the parent drug and another one is bioprecursor prodrugs

where the parent drugs are modified with functional groups by enzymatic reactions, hydration or redox reactions[6,22,24]. In most cases, the active substances are released in the organism through chemical or enzymatic reactions. However, the structure of prodrugs is mainly esters, oximes, amides and disulfate bridges which depends on the type of functional groups present in the parent drugs and carriers[10]. Conjugated prodrugs with a specific peptide, antibody, or agonist are also identified as target cell transporters in intestinal enterocytes or specific organs[10]. Recently, a quaternary ammonium-based bioreversible linkages are employed by conjugating with tertiary or heteroaryl amines for a targeted delivery. This strategy can be significantly decreased the hydrophobicity of drugs upon connecting with a linker by proteolytically or reductively cleaving or entering the target cell[25].

The **Carrier-linked prodrugs** are often used to simultaneously disclose the complication of poor water-soluble drugs and attain its targeted delivery. There are main four types of carrier moieties such as hydrophilic, hydrophobic, amino acids and macromolecules carriers, which covalently linked with a promoiety to the parent drug[6]. The hydrophilic carrier-linked prodrugs possess higher solubility compared with parent drugs. For example, Telzir® and Lexiva® (GlaxoSmithKline, Brentford, UK) contain fosamprenavir, which is a hydrophilic carrier-linked (phosphate ester) prodrugs displaying 10 times higher solubility as well as an increased bioavailability than patent amprenavir drug[6]. In case of hydrophobic carrier-linked prodrugs, the hydrogen bond-containing drug-drug interactions were disrupted in presence of hydrophobic carrier resulting in a higher dissolution rate. For example, the prodrug of anticancer drug 5-fluorouracil (5-FU) is Xeloda® (Hoffmann-LaRoche, Basel, Switzerland) contains capecitabine displaying high solubility, high absorption and low affinity for the intestine thymidine phosphatases[6,26]. Interestingly, a covalently linkage was formed between the doxifluridine backbone (a pre-prodrug of 5-FU) and hydrophobic hydrocarbon chains or amides, which is biotransformed by deaminases, carboxylesterases and tumor-specific thymidine phosphorylases. As a result, the cytotoxic 5-FU was released at the target site of tumor tissue as well as enhanced oral bioavailability. However, amino acids carrier-linked prodrugs is another promising approach for increasing water solubility and transporter-mediated absorption (using amino acid transporters) because of the versatile physical properties of amino acids. For example, valacyclovir marketed as Valtex® (GlaxoSmithKline, Brentford, UK) is the L-valyl ester prodrug of acyclovir displaying two times higher bioavailability than that of acyclovir due to the active transport via amino acid receptors[6]. The active acyclovir is generated through hydrolysis of valacyclovir where needs to inhibit herpes virus DNA polymerase through activation of viral thymidine kinase and cellular kinases. Finally, Drug-

macromolecule conjugated prodrugs are the latest approach of prodrugs strategy for assisting the solubilization, decreasing the toxicity, preventing the degradation and achieving the targeting delivery of drugs[6,23]. There are variety of macromolecules such as olyethylene glycol, hyaluronic acid, droxypropylmetacrylamide and nitrodiol or polyamidoamines dendrimers used for designing macromolecule prodrug[6]. De Groot et al. presented nitrodiol dendrimer-based paclitaxel anticancer drug and reported the site-specific release of paclitaxel. Regarding **bioprecursor** prodrugs, the sulindac marketed as Clinoril® (Merck, New Jersey, US) oral tablets are the prodrugs of Sulfinylindene displaying 100-fold increased solubility and oral absorption than that of its parent drug[6].

The prodrug approach is therefore a powerful and versatile strategy to not only address issues with poor water solubility, but also to develop a myriad of strategies for an efficient site-specific drug delivery. Nevertheless, the stability of prodrug formulations can be a hurdle since prodrugs require a high reactivity for a quick biotransformation, but also need an excellent stability for a long product shelf-life.

1.3.3. Cocrystal formation

Cocrystal formation strategy has received more attention in the last decade owing to its successful delivery of insoluble drugs. The crystal lattice of insoluble drugs is generally disturbing or disrupting using salts and cocrystals formation techniques. If a drug is an ionizable, salt formation technique is usually used to increase its solubility. But if the drugs cannot be ionized then cocrytal may be used[10]. In the cocrystal technique, the crystal drugs are converted into cocrystal using conformer, which disrupted the high lattice structure of drugs molecules and hold in a stoichiometric ratio with drug molecules via non-covalent interactions such as hydrogen bonding or van der Waals forces in acid–amide, acid–acid, and amide–amide interactions[4]. As a result, the cocrystal drugs poses higher solvent affinity with enhanced solubility. The generally regarded as safe (GRAS)-listed excipients such as glutaric acid, succinic acid, fumaric acid, oxalic acid, quercetin, p-coumaric acid, saccharine can act as a conformer[4]. The solubility enhancement of some insoluble drugs like itraconazole, gabapentinin, carbamazepine, modafinil, piroxi- cam and caffeine already reported using the cocrystal technology[27]. However, there is no approved product in market with drug cocrystals till today, although there have enormous potential for delivery of insoluble drugs[4]. Therefore, the future of cocrystals is promising.

1.3.4. Amorphous forms and solid dispersions

Amorphous forms of crystalline drugs can be enhanced the solubility by disordering the stable crystal form and changing the solid state characteristics of drug molecules who renders the molecule more water soluble. However, the formation process of amorphous drug systems is complicated and affected the stability by various factors resulted in reduced generic competition for already approved amorphous products[4]. Ceftin® by GSK (amorphous form of Cefuroxime axetil) and Accolate® (amorphous form of zafirlukast) are now available commercial market[4].

The solid dispersion strategy was also extensively explored in recent decades for the delivery of insoluble drugs, which contain polymer carriers for stabilizing the drugs molecules[10]. Sporanox® (Solid dispersion based formulation of itraconazole) is now available commercial market[4].

1.3.5. Solvents/ co-solvents

Addition of alternative solvents/ co-solvents for developing an effective formulation of insoluble drugs is also one of the oldest and widely used techniques for liquid dosages of oral and intravenous administration. By reducing the dielectric constant of non-polar drug molecules, solvents are maximized the solubility and prevented the precipitation formation upon dilution. Solvents/ co-solvents are also used in conjunction with surfactants and as pH modifiers during formulations of drug molecules[4,28]. For example, Taxol, an intravenous injection of paclitaxel, formulated using 49% of dehydrated alcohol and 527 mg of cremophore EL which is responsible owing to a hypersensitivity reaction in patients. Abraxane (albumin as cosolvent) and Genexol (PEG as cosolvents) are new formulation of paclitaxel, which is free from cremophore EL[4].

Nonetheless, their low solubility in water represents a challenge to the pharmaceutical industry and thus it is fundamental to find alternatives that allow us to incorporate this drugs in delivery systems. In this sense, ionic liquids, ILs, may be valuable as functional ingredients by enhancing drug solubility and/or drug permeation.

1.4. Ionic liquids as designer solvents

Ionic liquids (ILs) have gained widely attention and considered as green designer solvents for more than two decades. As a novel family of “green solvents”, ILs are remarkable chemical compounds and explore their applications in different areas of modern science due to their highly tunable and exceptional physico-chemical properties. Beside their traditional usage as

solvents, ILs have drawn attention for their overwhelming applications in biomedical fields not only as suitable catalytic media for drug synthesis, but also as potential components for effective biocompatible drug delivery systems. To date, several notable works have reported to emphasize the advantages of ILs in drug development. Surprisingly, the pharma industries are only focused on the salt forms or prodrugs of solid APIs to overcome the difficulties, have not deeply studied the ILs. Although, ILs could offer a virtually unlimited number of possibilities for effective drug formulations due to the vast variation of cation-anion combinations. ILs are now tailored as innovative solutions to improve many problems in solid pharmaceuticals such as design to promote dissolution, disrupt physiological barriers to transport drugs to targeted sites and/or new delivery options.

However, the widely use of ILs as solvents in chemical processes such as synthesis, separation and catalysis has recently become significant. To date, IL remains one of the most dynamic and remarkable areas of research with over 7000 contributions in 2018 alone. A literature search for IL in Scopus ® database has shown that only 3 works had in 1990 and 609 works in 2000, which rapidly increased in 2018 for 7000 works (Figure 1.4). It was reported that millions of ILs have been prepared, among them only about 300 ILs are available in market. In the light of the above facts, one can imagine the opportunities still to be uncovered in ionic liquids.

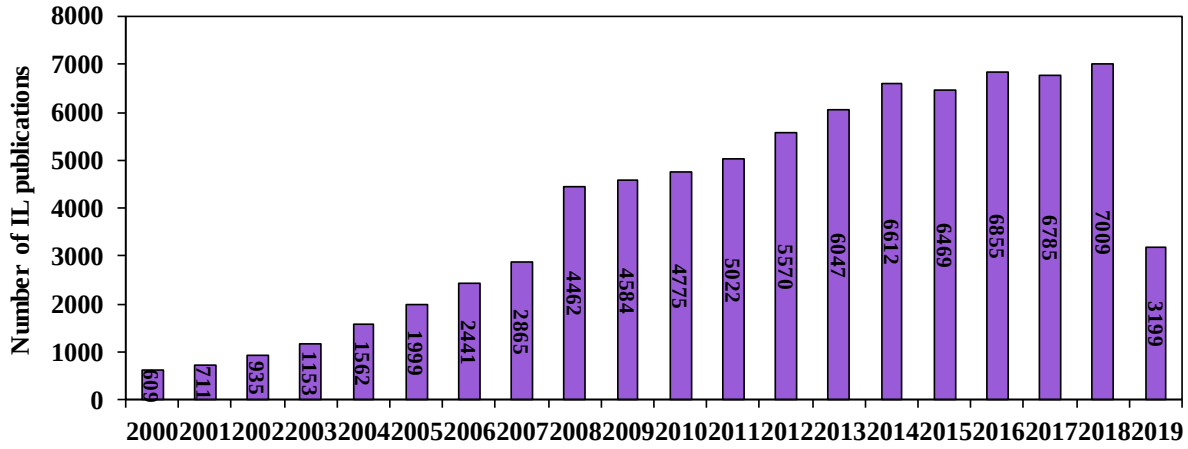

Figure 1.4. Publication frequency of the term "Ionic Liquids" obtained from Scopus® database.

1.4.1. Fundamentals of ILs and its physicochemical properties

For over a century, ILs have been a topic of scientific interest for researchers and risen the attention in many areas of modern science since the mid-1990s[1]. Generally, ILs are defined as the class of molten organic salts, which are typically composed of unsymmetrical organic cations and inorganic/organic anions with melting points at or below 100 °C[1,11,29]. ILs compounds have some attractive physico-chemical properties such as superior solvation

properties, negligible vapor pressures, wide liquid ranges, high thermal and chemical stability, non-volatility, and non-flammability[2,11,29,30]. The preparation of ILs is not so difficulties, even in large scale. The structural or physico-chemical properties modification of ILs mainly depends on the nature of either cation, anion or to the substituents on the cation or anion[1,11]. Therefore, a vast number of ILs are possible to prepare by changing the cation or anion of ILs (Figure 1.5).

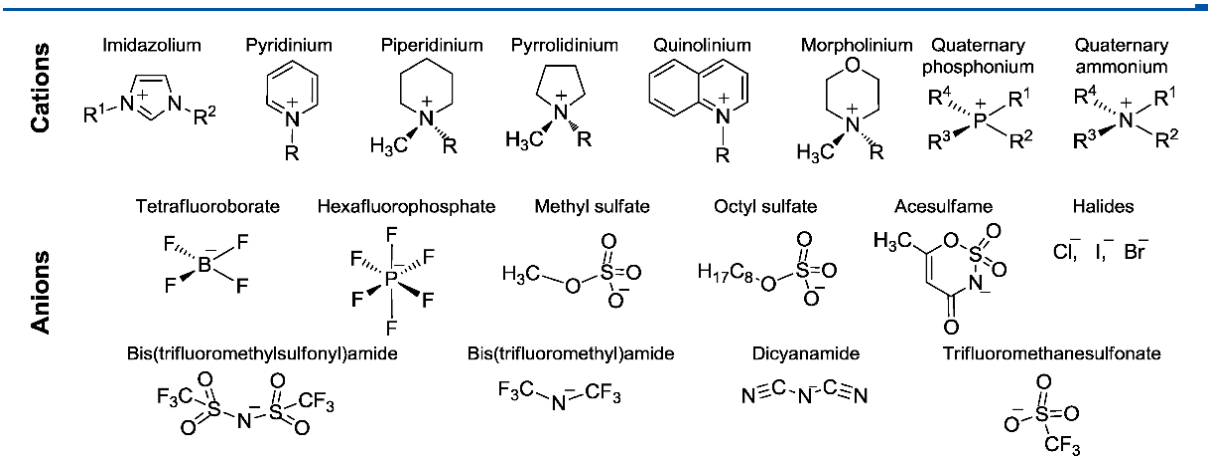

Figure 1.5. Examples of cations and anions commonly used in ILs. Figure reproduced with permission from ref.[10]

However, ILs have been known for all over the past few decades. The first appearance of IL was in 1914 by Paul Walden et al. and reported about the physical properties of ethylammonium nitrate ($[EtNH_3][NO_3]$)[1,11]. The first air and water stable imidazolium-based IL was reported in 1992 by Wilkes et al. which challenged the previous concept of ILs (most of previous ILs were highly hygroscopic)[31]. After this report, significantly increased the number of air- and water stable-based ILs. In 1998, Davis et al. firstly reported "functionalised ionic liquids" as a new class of IL in where the cation derived from the antifungal drug miconazole[32]. Recently, ILs are considered to be potential candidate as green or designer solvents due to their advantageous toxicity, flexibility and variability, hence redefining the definition of ILs as low melting salts below 100 °C with an boundless suite of tunable properties including biological activity, volatility, flammability, and instability[1,10,11].

The desirable physico-chemical properties of ILs are designed by considering the nature of cations as well as the anions. Some representative structures of cations and anions are shown in Figure 1.5. Among them, four main categories of cations such as ammonium, imidazolium,

pyrrolidinium or pyridinium, and phosphonium that are often used by pairing with various anions in the design of ILs[10,11]. The imidazolium-based ILs can be used as solubility promoters, solvents and catalysts due to their easy synthesis, low viscosity and stability in redox reactions[33,34]. ILs with a long alkyl chain of imidazolium cation have greater toxicity which is the main drawbacks for their biological applications[35]. The pyridinium-based ILs are more active in catalytic reactions but poor regioselectivity in palladium-catalyzed telomerization and Diels-Alder reactions[33,36]. The quaternary ammonium-based ILs have shown lower toxicity in biological applications as compared to imidazole-based and pyridinium-based ILs. These ILs are used as electrolytes for their lower viscosity and melting points[10,33,36]. Recently, quaternary ammonium-based ILs have been used to improve the antibiotic activity and topical drug delivery[10]. In addition, these ILs are appropriate solvents for pharmaceutical processing as an alternative to the conventional solvents of pharmaceutical industry. The Phosphonium-based ILs are more thermally stable than ammonium and imidazolium-based ILs, even at high temperature (>100 °C). Recently, these ILs are used as solvents and catalysts in several reactions and more recently for CO_2 capture[10,11,36].

To understand the useful properties and potential applicability, ILs are classified into three generations depending on their properties and chemical structures. The first generation ILs were basically prepared by using dialkylimidazolium and alkylpyridinium cations with metal halide anions. These ILs were attracted attention because of their desirable physico-chemical properties but highly sensitive to air and water. The second generation focused on the deliberate tuning of physico-chemical characteristics of ILs for adaptation of properties to a specific task. These ILs are stable to air and water, and prepared by the combination of most commonly used cations such as ammonium, phosphonium, alkylimidazolium and alkylpyridinium and anions included halides, tetrafluoroborate and hexafluorophosphate that are the most commonly used during IL synthesis. Initially, ILs of second generation had been considered as an environmentally safe and green solvent, but belief has changed when the data of biological activity were explored. Now it is reported that many ILs have shown similar or even higher biological activity as compared to toxic conventional organic solvents. Finally, the third generation of ILs is composed of biodegradable and natural ions, such as amino acids and choline, or ions with known biological activity. This generation has shown interest because of its chemical properties and possible applications in the field of ecology, biology and pharmaceutical.

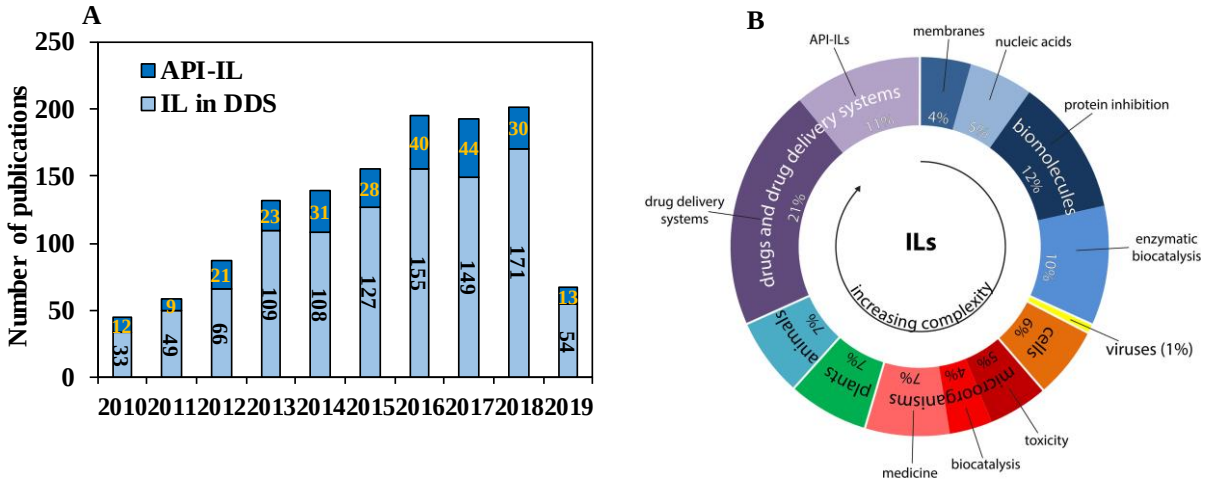

Figure 1.6. Ionic liquids as component of drug formulations. A) Publication frequency of the term "Ionic Liquids in drug delivery system" and "Active pharmaceutical ingredients ionic liquids" obtained from Web of science® database. B) Active research directions for studies on biological activity of ionic liquids published in 2017–2018 (for illustrative purpose only). Figure B reproduced with permission from ref.[35].

In general, ILs were considered for use as catalysts and reaction media for extractions and separations, as electrolytes for electrochemistry, application in biomass convention, biotransformation, nanotechnology, lubricants or propellants fluids, and many other fields. In medical field, ILs have attracted distinct attention to address the potential challenges of solid pharmaceuticals for effective drug delivery. Because many drug candidates exhibit polymorphism, poor solubility, permeability and bioavailability profiles, eventually leading to clinical failure and pursue the new strategies to solubilize and/or formulate them. ILs have the extraordinary solvating power to improve the solubility of many poorly soluble drugs and significantly enhances the drug permeation through physiological barriers to boost therapeutic efficacy. Figure 1.6 shows the literature analysis that has identified the leading directions and driving forces of the current research in the field.

1.4.2. ILs for delivery of pharmaceuticals

1.4.2.1. Solubility of drug molecules in ILs

Remarkable solvent abilities of ILs have been widely known as solvents since their revival in the mid-1990s[1]. The excellent solvating power of ILs can be enhanced the physico-chemical properties of solid API by converting into the liquid form. Many APIs are notoriously challenging to dissolve with physiological fluids and/or FDA approved solvents. Currently, the

use of organic solubilizers is an undeniable challenge for effective drug delivery due to their toxicity and contamination ability of pharmaceutical products[10,29]. As a suitable alternative of organic solvents, ILS can be tailored to dissolve hard-to-dissolve drugs with increased shelf stability and drug concentration for delivery (Table 1.1)[11]. The dissolving mechanism already explored by experimental data and/or molecular dynamic simulations that suggested the continuous polar network is found in ILs which disrupted into smaller domains so that the ILs solutions are resembled with water matrix where the ionic filaments are incorporated[37]. The anions of ionic filaments form H-bonds with water molecules and stabilize the structure of IL filaments in the water solution. Claudio et al. reported the snapshots of the equilibrated simulation for revealing the existence of co-aggregates between the hydrophobic solute and the IL ions in an aqueous solution (Figure 1.7)[37]. Simulation snapshots show the vanillin molecules properly mix with water and form cation−vanillin clusters via dispersion forces and other specific interactions, such as hydrogen bonds and π−π interactions. Other studies support the correlation between excellent solubilizing properties of ILs and their ability to form numerous interactions with the solute[37].

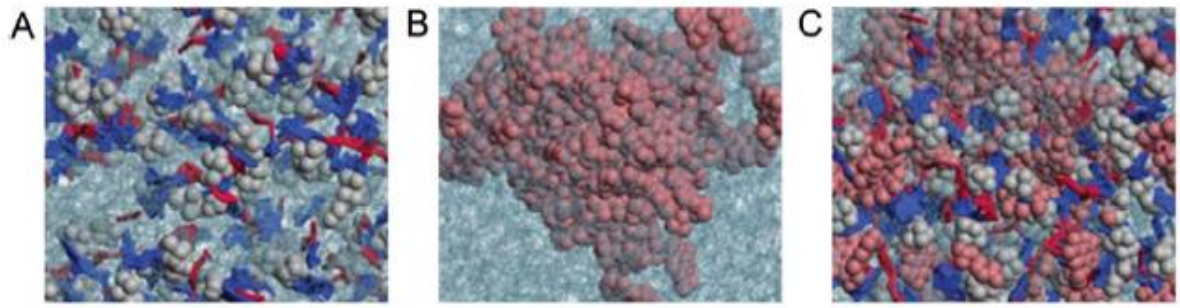

Figure 1.7. Simulation snapshots. (A) IL ([C_4MIM][$N(CN)_2$]) in water; (B) Vanilla in water; (C) IL and vanilla in water. (Light green): ionic liquid polar aggregates (strands); (blue): anion-water network; (light red) vanillin clusters. Figure reproduced with permission from ref.[10]

In general, ILs may be used as solvents or antisolents, cosolvents, copolymers and emulsifiers for designing the problematic drugs. The hydrophobic ILs can easily solubilize the hydrophobic drugs, whereas hydrophilic drugs prefer hydrophilic ILs[10]. It is clear that both IL anion and cation can play vital roles to dissolve the APL in the IL solution although the influence of the anion is still complicated[38]. The alkyl chain length of cations correlates with the solubility of solid APIs. As increased the alkyl length of cations, the solubility of APIs led to a decreased. Jaitely et al. reported the solubilities of penicillin, dexametasone, progesterone and dehydro-

epiandrosterone in imidazolium based-ILs with varying alkyl lengths (C_4, C_6 and C_8). The solubilities of these drugs are decreased with increases the alkyl lengths[39].

Table 1.1. ILs as solubility enhancers in drug delivery. Table reproduced with permission from ref.[10]

Drug	Activity	IL
N-acetyl-L-cysteine	antioxidant	$[C_2MIM][OTf]$, $[(C_6)_3C_{14}P][Cl]$, $[(C_6)_3C_{14}P][NTf_2]$
acetaminophen	analgesic	$[C_4MIM][BF_4]$, $[C_8MIM][BF_4]$, $[C_4MIM][PF_6]$, $[C_4MIM][Br]$, $[C_6MIM][Br]$
acyclovir	antiviral drug	$[C_1MIM][DMP]$
albendazole	antiparasitic	$[C_4MIM][PF_6]$, $[C_6MIM][PF_6]$, $[C_8MIM][PF_6]$
amphotericin B	antifungal agent	$[C_2MIM][OAc]$, $[CnNH_3][OAc]$ (n = 4, 6, 8), $[m\text{-}PEG350\text{-}NH_3][OAc]$
coumarin	anticoagulant	$[C_{10}MIM][NTf_2]$, $[(C_6)_3C_{14}P][Cl]$, $[(C_6)_3C_{14}P][NTf_2]$
4-hydroxycoumarin	anticoagulant	$[C_2MIM][OTf]$
curcumin	antioxidant	$[C_4MIM][BF_4]$
danazol	steroid drug	$[C_6C_6OCOPy][NTf_2]$,$[C_6C_6OCOPy][N(CN)_2]$, $[C_4MIM][PF_6]$, $[C_8MIM][PF_6]$,$[C_4MIM][BF_4]$
dantrolene sodium	muscle relaxant	$[C_1MIM][DMP]$
dehydroepiandrosterone	steroid hormone	$[C_4MIM][PF_6]$, $[C_6MIM][PF_6]$, $[C_8MIM][PF_6]$
dexametasone	steroid drug	$[C_4MIM][PF_6]$, $[C_6MIM][PF_6]$, $[C_8MIM][PF_6]$
diclofenac	NSAID	$[C_6MIM][Br]$, $[C_{12}MIM][Br]$, $[C_{14}MIM][Br]$
ibuprofen	NSAID	$[(C_6)_3C_14P][Cl]$, $[(C_6)_3C_14P][_{NTf2}]$, $[C_2MIM][NTf_2]$
etodolac	NSAID	$[C_4MIM][PF_6]$
isoniazid	antituberculosis	$[C_{10}MIM][OTf]$, $[(C_{10})_2(C_1)_2N][NO_3]$
itraconazole	antifungal drug	$[C_6C_6OCOPy][NTf_2]$,$[C_6C_6OCOPy][N(CN)_2]$, $[m\text{-}PEG350\text{-}NH_3][OAc]$, $[m\text{-}PEG350\ NH_3][C_nCOO]$ (n = 3, 5, 7, 9)
methotrexate	anticancer	$[C_1MIM][DMP]$

1.4.2.2. IL-based topical and transdermal drug delivery

The solvation power of ILs is remarkable, leading to their use not only limited to solubilizing agents, but also oral, topical and transdermal systems for an effective delivery of poorly bioavailable drug molecules. Among the various targeted routes of delivery, topical or transdermal drug delivery (TDD) potentially is a safe and non-invasive system as compared with conventional delivery strategies (i.e., oral, injection and nasal) because of easily usage, painless, avoidance of first-pass hepatic elimination and reduction of some side effects[1,11,29]. TDD can be improved the drug bioavailability and reduced undesirable metabolism in the oral cavity, GI tract and liver[29]. Several transdermal drugs such as estradiol, testosterone, fentanyl, nitroglycerin, clonidine, nicotine and scopolamine are existing in the market[40]. However, the effectiveness or efficacy of TDD mainly depends upon the drugs physicochemical characteristics and the outermost layer of the skin, the stratum corneum (SC)[11,29,40]. The skin is the largest and most important organs of the body, representing about 10% of total body mass and covering about 1.7 m^2[41]. The main function of skin is to act as a natural protective barrier against the ultraviolet radiation, microorganisms, penetration of toxic exogenous compounds and preventing the excessive loss of water and body nutrients, or as a favorable portal of entry for drugs with local and/or systemic action[29,41,42]. The skin is composed of three different main layers; the stratum corneum, the viable epidermis and dermis with hair follicles, appendages and eccrine and apocrine sweat glands[40,41,43]. The SC, a structurally well-organized corneocytes and lipid layers, poses a formidable barricade to the drug transport into the skin[11,40,44]. Hence, many hydrophilic or macromolecule drugs (> 500 Da) cannot be penetrated through the skin without reducing barrier properties by either disrupting the SC or altering the lipid structure through the use of physical (device based) or chemical (formulation based) penetration enhancement techniques[40].

Thus, for developing an effective TDD through the skin, it is necessary to carefully understand their properties, not only API molecules, but also the excipients used in formulations. However, many sparingly water soluble drugs were targeted for TDD and formulated to perturb the formidable barrier of impervious stratum corneum (SC) using chemical enhancers which causes toxicity, skin irritation and infections, burns and scars in their clinical application[11,40,45]. ILs have fascinated attention to disrupt the SC barriers for ensuring the efficient transcellular and paracellular drug transport[11]. It has been proven the feasibility of ILs to enhance the drug transport through the skin by the experimental data, as well as molecular dynamics. Lin GS et al. [46] simulated the model membrane with amphiphilic 1-octyl-3- methylimidazolium-based IL by using molecular dynamics combined with empirical

force fields and reported that the cationic head of IL inserts into a model of a bacterial cell membrane. As a result, the structural integrity of cell membrane disrupted to increase the membrane permeability of polar ammonia molecules. The imidazolium-based hydrophilic IL can fluidize the cell membrane to generate pathways for the diffusion of molecules and causes membrane permeabilization[47]. Although these findings linked with the cytotoxicity generated by IL and assume that a similar mechanism should permit to drugs transport in target sites. In addition, ILs have an ability to extract the lipids from physiological structures of SC and enhanced the transport by creating channels for drug molecules[40]. Recently, deep eutectic solvents (DESs) used as a skin enhancer to increase the transdermal delivery of drugs as well as disrupt/neutralize biofilm-forming bacteria[40,45,48]. DESs are a mixture of compounds that jointly have a lower melting points than individual components. Mitragotri S and co-worker reported choline and geranate (CAGE) as DES, have a potent antibacterial activity and significantly enhanced transdermal delivery of antibacterial drugs without causing notable toxicity to keratinocytes and mice[48]. They demonstrated that the transdermal delivery of hydrophilic drug molecules (i.e., mannitol and cefadroxil) and macromolecules (i.e., bovine serum albumin, ovalbumin, and insulin) were significantly improved for using CAGE as compared with conventional chemical permeation enhancers such as ethanol and Transcutol[40,45].

Microemulsions (MEs) are the promising widely formulated and implemented techniques to deliver the drug molecules across the skin barrier. MEs are the transparent systems consisting of two immiscible fluids and stabilized by an interfacial film of surfactant, frequently with co-surfactants[29,49]. There are three different categories depending on their microstructure such as oil-in-water, water-in-oil and bicontinuous, which is influenced by their physicochemical properties and the proportions of their ingredients[29]. Recently, ILs have been used to stabilize the ME systems for the transdermal delivery of sparingly soluble drugs. Goto and co-workers pioneered this concept[1], have developed IL-based ME systems (IL-in-oil microemulsions) in which the drugs loaded-IL (drugs loaded in the IL core) is dispersed in oil in the presence of a surfactant (Figure 1.8)[30,42,49]. They reported that the solubility of acyclovir was increased 500 times more in dimethylimidazolium dimethylphosphate IL and increased six times higher the transdermal delivery than current acyclovir creams. Recently, they developed a solid-in-oil nanodispersion by using 1-dodecyl-3-methylimidazolium-based IL to deliver ovalbuminin vitro[50]. In a related study, an IL-in-water (IL/water) microemulsion was reported in where ex-vivo permeation studies of a poorly water soluble drug, etodolac was conducted for topical delivery using 1-butyl-3- methylimidazolium hexafluorophosphate) as IL, Tween 80 as

surfactant and ethanol as co-surfactant. The IL/water microemulsion was more efficient to transport drugs than oily solution, o/w ME and marketed formulation of ETO.

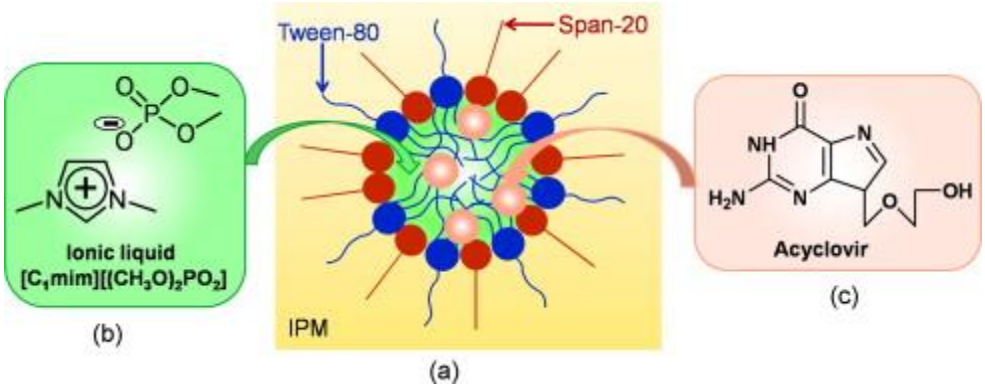

Figure 1.8. (a) Schematic representation of ionic liquid-in-oil (IL/o) microemulsions containing drug molecules. Chemical structure of IL (b) and acyclovir (c). Figure reproduced with permission from ref.[30]

1.4.2.3. IL-based oral drug delivery

Oral delivery of drugs is the most preferred route of administration due to its convenience and safety including ease of use, being painless, lesser cost of care, lesser patient supervision, and high patient compliance as compared to injection and, other methods. The oral delivery route is more natural and less invasive. However, there are existed some complications in the oral route of drug administration due to exhibit low solubility and permeability, low absorption in GIT and high degradation rates of drug molecules. To address these issues, several strategies already applied to enhance its solubility and bioavailability through oral administration, IL-based oral delivery is one of the potential candidates for the effective delivery of these problematic drugs. To date, several notable works have been done to emphasize the advantages of IL-based oral delivery. Porter and co-workers pioneered ILs based-oral delivery for improving pharmacokinetics of poorly bioavailable drugs. They demonstrated that the solubility and absorption of poorly water-soluble drugs such as danazol, itraconazole and fenofibrate were significantly improved using 1-hexyl-3-hexyloxycarbonylpyridinium dicyanamide ILs as compared with crystalline drugs through the oral delivery[51]. Similar studies were conducted using various weakly acidic poorly water-soluble drugs such as tolfenamic acid (Tolf), meclofenamic acid, diclofenac, ibuprofen, amlodipine fexofenadine, ranitidine, and metformin using a series of lipophilic cations[52]. Recently, Wang *et al.* reported that the protic ionic liquids of naproxen and ibuprophen with iphenhydramine displayed rapid dissolution and improved bioavailability in capsule forms[53]. Mitragotri S.

and co-workers reported about geranate and choline (CAGE) ionic liquid and developed a highly effective oral insulin formulation using IL, which enhanced significantly the paracellular transport of insulin[54]. Even, at low doses of Insulin (3–10 U/kg), IL based insulin had shown about 45% decrease of glucose levels in blood with sustained release up to 12 h. While IL-based oral delivery is proving advantageous in the effective delivery of poorly bioavailable drug molecules but the safety of such delivery vehicles remains to be established.

1.4.2.4. API-ILs as pharmaceuticals in drug delivery

An estimated 40-70% of FDA-approved drugs are failed to attain the therapeutic excellence because of their polymorphism, limited solubility and poor bioavailability[2]. Consequently, the pharmaceutical researchers are actively exploring several approaches to improve the pharmacological properties such as controlled drug release, solubility, bioavailability and stability that ensure therapeutic efficacy. The active pharmaceutical ingredient–ionic liquid (API-IL) is an innovative approach to address the innate difficulties of many drug candidates. Rogers and coworkers pioneered this concept, generally converting the solid APIs in an ionic liquid form by combining distinct cationic and anionic derivatives of drug molecules to fine-tuning their various pharmaceutical cocktail properties. The first endeavor to prepare API-ILs was in 2007 by Rogers and coworkers and obtained [lidocainium][docusate] (LD) API-IL by pairing lidocaine, a widely used local anesthesia, with sodium docusate, a laxative[1,11]. A significant enhancement with improved solubility and thermal stability was achieved as compared with lidocaine hydrochloride in the topical analgesia treatment[55]. Also, the polymorphism of ranitidine hydrochloride was successfully eliminated by designing [ranitidine][docusate] as a room temperature API-IL. Biological activity of API-ILs also investigated using pheochromocytoma (PC12) cells in where LD exerted a distinct effect than that of lidocaine hydrochloride [55]. Following this, an increasing number of research groups turned their attention to API-ILs.

Egorova KS and co-workers[56] demonstrated the three strategies to introduce API into IL systems; A) API-ILs containing ionic API as anion, B) covalently linked API in the cation and C) API-ILs by combining both ways with dual activities (Figure 1.9). Most of cases, type A strategy is used to prepare the API-ILs in which the readily ionizable API can be act as IL cations or anions. They described the above three strategies to prepare the API-ILs using salicylic acid (SA) as a model drug and the imidazolium head group as the cation with on various alkyl side chains. The API-ILs showed improved solubility compared with SA, and

significantly higher cytotoxicity than that of conventional imidazolium-based ILs in human colon cancer cell line which was also comparable to pure SA[56].

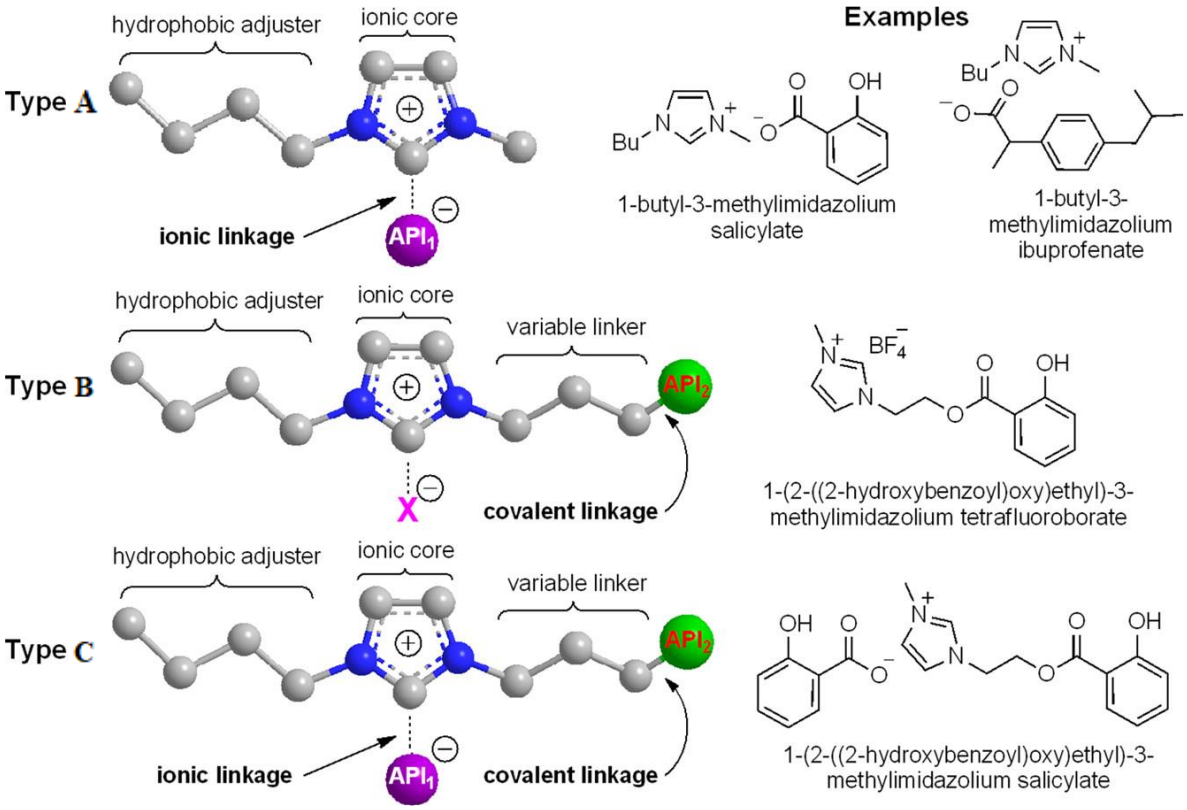

Figure 1.9. Drug development platforms of API-ILs. A) API-ILs containing ionic API as anion, B) covalently linked API in the cation and C) API-ILs by combining both ways with dual activities. Figure reproduced with permission from ref.[10].

When the crystalline solid APIs converted into ionic liquids form, the physicochemical or biological properties of API-ILs are affected by the appropriate choice of counterions. Several notable works have been conducted to emphasize the effect of counterion on API-ILs for tuning their various pharmaceutical cocktail properties i.e., solubility, thermal stability, toxicity and bioavailability[1,2,11,29,57]. Recently, Rogers and co-workers demonstrated a series of various IL-forming ions such as cholinium, tetrabutylammonium, tetrabutylphosphonium, tetramethylhexadecyl- ammonium cations, and docusate and chloride anions were paired with acyclovir as the counterion to form ionic liquids[58]. Acyclovir API-ILs exhibited excellent solubility not only in water, but also in simulated body fluids (phosphate-buffered saline, simulated gastric, and simulated intestinal fluids) as compared with neutral acyclovir. Cholinium-based acyclovir API-IL showed higher solubility than that of other cations-based acyclovir API-ILs in both water and simulated body fluids due to the presence of hydrophilic cholinium cation with hydroxyl groups. A similar finding also obtained when they prepared

cholinium based-sulfasalazine ionic liquid (Sulfa-IL), wherein Sulfa-IL exhibited about 4000-fold enhanced solubility and 2.4-fold improved bioavailability as compared with neutral Sulfa in both *in vitro* and *in vivo* models[59]. Also, Marrucho groups investigated the physicochemical and pharmaceutical properties of API-ILs, derived by pairing the biocompatible and low toxic cholinium cation with various API anions such as nalidixic acid, niflumic acid, 4-aminosalicylic acid, pyrazinoic acid, or picolinic acid, and exhibited enhanced solubility and bioavailability as compared with neutral APIs[60].

Dual-functional API-ILs strategy is also an effect tool to develop, design and delivery of solid drugs. The pharmacological activity of this API-IL not only act independently, but also synergistically affect the pharmacokinetics, suggesting not achievable with separate APIs. Some notable works of dual active API-ILs have been reported to emphasize their synthesis and attracting properties[1,10,11]. Antibacterial cations such as Benzalkonium and didecyldimethylammonium were paired with saccharinate and acesulfame anions to form dual-active API-ILs that demonstrated improved antimicrobial activity as compared with individual ones[61]. Ampicillin is the popular antibiotic which forms API-IL by combing with the antiseptic cetylpyridinium ($C_{16}Py$) and exhibited higher activity against several Gram-positive and Gram-negative bacterial strains as [Na][Amp] or [$C_{16}Py$][Cl][10,62]. Recently, Rogers's groups and Ishida groups reported a dual-active API-IL by combining lidocaine as local anesthesia or painkiller and etodolac or ibuprofen as a nonsteroidal anti-inflammatory drug[63,64]. The resulting lidocainium etodolac API-IL demonstrated significantly higher saturation solubility in water and more efficient permeability through the skin than etodolac alone[63].

API-IL Prodrugs are another promising strategy to enlarge the role of API-ILs in drug delivery derives from a combination with the familiar prodrug approach. Generally, prodrugs are pharmacologically inactive drug molecules that are converted into the active drug through a metabolic biotransformation within the body[1,2]. Although, prodrugs approaches are used to increase the solubility and site specificity, reduce the rapid drug metabolism and cellular toxicity and controlled release of drugs, but some cases can suffer the same polymorphic issues as the solid drugs[1,2]. For example, a prodrug of chloromycetin (chloramphenicol palmitate) exists three polymorphic forms, A, B and C, but only the B polymorph is able to transfer at the required level into the blood plasma[65].

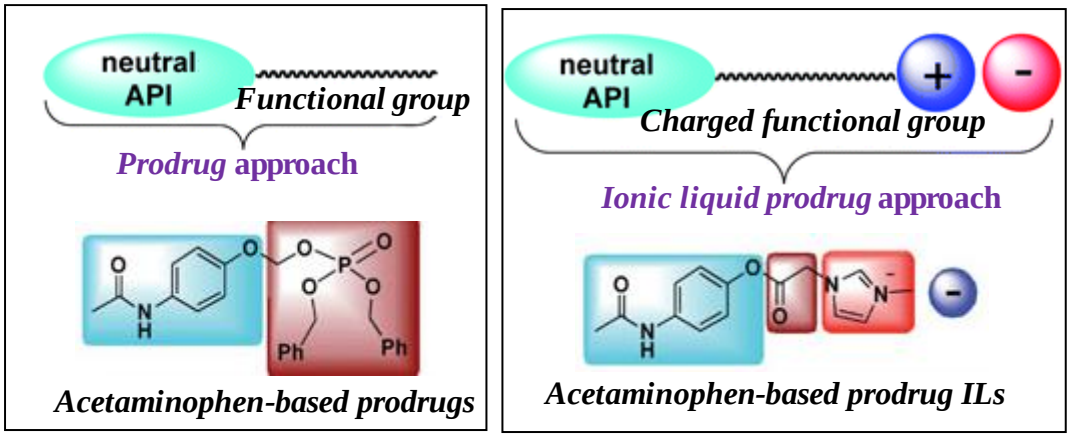

Figure 1.10. A schematic view of prodrug strategy vs ionic liquid prodrug (API-IL prodrug) strategy. Figure reproduced with permission from ref.[10]

However, API-IL prodrugs offer advantages by eliminating unwanted properties of a solid drugs. API-IL prodrug was prepared by adding the hydrolizable functional groups that are charged or ionizable with a neutral API and, then paired with the appropriate counterions to form ILs (Figure 1.10)[57,61]. By selecting appropriate counterions, desirable API-IL prodrugs can be prepared with designing properties such as dual-functionality, transdermal penetration enhancer or other favorable action. A series of API-IL prodrugs were prepared from an acetaminophen-derived imidazolium, phosphonium, pyridinium and pyrrolidinium paired with docusate[66]. The new prodrugs are liquids with no melting point and release faster drugs in PBS and SIF, suggesting that controlled release might be achievable.

1.5. Aim and outline of this thesis

Pharmaceutical industries are mainly dependents on that drug molecules, which get approved by the Food and Drug Administration (FDA). The FDA approval procedure of a drug also depends on their biopharmaceutical performance such as solubility, stability, bioavailability and permeability. However, these properties can be variable because of their different polymorphic forms, which can also have a significant impact on the manufacturing process, storage and transport of the final product. Therefore, the commercial volumes of manufactured drug products can also depend on the final crystallization product.

The problems of obtaining pure drugs in the correct form, as discussed above, can be solved by the formation of stable liquid drugs from the solid crystalline form. Unfortunately, limited research is available on liquid drugs. Liquefaction of a drug could be achieved by the solubilisation of solid drugs by using potent counterions and the delivery of drugs in various

routes such as emulsions, suspensions, and liposomes. Thus, a new form of liquid drugs could reduce the problems associated with the solid state.

In recent years, ionic liquids have been emerging as novel media in pharmaceuticals applications. Specifically in crystallisation and liquid drug conversion, ionic liquids could play a vital role due to their solvents properties such as wide liquid range from -100 to 300 °C, good solvation power, almost zero vapour pressure, thermally stability up to 200 °C, recyclable, tuneability of cations and anions and easy preparation. In addition, the multifunctionality of ionic liquids can provide a unique opportunity to design a specific process which could potentially reduce the process cost and a significant impact on environmental factors.

The present work focused on synthesis and characterization of biocompatible counterions for transforming the poorly water-soluble drugs into ionic liquids and investigated its pharmaceutical performances. A review of the literature showed that ionic liquids are used in many applications such areas as catalysis, electrochemistry, lubrication and solvents for synthetic chemistry but there are a limited number of publications on crystal engineering and drug delivery. Thus ionic liquids have enormous potential to be explored in these fields due to their unique properties. Hence the focus of this research was the investigation of some biocompatible IL-forming cations based ionic liquids for the use in drug delivery.

The aim of the research is to get a better understanding on the fascinating behavior of different biocompatible cations that could be transferred the poorly water-soluble drugs into ionic liquids for envisaging their biomedical applications. The general objectives of the present work were illustrated as below:

A. Synthesis a series of potent biocompatible IL-forming cations such as amino acid esters, choline and *N*-methyl-2-pyrrolidone, and API-ILs of three model poorly water-soluble APIs (salicylic acid, methotrexate and ibuprofen).

B. Study on the physico-chemical and thermal properties of the newly synthetized API-ILs.

C. Study on *in vitro* solubility and skin permeability of API-ILs.

D. Study on the biological properties of API-ILs with IL-forming counterions.

- **a)** Study on *in vitro* cellular viability and the cytotoxicity of the IL-forming counterions obtained on mammalian cell lines L929, HeLa and NIH3T3.
- **b)** Study on *in vitro* cellular viability and the cytotoxicity of API-ILs obtained on mammalian cell lines L929 and NIH3T3.
- **c)** Study on *in vitro* antitumor activity of the newly synthesized methotrexate ionic liquids.

E. Study on in vivo pharmacokinetics and antitumor activity of methotrexate ionic liquids.

The particular objectives in each chapter are described as follows:

Chapter 2 – A series of amino acid esters (AAEs) were synthesized from natural amino acids and introduced as biocompatible cations for generating the IL forms of salicylic acid (Sal-ILs). The synthesized AAEs and Sal-ILs were characterized using ^{1}H and ^{13}C NMR, FTIR, elemental, and thermogravimetric analyses. The solubility, cytotoxicity and skin permeability of Sal-ILs evaluated for envisaging their biomedical applications.

Chapter 3 – Several types of IL-forming cations from amino acids, cholinium, imidazolium, ammonium, phosphonium groups were synthesized by considering the lower toxicities among their corresponding groups for converting the poorly water-soluble methotrexate into IL forms (MTX-ILs). The synthesized MTX-ILs were characterized through ^{1}H NMR, FTIR, p-XRD, DSC and thermogravimetric analysis. *In vitro* solubilities and antitumor activity also evaluated for representing potential drug formulations. Finally, *In vivo* biocompatibility, pharmacokinetics and antitumor efficacy of methotrexate ionic liquid moieties are investigated for envisaging their therapeutic application as a biocompatible component of a drug delivery system.

Chapter 4 – *N*-Methyl-2-pyrrolidone (NMP) cation was firstly introduced as a potent biocompatible promising counter ion to ionic liquefied the poorly water insoluble ibuprofen as a model drug for the topical drug delivery. The synthesized NMP-based ionic liquid (NMP-IL) was characterized using ^{1}H & ^{13}C-NMR, FT-IR, DSC and TGA. *In vitro* cytotoxicities, skin penetration and permeation studies of NMP-IL were conducted for developing the novel API-IL formulations for the topical treatment of skin diseases.

Chapter 5 – We summarized the findings of this research and briefly discussed further research directions related to this research.

1.6. ***References***

[1] J.L. Shamshina, P.S. Barber, R.D. Rogers, Ionic liquids in drug delivery, Expert Opin. Drug Deliv. 10 (2013) 1367–1381. doi:10.1517/17425247.2013.808185.

[2] G. Shamshina, Julia L, Steven P. Kelley, R.D.R. Gurau, Develop ionic liquid drugs, Nature. 528 (2015) 188–189. http://www.nature.com/polopoly_fs/1.18964!/menu/main/topColumns/topLeftColumn/pdf/528188a.pdf.

[3] Y. Kawabata, K. Wada, M. Nakatani, S. Yamada, S. Onoue, Formulation design for

poorly water-soluble drugs based on biopharmaceutics classification system: Basic approaches and practical applications, Int. J. Pharm. 420 (2011) 1–10. doi:10.1016/j.ijpharm.2011.08.032.

[4] S. Kalepu, V. Nekkanti, Insoluble drug delivery strategies: Review of recent advances and business prospects, Acta Pharm. Sin. B. 5 (2015) 442–453. doi:10.1016/j.apsb.2015.07.003.

[5] A. Mullard, 2018 FDA drug approvals, Nat. Rev. Drug Discov. 18 (2019) 85–89. doi:10.1038/d41573-019-00014-x.

[6] M. Rodriguez-Aller, D. Guillarme, J.L. Veuthey, R. Gurny, Strategies for formulating and delivering poorly water-soluble drugs, J. Drug Deliv. Sci. Technol. 30 (2015) 342–351. doi:10.1016/j.jddst.2015.05.009.

[7] Z. Gao, S. Rohani, J. Gong, J. Wang, Recent Developments in the Crystallization Process: Toward the Pharmaceutical Industry, Engineering. 3 (2017) 343–353. doi:10.1016/J.ENG.2017.03.022.

[8] J. Hodgson, ADMET - Turning chemicals into drugs. Rapidly resolving the pharmacokinetic and toxicological properties of drug candidates remains a key challenge for drug developers, Nat. Biotechnol. 19 (2001) 722–726. doi:10.1038/90761.

[9] B. Homayun, X. Lin, H.-J. Choi, Challenges and Recent Progress in Oral Drug Delivery Systems for Biopharmaceuticals, Pharmaceutics. 11 (2019) 129. doi:10.3390/pharmaceutics11030129.

[10] K.S. Egorova, E.G. Gordeev, V.P. Ananikov, Biological Activity of Ionic Liquids and Their Application in Pharmaceutics and Medicine, Chem. Rev. 117 (2017) 7132–7189. doi:10.1021/acs.chemrev.6b00562.

[11] C. Agatemor, K.N. Ibsen, E.E.L. Tanner, S. Mitragotri, Ionic liquids for addressing unmet needs in healthcare, Bioeng. Transl. Med. (2018) 7–25. doi:10.1002/btm2.10083.

[12] G.K. Kaur, M. Arora, R.K. Majeti, Oral Drug Delivery Technologies-A Decade of Developments, J. Pharmacol. Exp. Ther. (2019) jpet.118.255828. doi:10.1124/jpet.118.255828.

[13] D. Hörter, J.. Dressman, Influence of physicochemical properties on dissolution of drugs in the gastrointestinal tract1PII of original article: S0169-409X(96)00487-5. The article was originally published in Advanced Drug Delivery Reviews 25 (1997) 3–14.1, Adv. Drug Deliv. Rev. 46 (2002) 75–87. doi:10.1016/s0169-409x(00)00130-7.

[14] I. Ali, M.N. Lone, Z.A. Alothman, A. Alwarthan, Insights into the pharmacology of new heterocycles embedded with oxopyrrolidine rings: DNA binding, molecular docking,

and anticancer studies, J. Mol. Liq. 234 (2017) 391–402. doi:10.1016/j.molliq.2017.03.112.

[15] R. Shaikh, R. Singh, G.M. Walker, D.M. Croker, Pharmaceutical Cocrystal Drug Products: An Outlook on Product Development, Trends Pharmacol. Sci. 39 (2018) 1033–1048. doi:10.1016/j.tips.2018.10.006.

[16] D. Giron, Review article of using calorimetry to study polymorphs.pdf, 64 (2001) 37–60.

[17] G. Ghielmetti, T. Bruzzese, C. Bianchi, F. Recusani, Relationship between acute toxicity in mice and polymorphic forms of polyene antibiotics, J. Pharm. Sci. 65 (1976) 905–907. doi:10.1002/jps.2600650625.

[18] T.L. Chang, H. Zhan, D. Liang, J.F. Liang, Nanocrystal technology for drug formulation and delivery, Front. Chem. Sci. Eng. 9 (2015) 1–14. doi:10.1007/s11705-015-1509-3.

[19] S.L. Childs, G.P. Stahly, A. Park, The salt-cocrystal continuum: The influence of crystal structure on ionization state, Mol. Pharm. 4 (2007) 323–338. doi:10.1021/mp0601345.

[20] P.L. Gould, Salt selection for basic drugs, Int. J. Pharm. 33 (1986) 201–217. doi:10.1016/0378-5173(86)90055-4.

[21] D.A. Haynes, W. Jones, W.D.S. Motherwell, Occurrence of pharmaceutically acceptable anions and cations in the Cambridge Structural Database, J. Pharm. Sci. 94 (2005) 2111–2120. doi:10.1002/jps.20441.

[22] J. Rautio, J. Kärkkäinen, K.B. Sloan, Prodrugs – Recent approvals and a glimpse of the pipeline, Eur. J. Pharm. Sci. 109 (2017) 146–161. doi:10.1016/j.ejps.2017.08.002.

[23] A. Najjar, R. Karaman, The prodrug approach in the era of drug design, Expert Opin. Drug Deliv. 16 (2019) 1–5. doi:10.1080/17425247.2019.1553954.

[24] R.D. Rogers, Review / Preview : Prodrug Ionic Liquids, 31 (2013).

[25] L.R. Staben, S.G. Koenig, S.M. Lehar, R. Vandlen, D. Zhang, J. Chuh, S.F. Yu, C. Ng, J. Guo, Y. Liu, A. Fourie-O'Donohue, M. Go, X. Linghu, N.L. Segraves, T. Wang, J. Chen, B. Wei, G.D.L. Phillips, K. Xu, K.R. Kozak, S. Mariathasan, J.A. Flygare, T.H. Pillow, Targeted drug delivery through the traceless release of tertiary and heteroaryl amines from antibody-drug conjugates, Nat. Chem. 8 (2016) 1112–1119. doi:10.1038/nchem.2635.

[26] C.M. Walko, C. Lindley, Capecitabine: a review., Clin. Ther. 27 (2005) 23–44. doi:10.1016/j.clinthera.2005.01.005.

[27] R. Thakuria, A. Delori, W. Jones, M.P. Lipert, L. Roy, N. Rodríguez-Hornedo, Pharmaceutical cocrystals and poorly soluble drugs, Int. J. Pharm. 453 (2013) 101–125.

doi:10.1016/j.ijpharm.2012.10.043.

[28] K. Kawakami, N. Oda, K. Miyoshi, T. Funaki, Y. Ida, Solubilization behavior of a poorly soluble drug under combined use of surfactants and cosolvents, Eur. J. Pharm. Sci. 28 (2006) 7–14. doi:10.1016/j.ejps.2005.11.012.

[29] N. Adawiyah, M. Moniruzzaman, S. Hawatulaila, M. Goto, Ionic liquids as a potential tool for drug delivery systems, Med. Chem. Commun. 7 (2016) 1881–1897. doi:10.1039/C6MD00358C.

[30] M. Moniruzzaman, M. Tamura, Y. Tahara, N. Kamiya, M. Goto, Ionic liquid-in-oil microemulsion as a potential carrier of sparingly soluble drug: Characterization and cytotoxicity evaluation, Int. J. Pharm. 400 (2010) 243–250. doi:10.1016/j.ijpharm.2010.08.034.

[31] J.S.. Wilkes, M.J. Zaworotko, Air and Water stable emim-based ionic liquids, J. Chem. Soc., Chem. Commun. 04 (1992) 965–967.

[32] J.H. Davis, K.J. Forrester, T. Merrigan, Novel organic ionic liquids (OILS) incorporating cations derived from the antifungal drug miconazole, Tetrahedron Lett. 39 (1998) 8955–8958. doi:10.1016/S0040-4039(98)02070-X.

[33] D. Dobler, T. Schmidts, I. Klingenhöfer, F. Runkel, Ionic liquids as ingredients in topical drug delivery systems, Int. J. Pharm. 441 (2013) 620–627. doi:10.1016/j.ijpharm.2012.10.035.

[34] S. Goindi, R. Kaur, R. Kaur, An ionic liquid-in-water microemulsion as a potential carrier for topical delivery of poorly water soluble drug: Development, ex-vivo and in-vivo evaluation, Int. J. Pharm. 495 (2015) 913–923. doi:10.1016/j.ijpharm.2015.09.066.

[35] K.S. Egorova, V.P. Ananikov, Fundamental importance of ionic interactions in the liquid phase: A review of recent studies of ionic liquids in biomedical and pharmaceutical applications, J. Mol. Liq. 272 (2018) 271–300. doi:10.1016/j.molliq.2018.09.025.

[36] K. Ghandi, A Review of Ionic Liquids, Their Limits and Applications, Green Sustain. Chem. 04 (2014) 44–53. doi:10.4236/gsc.2014.41008.

[37] A.F.M. Cláudio, M.C. Neves, K. Shimizu, J.N. Canongia Lopes, M.G. Freire, J.A.P. Coutinho, The magic of aqueous solutions of ionic liquids: Ionic liquids as a powerful class of catanionic hydrotropes, Green Chem. 17 (2015) 3948–3963. doi:10.1039/c5gc00712g.

[38] H. Mizuuchi, V. Jaitely, S. Murdan, A.T. Florence, Room temperature ionic liquids and their mixtures: Potential pharmaceutical solvents, Eur. J. Pharm. Sci. 33 (2008) 326–

331. doi:10.1016/j.ejps.2008.01.002.

[39] V. Jaitely, A.T. Florence, Water-immiscible room temperature ionic liquids (RTILs) as drug reservoirs for controlled release, 354 (2008) 168–173. doi:10.1016/j.ijpharm.2008.01.034.

[40] A. Banerjee, K. Ibsen, Y. Iwao, M. Zakrewsky, S. Mitragotri, Transdermal Protein Delivery Using Choline and Geranate (CAGE) Deep Eutectic Solvent, Adv. Healthc. Mater. 6 (2017) 1–11. doi:10.1002/adhm.201601411.

[41] J. Krug, Kinetic pattern formation at solid surfaces, 2005. doi:10.1007/3-540-26869-3_2.

[42] M. Moniruzzaman, Y. Tahara, M. Tamura, N. Kamiya, M. Goto, Ionic liquid-assisted transdermal delivery of sparingly soluble drugs, Chem. Commun. 46 (2010) 1452–1454. doi:10.1039/b907462g.

[43] T. Gabriel, Topical Antiacne Drugs Delivery Systems, Open Dermatol. J. 10 (2016) 85–95. doi:10.2174/1874372201610010085.

[44] D. Lee, J.N. Ashcraft, E. Verploegen, E. Pashkovski, D.A. Wertz, Permeability of model stratum corneum lipid membrane measured using quartz crystal microbalance, Langmuir. 25 (2009) 5762–5766. doi:10.1021/la804105t.

[45] M. Zakrewsky, K.S. Lovejoy, T.L. Kern, T.E. Miller, V. Le, A. Nagy, A.M. Goumas, R.S. Iyer, R.E. Del Sesto, A.T. Koppisch, D.T. Fox, S. Mitragotri, Ionic liquids as a class of materials for transdermal delivery and pathogen neutralization, Proc. Natl. Acad. Sci. 111 (2014) 13313–13318. doi:10.1073/pnas.1403995111.

[46] G.S. Lim, S. Jaenicke, M. Klähn, How the spontaneous insertion of amphiphilic imidazolium-based cations changes biological membranes: A molecular simulation study, Phys. Chem. Chem. Phys. 17 (2015) 29171–29183. doi:10.1039/c5cp04806k.

[47] N. Kundu, S. Roy, D. Mukherjee, T.K. Maiti, N. Sarkar, Unveiling the Interaction between Fatty-Acid-Modified Membrane and Hydrophilic Imidazolium-Based Ionic Liquid: Understanding the Mechanism of Ionic Liquid Cytotoxicity, J. Phys. Chem. B. 121 (2017) 8162–8170. doi:10.1021/acs.jpcb.7b06231.

[48] M. Zakrewsky, A. Banerjee, S. Apte, T.L. Kern, M.R. Jones, R.E.D. Sesto, A.T. Koppisch, D.T. Fox, S. Mitragotri, Choline and Geranate Deep Eutectic Solvent as a Broad-Spectrum Antiseptic Agent for Preventive and Therapeutic Applications, Adv. Healthc. Mater. 5 (2016) 1282–1289. doi:10.1002/adhm.201600086.

[49] M. Moniruzzaman, N. Kamiya, M. Goto, Ionic liquid based microemulsion with pharmaceutically accepted components: Formulation and potential applications, J. Colloid Interface Sci. 352 (2010) 136–142. doi:10.1016/j.jcis.2010.08.035.

[50] S. Araki, R. Wakabayashi, M. Moniruzzaman, N. Kamiya, M. Goto, Ionic liquid-mediated transcutaneous protein delivery with solid-in-oil nanodispersions, Medchemcomm. 6 (2015) 2124–2128. doi:10.1039/c5md00378d.

[51] H.D. Williams, Y. Sahbaz, L. Ford, T.H. Nguyen, P.J. Scammells, C.J.H. Porter, Ionic liquids provide unique opportunities for oral drug delivery: Structure optimization and in vivo evidence of utility, Chem. Commun. 50 (2014) 1688–1690. doi:10.1039/c3cc48650h.

[52] Y. Sahbaz, H.D. Williams, T.H. Nguyen, J. Saunders, L. Ford, S.A. Charman, P.J. Scammells, C.J.H. Porter, Transformation of poorly water-soluble drugs into lipophilic ionic liquids enhances oral drug exposure from lipid based formulations, Mol. Pharm. 12 (2015) 1980–1991. doi:10.1021/mp500790t.

[53] C. Wang, S.A. Chopade, Y. Guo, J.T. Early, B. Tang, E. Wang, M.A. Hillmyer, T.P. Lodge, C.C. Sun, Preparation, Characterization, and Formulation Development of Drug-Drug Protic Ionic Liquids of Diphenhydramine with Ibuprofen and Naproxen, Mol. Pharm. 15 (2018) 4190–4201. doi:10.1021/acs.molpharmaceut.8b00569.

[54] E.E.L. Tanner, K.N. Ibsen, S. Mitragotri, Transdermal insulin delivery using choline-based ionic liquids (CAGE), J. Control. Release. 286 (2018) 137–144. doi:10.1016/j.jconrel.2018.07.029.

[55] W.L. Hough, M. Smiglak, H. Rodríguez, R.P. Swatloski, S.K. Spear, D.T. Daly, J. Pernak, J.E. Grisel, R.D. Carliss, M.D. Soutullo, J.H. Davis, R.D. Rogers, The third evolution of ionic liquids: Active pharmaceutical ingredients, New J. Chem. 31 (2007) 1429–1436. doi:10.1039/b706677p.

[56] K.S. Egorova, M.M. Seitkalieva, A. V. Posvyatenko, V.N. Khrustalev, V.P. Ananikov, Cytotoxic Activity of Salicylic Acid-Containing Drug Models with Ionic and Covalent Binding, ACS Med. Chem. Lett. 6 (2015) 1099–1104. doi:10.1021/acsmedchemlett.5b00258.

[57] A. Balk, T. Widmer, J. Wiest, H. Bruhn, J.C. Rybak, P. Matthes, K. Müller-Buschbaum, A. Sakalis, T. Lühmann, J. Berghausen, U. Holzgrabe, B. Galli, L. Meinel, Ionic liquid versus prodrug strategy to address formulation challenges, Pharm. Res. 32 (2015) 2154–2167. doi:10.1007/s11095-014-1607-9.

[58] J.L. Shamshina, O.A. Cojocaru, S.P. Kelley, K. Bica, S.P. Wallace, G. Gurau, R.D. Rogers, Acyclovir as an Ionic Liquid Cation or Anion Can Improve Aqueous Solubility, ACS Omega. 2 (2017) 3483–3493. doi:10.1021/acsomega.7b00554.

[59] M. Shadid, G. Gurau, J.L. Shamshina, B.C. Chuang, S. Hailu, E. Guan, S.K. Chowdhury,

J.T. Wu, S.A.A. Rizvi, R.J. Griffin, R.D. Rogers, Sulfasalazine in ionic liquid form with improved solubility and exposure, Medchemcomm. 6 (2015) 1837–1841. doi:10.1039/c5md00290g.

[60] J.M.M. Araújo, C. Florindo, A.B. Pereiro, N.S.M. Vieira, A.A. Matias, C.M.M. Duarte, L.P.N. Rebelo, I.M. Marrucho, Cholinium-based ionic liquids with pharmaceutically active anions, RSC Adv. 4 (2014) 28126–28132. doi:10.1039/c3ra47615d.

[61] O.A. Cojocaru, K. Bica, G. Gurau, A. Narita, P.D. McCrary, J.L. Shamshina, P.S. Barber, R.D. Rogers, Prodrug ionic liquids: Functionalizing neutral active pharmaceutical ingredients to take advantage of the ionic liquid form, Medchemcomm. 4 (2013) 559–563. doi:10.1039/c3md20359j.

[62] M.R. Cole, M. Li, B. El-Zahab, M.E. Janes, D. Hayes, I.M. Warner, Design, synthesis, and biological evaluation of β-lactam antibiotic-based imidazolium- and pyridinium-type ionic liquids, Chem. Biol. Drug Des. 78 (2011) 33–41. doi:10.1111/j.1747-0285.2011.01114.x.

[63] Y. Miwa, H. Hamamoto, T. Ishida, Lidocaine self-sacrificially improves the skin permeation of the acidic and poorly water-soluble drug etodolac via its transformation into an ionic liquid, Eur. J. Pharm. Biopharm. 102 (2016) 92–100. doi:10.1016/j.ejpb.2016.03.003.

[64] P. Berton, K.R. Di Bona, D. Yancey, S.A.A. Rizvi, M. Gray, G. Gurau, J.L. Shamshina, J.F. Rasco, R.D. Rogers, Transdermal Bioavailability in Rats of Lidocaine in the Forms of Ionic Liquids, Salts, and Deep Eutectic, ACS Med. Chem. Lett. 8 (2017) 498–503. doi:10.1021/acsmedchemlett.6b00504.

[65] A.J. Aguiar, J. Krc, A.W. Kinkel, J.C. Samyn, Effect of polymorphism on the absorption of chloramphenicol from chloramphenicol palmitate, J. Pharm. Sci. 56 (1967) 847–853. doi:10.1002/jps.2600560712.

[66] J.H. Davis, Jr., P.A. Fox, From curiosities to commodities: ionic liquids begin the transition, Chem. Commun. (2003) 1209–1212. doi:10.1039/b212788a.

CHAPTER 2: CHARACTERIZATION AND CYTOTOXICITY EVALUATION OF BIOCOMPATIBLE AMINO ACID ESTERS USED TO CONVERT SALICYLIC ACID INTO IONIC LIQUIDS

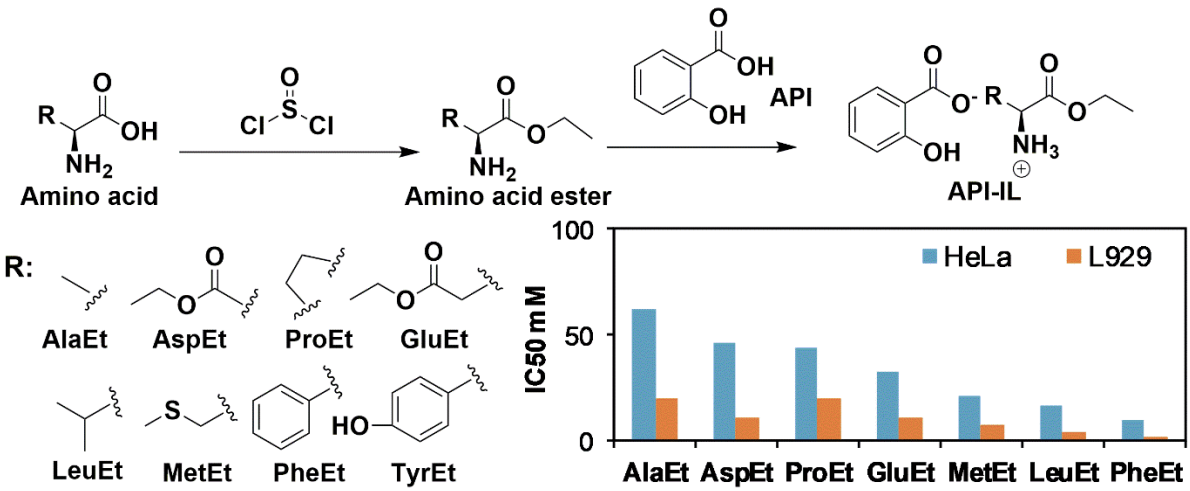

This chapter was originally published in International Journal of Pharmaceutics 546 (**2018**) 31–38; https://doi.org/10.1016/j.ijpharm.2018.05.021 with permission of Elsevier.

2.1. Abstract

The technological utility of active pharmaceutical ingredients (APIs) is greatly enhanced when they are transformed into ionic liquids (ILs). API-ILs have better solubility, thermal stability, and the efficacy in topical delivery than solid or crystalline drugs. However, toxicological issue of API-ILs is the main challenge for their application in drug delivery. To address this issue, 11 amino acid esters (AAEs) were synthesized and investigated as biocompatible counter cations for the poorly water-soluble drug salicylic acid (Sal) to form Sal-ILs. The AAEs were characterized using ^{1}H and ^{13}C NMR, FTIR, elemental, and thermogravimetric analyses. The cytotoxicities of the AAE cations, Sal-ILs, and free Sal were investigated using mammalian cell lines (L929 and HeLa). The toxicities of the AAE cations greatly increased with inclusion of long alkyl chains, sulfur, and aromatic rings in the side groups of the cations. Ethyl esters of alanine, aspartic acid, and proline were selected as a low cytotoxic AAE. The cytotoxicities of the Sal-ILs drastically increased compared with the AAEs on incorporation of Sal into the cations, and were comparable to that of free Sal. Interestingly, the water miscibilities of the Sal-ILs were higher than that of free Sal, and the Sal-ILs were miscible with water at any ratio. A skin permeation study showed that the Sal-ILs penetrated through skin faster than the Sal sodium salt. These results suggest that AAEs could be used in biomedical applications to eliminate the use of traditional toxic solvents for transdermal delivery of poorly water-soluble drugs.

2.2. Introduction

The pharmaceutical industry is facing unprecedented challenges to overcome physicochemical obstacles to achieve optimum pharmacological responses for many drugs because of their low solubility, polymorphism, and low bioavailability[1,2]. Currently, poorly water-soluble drugs represent about 40% of available oral drugs, 40%–50% of innovative active pharmaceutical ingredient (API) drugs, and 90% of new chemical entities[1,3]. These drugs have poor and variable absorption rates in their therapeutic applications. High doses of these drugs need to be administrated to reach the target therapeutic responses in oral administration, which can cause inadequate bioavailability and long term gastrointestinal mucosal toxicity in patients[4]. To improve drug solubilities and therapeutic effects, researchers are investigating changing the dosage forms, physical forms, and routes of administration to develop efficacious drug delivery systems. Recently, the solubility characteristics of these drugs have been evaluated by applying several techniques, either alone or in combination, such as lyophilization, solid dispersion,

nanosuspensions, nanoprecipitation, microencapsulation, soluble salt formation, inclusion complexes with β-cyclodextrins, cocrystal formation, and ionic liquefaction[1–3,5].

Scientists have investigated ionic liquids (ILs) as potential candidates for effective biocompatible drug delivery systems of poorly water-soluble drugs[6]. ILs have gained considerable attention as green designer solvents with unique physiochemical properties, such as superior solvation properties, wide liquid ranges, negligible vapor pressures, non-volatility, and non-flammability[5,7,8]. Recently, the cytotoxic effects of ILs have been evaluated in different human and animal cell lines, bacteria, plants, and fungi[2,9]. However, ILs do not satisfy all green chemistry criteria, and in some cases, ILs show higher toxicity than conventional organic solvents in various biotechnological processes[10]. Most commonly used imidazolium- and pyridinium-based ILs are not considered ecofriendly[10]. Therefore, non-toxic and ecofriendly ILs need to be developed for sustainable pharmaceutical applications[9]. Natural amino acids are potential candidates for synthesis of green ILs because of their abundance, nontoxicity, biodegradability, biocompatibility, relatively low price, and environmentally friendly behavior[10,11]. Amino acids have prolific structural diversity and can act as cations or anions in IL synthesis. Recently, amino acid-based ILs, with an amino acid as the anion and phosphonium, choline, alkyl ammonium, or dialkylimidazolium as the cation, have been developed[2]. These amino acid-based ILs possess interesting physicochemical and biological activities. For example, addition of an amino acid decreases the cytotoxicity of 1-(2(glycyloxy)ethyl)-3-methylimidazolium tetrafluoroborate compared with that of 1-ethyl-3-methylimidazolium tetrafluoroborate[7]. Amino acid derivatization at the carboxyl group was used to reduce the possibility of formation of strong hydrogen bonds involving carboxylic acid, which led to production of room temperature ILs in many cases. As biocompatible counter cations, amino acid esters (AAEs) could be used to formulate poorly water-soluble anionic drugs with attractive physicochemical properties, such as high water solubility, thermal stability, and skin permeability[12]. However, the cytotoxicities of ILs synthesized with AAE cations have not been investigated.

Derivatization of poorly water-soluble APIs to their ionized forms in API-ILs is an excellent approach to increase water solubility. This approach was first reported for pairing of salicylic acid (Sal) with alkyl amines in propylene ethanol glycol solutions[13]. Sal is commonly used as anti-inflammatory, analgesic, and antipyretic because of its excellent bacteriostatic, fungicidal, keratolytic, and photoprotective properties[14–16]. Recently, many researchers have formulated API-ILs using both single active drugs (e.g., lidocaine, ibuprofen, procaine, and docusate) and multiple active drugs (e.g., lidocaine–ibuprofen, salicylate–ibuprofen, and

ephedrine–ibuprofen)[2]. The API-IL formulation improves the physicochemical or biological properties and is an efficient drug carrier in drug delivery systems[2,12].

The aim of this study was to develop biocompatible amino acid-based API-ILs and to evaluate their toxicities and skin permeation behavior using Sal as a model drug. We synthesized and characterized various AAEs as cations, and optimized the alkyl chain length based on the cytotoxicities with mammalian cell lines. Then, we synthesized Salicylate ionic liquids (Sal-ILs) by incorporating the model drug into those AAEs with low cytotoxicities, and investigated the toxicological effects of the Sal-ILs. Finally, skin permeation was evaluated for selected Sal-ILs.

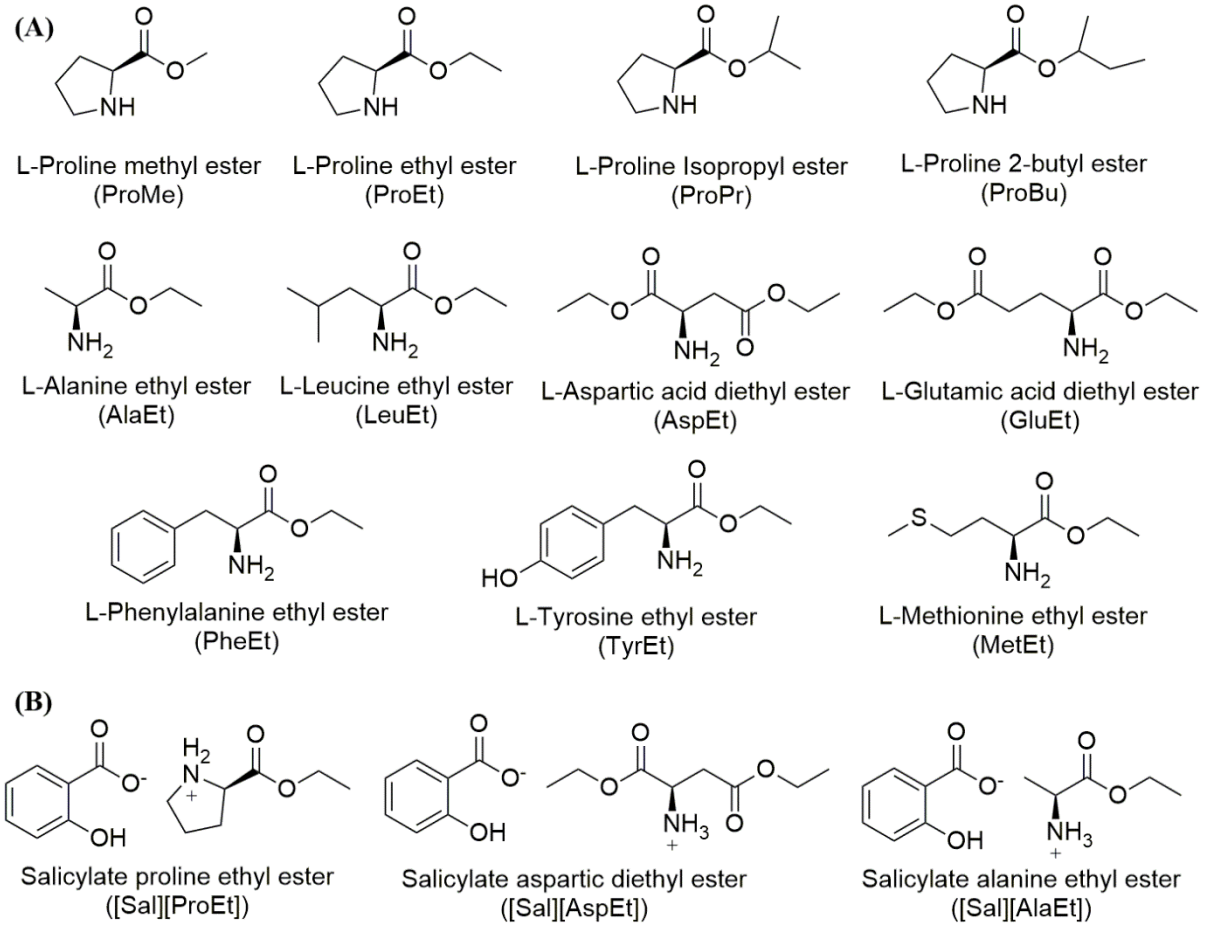

Figure 2.1. Structures, names, and abbreviations for (A) amino acid ester cations and (B) Sal-ILs used in this study.

2.3. Experimental

2.3.1. Materials

Salicylic acid (anhydrous, > 99% purity) was purchased from Sigma-Aldrich (Munich, Germany). L-Proline, L-alanine, L-leucine, L-aspartic acid, sodium salicylate, and thionyl

chloride with high purity (>98.0 %) were obtained from Wako Pure Chemical Industries Ltd. (Osaka, Japan). L-Glutamic acid, L-methionine, L-cysteine, L-tyrosine, and L-phenylalanine with high purity (>98.0 %) were purchased from Kishida Chemical Co. Ltd (Osaka, Japan). Methanol, ethanol, isopropanol, isobutanol, ammonia solution, diethyl ether, sodium chloride, and octanol were purchased from Wako Pure Chemicals Industries. All reagents, solvents, and other materials were of analytical grade and were used without any further purification.

Gibco minimum essential media (MEM), Opti-MEM, fetal bovine serum, and antibiotic-antimycotic were purchased from Thermo Fisher Scientific (Waltham, MA, USA). Dulbecco's phosphate buffered saline and trypsin/ethylenediaminetetraacetic acid (0.25% trypsin/1 mM ethylenediaminetetraacetic acid) were purchased from Nacalai Tesque (Kyoto, Japan). A WST-8 cell counting kit containing 2-(2-methoxy-4-nitrophenyl)-3-(4-nitrophenyl)-5-(2,4-disulfophenyl)-2H-tetrazolium monosodium salt was purchased from Dojindo Molecular Technologies, Inc. (Kumamoto, Japan). Mammalian cell lines L9292 and HeLa were provided by the RIKEN cell bank (Tsukuba, Japan).

2.3.2. General synthetic procedure for AAE

AAEs were synthesized using a slight modification of an established method[12]. Briefly, a suspension of 2.0 g of an amino acid in 20 mL of the required alcohol (e.g., methanol for methyl ester, ethanol for ethyl ester) was stirred vigorously in an ice bath. Then, thionyl chloride (mole ratio of thionyl chloride: amino acid = 1.5:1) was added dropwise to the slurry, and the mixture was kept on ice for 1 h. The resultant solution was stirred thoroughly for 24 h at room temperature and then concentrated under reduced pressure after completion of the reaction. The oily residue was dissolved in alcohol (10 mL) and the solvent was evaporated under reduced pressure to yield the AAE hydrochloride salt. Then, 10 mL of distilled water was added to the solution, followed by neutralization with ammonia solution (mole ratio of ammonia: AAE salt = 2:1). Diethyl ether (50 mL) was added, and the solution was stirred for 2 h at room temperature. The organic layer was extracted and concentrated under reduced pressure to yield the AAE. The yields of all the synthesized compounds were ≥ 72.0% (Table 2.S1). All the synthesized compounds were characterized by ^{1}H and ^{13}C nuclear magnetic resonance spectroscopy (NMR) and elemental analysis to check their structures and purities.

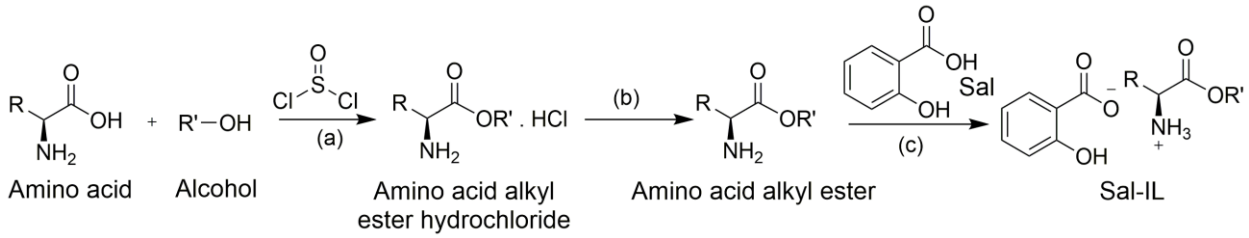

Scheme 2.1. General synthetic procedure for amino acid alkyl ester. (a) Thionyl chloride-mediated esterification in alcohol on ice for 1 h, and then at room temperature for 24 h; (b) ammonia solution and diethyl ether at room temperature for 2 h; and (c) in the dark at 40 °C for 2 h.

2.3.3. Synthesis of API-ILs

An equimolar mixture of the synthesized AAE (Section 2.2.2) and Sal was stirred thoroughly in the dark for 2 h at 40 °C (Scheme 2.1)[12]. The derived Sal-ILs were clear and colorless liquids, and their ionization and purities were evaluated using ^{1}H and ^{13}C NMR spectroscopy.

2.3.4. Measurements

All NMR measurements were recorded on a JEOL ECZ400S 400 MHz spectrometer (Tokyo, Japan) operating at 25 °C. Deuterated chloroform (2.0 ppm) or methanol (7.3 ppm) was used as the solvent, and tetramethylsilane as the internal standard. The NMR solvents were purchased from Wako Pure Chemical Industries Ltd. The coupling constants (*J*) are reported in Hertz (Hz). The same instrument was used to record ^{13}C NMR spectra with complete proton decoupling (deuterated chloroform, 76.8–77.5 ppm). The spectra were processed using the DeltaV software package (version 5.0.5.1, JEOL).

The purities of the synthesized compounds were calculated using the following equation:

Purity (%) = [Σ *I* (product)/Σ *I* (total)] × 100……. (2.1)

where, *I* represents the relative area of each signal[16].

The Fourier transform infrared (FT-IR) analyses of the Sal-ILs were carried out on a Perkin Elmer (Frontier FT/IR, Waltham, MA), in attenuated total reflectance mode. All spectra were obtained with accumulation of 20 scans in the wavenumber range 400–4000 cm^{-1}. Elemental analysis was carried out for quantitative analysis of carbon, hydrogen, and nitrogen in organic matter using a Yanaco CHNC MT-5 analyzer (Yanagimoto Seisakusho, Kyoto, Japan). Thermogravimetric analysis (TGA) was carried out on Hitachi High-Technologies TG/DTA 7300 (Tokyo, Japan). Samples weighing about 10 to 20 mg were analyzed in an alumina crucible using nitrogen as a purge gas. The sample analysis was conducted from 30 to 500 °C

using a constant heating rate of 5 °C min^{-1}. An isothermal hold at 70 °C for 30 min was performed to remove excess volatile solvents.

Characterization of L-Proline methyl ester

Yield 74.3%. Purity 99.2%. Clear colorless liquid. ^{1}H-NMR ($CDCl_3$, 400 MHz, TMS) δ ppm: 1.90-1.72 (m, 3H), 2.18-2.09 (m, 1H), 2.94-2.89 (m, 1H), 3.11-3.05 (m, 1H), 3.79-3.70 (m, 4H). ^{13}C-NMR ($CDCl_3$, 400 MHz, TMS) δ ppm: 25.56, 30.27, 47.06, 52.12, 59.66, 76.86, 77.17, 77.49, 175.98. Elemental analysis: Found: C, 55.8; H, 8.5; N, 10.7%. Calc. for $C_6H_{11}NO_2$: C, 55.8; H, 8.6; N, 10.8%.

Characterization of L-Proline ethyl ester

Yield 76.4%. Purity 98.2%. Clear colorless liquid. ^{1}H-NMR ($CDCl_3$, 400 MHz, TMS) δ ppm: 1.28 (tt, J = 22.3, 7.2 Hz, 3H), 1.92-1.65 (m, 3H), 2.19-2.05 (m, 1H), 2.97-2.82 (m, 1H), 3.15-3.02 (m, 1H), 3.80-3.61 (m, 1H), 4.26-4.08 (m, 2H). ^{13}C-NMR ($CDCl_3$, 400 MHz) δ ppm: 14.21, 25.51, 30.28, 47.06, 59.79, 60.84, 76.89, 77.20, 77.52 and 175.48. Elemental analysis: Found: C, 58.15; H, 9.2; N, 9.8%. Calc. for $C_7H_{13}NO_2$: C, 58.7; H, 9.15; N, 9.8%.

Characterization of L-Proline Isopropyl ester

Yield 81.3%. Purity 97.0%. Clear colorless liquid. ^{1}H-NMR ($CDCl_3$, 400 MHz, TMS) δ ppm: 1.30-1.20 (m, 6H), 1.86-1.68 (m, 3H), 2.17-2.08 (m, 1H), 2.92-2.86 (m, 1H), 3.12-3.06 (m, 1H), 3.70 (dd, J = 8.7, 5.5 Hz, 1H), 5.07-5.01 (m, 1H). ^{13}C-NMR ($CDCl_3$, 400 MHz) δ ppm: 21.78, 25.49, 30.35, 47.08, 59.95, 68.19, 76.86, 77.17, 77.50 and 175.03. Elemental analysis: Found: C, 59.0; H, 9.5; N, 8.8%. Calc. for $C_8H_{15}NO_2$ 0.3 H_2O: C, 59.1; H, 9.7; N, 8.6%.

Characterization of L-Proline Isobutyl ester

Yield 79.1%. Purity 98.1%. Clear colorless liquid. ^{1}H-NMR ($CDCl_3$, 400 MHz, TMS) δ ppm: 0.90 (t, J = 7.3 Hz, 3H), 1.22 (dd, J = 6.2, 3.9 Hz, 3H), 1.88-1.50 (m, 5H), 2.18-2.08 (m, 1H), 2.93-2.87 (m, 1H), 3.12-3.06 (m, 1H), 3.74-3.70 (m, 1H), 4.92-4.84 (m, 1H). ^{13}C-NMR ($CDCl_3$, 400 MHz) δ ppm: 9.68, 19.42, 19.51, 25.50, 28.76, 28.82, 30.43, 30.47, 47.06, 47.11, 59.94, 60.06, 72.77, 76.85, 77.17, 77.49 and 175.21. Elemental analysis: Found: C, 63.0; H, 10.1; N, 8.1%. Calc. for $C_9H_{17}NO_2$: C, 63.1; H, 10.0; N, 8.2%.

Characterization of L-Alanine ethyl ester

Yield 83.6%. Purity 98.1%. Clear colorless liquid. ^{1}H-NMR ($CDCl_3$, 400 MHz, TMS) δ ppm: 1.34-1.21 (m, 6H), 3.53 (q, J = 7.2 Hz, 1H), 4.17 (q, J = 7.0 Hz, 2H). ^{13}C-NMR ($CDCl_3$, 400 MHz) δ ppm: 14.18, 20.65, 50.05, 60.80, and 176.59. Elemental analysis: Found: C, 49.7; H, 9.5; N, 11.5%. Calc. for $C_5H_{11}NO_2$ 0.2 H_2O: C, 49.7; H, 9.5; N, 11.6%.

Characterization of L-Leucine ethyl ester

Yield 72.8%. Purity 97.8%. Clear colorless liquid. ^{1}H-NMR ($CDCl_3$, 400 MHz, TMS) δ ppm:

0.94 (t, J = 7.1 Hz, 6H), 1.28 (t, J = 7.1 Hz, 3H), 1.45-1.38 (m, 1H), 1.59-1.53 (m, 1H), 1.84-1.73 (m, 1H), 3.45 (dd, J = 8.5, 5.7 Hz, 1H), 4.20-4.13 (m, 2H). ^{13}C-NMR ($CDCl_3$, 400 MHz) δ ppm: 14.29, 21.90, 23.04, 24.81, 44.19, 52.94, 60.77, 76.80, 77.12, 77.43, and 176.77. Elemental analysis: Found: C, 60.3; H, 10.7; N, 8.8%. Calc. for $C_8H_{17}NO_2$: C, 60.35; H, 10.8; N, 8.8%.

Characterization of L-Aspartic diethyl ester

Yield 82.1%. Purity 97.6%. Clear colorless liquid. ^{1}H-NMR ($CDCl_3$, 400 MHz, TMS) δ ppm: 1.36-1.19 (m, 6H), 2.87-2.63 (m, 2H), 3.86-3.75 (m, 1H), 4.27-4.10 (m, 4H). ^{13}C-NMR ($CDCl_3$, 400 MHz) δ ppm: 14.16, 39.06, 51.28, 61.01, 77.20, 171.21, and 174.24. Elemental analysis: Found: C, 50.8; H, 8.0; N, 7.4%. Calc. for $C_8H_{15}NO_4$: C, 50.8; H, 8.0; N, 7.4%.

Characterization of L-Glutamic diethyl ester

Yield 78.5%. Purity 98.1%. Clear colorless liquid. ^{1}H-NMR ($CDCl_3$, 400 MHz, TMS) δ 1.32-1.24 (m, 6H), 1.84 (td, J = 14.9, 6.9 Hz, 1H), 2.12-2.04 (m, 1H), 2.48-2.40 (m, 2H), 3.46 (dd, J = 8.5, 5.3 Hz, 1H), 4.25-4.11 (m, 4H). ^{13}C-NMR ($CDCl_3$, 400 MHz) δ 14.22, 29.78, 30.65, 53.79, 60.43, 60.97, 76.87, 77.18, 77.50, 173.15, 175.6. Elemental analysis: Found: C, 53.2; H, 8.4; N, 6.9%. Calc. for C9H17NO4: C, 53.2; H, 8.4; N, 6.9%.

Characterization of L-Phenylalanine ethyl ester

Yield 87.6%. Purity 98.3%. Clear colorless liquid. ^{1}H-NMR (CD_3OD, 400 MHz, TMS) δ ppm: 1.24 (t, J = 7.3 Hz, 3H), 2.86 (dd, J = 13.3, 7.8 Hz, 1H), 3.08 (dd, J = 13.5, 5.3 Hz, 1H), 3.71 (dd, J = 7.8, 5.5 Hz, 1H), 4.16 (q, J = 7.2 Hz, 2H), 7.32-7.19 (m, 5H). ^{13}C-NMR ($CDCl_3$, 400 MHz) δ ppm: 14.25, 41.24, 55.98, 60.95, 76.91, 77.23, 77.55, 126.77, 126.89, 128.54, 129.31, 129.47, 137.41, and 175.10. Elemental analysis: Found: C, 68.5; H, 7.85; N, 7.2%. Calc. for $C_{11}H_{15}NO_2$: C, 68.4; H, 7.8; N, 7.25%.

Characterization of L-Methionine ethyl ester

Yield 79.0%. Purity 98.0%. Clear colorless liquid. ^{1}H-NMR ($CDCl_3$, 400 MHz, TMS) δ ppm: 1.29 (t, J = 7.1 Hz, 3H), 1.80 (dt, J = 22.0, 6.9 Hz, 1H), 2.08-2.00 (m, 1H), 2.11 (s, 3H), 2.63 (dd, J = 8.5, 6.6 Hz, 2H), 3.57 (dd, J = 8.2, 5.0 Hz, 1H), 4.19 (q, J = 7.2 Hz, 2H). ^{13}C-NMR ($CDCl_3$, 400 MHz) δ ppm: 14.26, 15.39, 30.52, 34.03, 53.38, 53.42, 60.99, 76.89, 77.21, 77.53, and 175.78. Elemental analysis: Found: C, 47.2; H, 8.6; N, 7.9%. Calc. for $C_7H_{15}NO_2S$: C, 47.4; H, 8.5; N, 7.9%.

Characterization of L-Tyrosine ethyl ester

Yield 95.4%. Purity 98.7%. Solid powder. ^{1}H-NMR ($CDCl_3$, 400 MHz) δ ppm: 1.27 (t, J = 7.3 Hz, 3H), 2.82 (dd, J = 13.7, 7.8 Hz, 1H), 3.04 (dd, J = 13.7, 5.0 Hz, 1H), 3.74-3.69 (m, 1H), 4.19 (q, J = 7.2 Hz, 2H), 6.67 (td, J = 5.7, 3.7 Hz, 2H), 7.00 (dt, J = 9.1, 2.4 Hz, 2H). ^{13}C-NMR

($CDCl_3$, 400 MHz) δ ppm: 14.28, 39.72, 55.55, 61.36, 76.82, 77.15, 77.46, 115.89, 127.67, 130.45, 155.64, and 174.88. Elemental analysis: Found: C, 63.2; H, 7.2; N, 6.7%. Calc. for $C_9H_{17}NO_4$: 63.4; H, 7.2; N, 6.7%.

Characterization of salicylic acid

^{1}H-NMR ($CDCl_3$, 400 MHz, TMS) δ ppm: 7.03-6.93 (m, 2H), 7.56-7.51 (m, 1H), 7.94 (dd, J = 7.8, 1.8 Hz, 1H), 10.37 (s, 1H)

Characterization of salicylate proline ethyl ester

^{1}H-NMR ($CDCl_3$, 400 MHz, TMS) δ ppm: 1.26-1.20 (m, 3H), 2.44-1.99 (m, 4H), 3.51-3.37 (m, 2H), 4.20 (q, J = 7.2 Hz, 2H), 4.48-4.43 (m, 1H), 6.78-6.76 (m, 1H), 6.85 (d, J = 8.2 Hz, 1H), 7.33-7.28 (m, 1H), 7.86-7.83 (m, 1H). ^{13}C-NMR ($CDCl_3$, 400 MHz, TMS) δ ppm: 14.04, 24.01, 29.09, 45.68, 58.97, 62.72, 76.85, 77.16, 77.48, 116.74, 117.84, 118.10, 130.61, 133.40, 161.71, 170.03, 175.36.

2.3.5. Partitioning coefficient determination

The synthesized Sal-ILs were characterized by measuring the log *P* in octanol and water. Free Sal (2–3 mg) containing Sal-ILs was mixed with 5 mL of water and 5 mL of octanol. The mixtures were left overnight at room temperature with constant shaking in the dark. Then, each solution was centrifuged at 9100g for 30 min to separate the water and octanol layers. The concentration of Sal in each layer was quantified by ultraviolet–visible spectroscopy (V-750, JASCO, Tokyo, Japan) with known concentrations of standards at 297 nm. The partition coefficient, log $P_{o/w}$, was determined using the following equation:

$$\log P_{o/w} = \log (Solute_{octanol}/Solute_{water}) \quad (2.2)$$

where, $Solute_{octanol}$ and $Solute_{water}$ represent the concentration of free Sal dissolved in octanol and water, respectively.

2.3.6. Water miscibility determination

A viscous sample of Sal-IL (0.7215 g of [Sal][ProEt] containing 0.3565 g of free Sal) was mixed with 0.3 mL of water in a transparent glass tube. A clear solution without a precipitate was obtained after shaking for a few minutes. Then, the liquid phase was filtered using 0.2 µm syringe filter to remove the remaining any particles. The concentration of Sal was quantified by ultraviolet–visible spectroscopy (V-750, JASCO, Tokyo, Japan) with known concentrations of standards at 297 nm.

2.3.7. In vitro cytotoxicity evaluation

The WST cell viability assay was conducted using mammalian cell lines L9292 and HeLa as described in the literature, with some modifications[12]. The cells were cultivated until reaching approximately 70% monolayer and trypsinized to collect the cells from the cell culture dish. Then, the cells were seeded into 96-well flat-bottomed plates at 5000 cells/well and cultured in MEM (containing 10 % fetal bovine serum and 1% antibiotic-antimycotic) for 24 h at 37 °C in a CO_2 incubator. AAEs were dissolved in Opti-MEM at concentrations in the range 1–200 mM. For Sal-ILs and free Sal, the concentration range was 0.001–40 mM because of the limited water solubility of free Sal. One hundred microliters of each sample solution was replaced with the medium in each well, and the plates were incubated for 24 h. After incubation, the solution was removed from each well, and the wells were rinsed twice with Dulbecco's phosphate-buffered saline. Then, 100 µL of Opti-MEM containing 10 µL of WST assay reagent from the cell counting kit was added to each well to measure the mitochondrial activity of the cells. After incubation for 3 h at 37 °C in a CO_2 incubator, the absorbance of the supernatant at 450 nm ($A_{treated}$) was measured using a microplate spectrophotometer (Bio-Rad, Tokyo, Japan). The absorbance of cells soaked in Opti-MEM medium without AAEs or Sal-ILs was used as a control ($A_{control}$). The cytotoxicity is expressed as the relative cell viability, and was calculated using the following equation:

$$\text{Cell viability (\%)} = (A_{treated}/A_{control}) \times 100 \quad (2.3)$$

All tests were repeated three times and the average values are reported. Statistical analysis of the data was performed using Microsoft Excel 2016 (Microsoft, Washington, USA). The half maximal inhibitory concentration (IC_{50}) was calculated for each cation and Sal-IL. Data are present as the mean with the standard deviation.

2.3.8. Skin permeation study

Skin permeation tests were carried out using a temperature controlled Franz diffusion cell[12]. Phosphate buffer solution was used to dilute the samples. The buffer solution was prepared by mixing 8 g/L of NaCl, 0.2 g/L of KCl, 2.9 g/L of Na_2HPO_4 and 0.2 g/L of KH_2PO_4, respectively. Then, the pH of buffer solution was adjusted to 7.4 with NaOH or HCl solution.

Shoulder skin of a female Yucatan micro pig (Charles River Japan Inc., Tokyo, Japan) was used for this study. The fat layer was carefully removed from the skin, and then the skin was cut into small pieces and placed in the Franz diffusion cell with the inside of the skin facing the receptor phase. The receptor phase was 5 mL of phosphate solution with constant stirring

at 32.5 °C. [Sal][Na] and Sal-IL solutions were prepared using the diluent. Then, a 0.3 mL aliquot of each sample solution, with an approximate concentration of 3.2 μmol/cm2, was applied on the outside of skin (donor phase). The donor chamber was covered with parafilm to minimize adsorption of water from the atmosphere. Aliquots (0.1 mL) of the receiving phase were withdrawn at fixed intervals for 60 h. After each sampling, 0.1 mL of fresh diluent was added to maintain a constant volume in the receiving chamber.

The withdrawn samples were diluted and the concentration of Sal was quantified using high performance liquid chromatography (HPLC) after calibration with known concentrations of free Sal standard at 245 nm.

2.3.9. Statistical Analysis

Statistical analysis was performed using GraphPad Prism version 6 software (GraphPad Software, Inc., La Jolla, CA). Statistical significance was evaluated by one-way analysis of variance (ANOVA) followed by Tukey's post hoc test for multiple comparisons.

2.4. Results and discussion

2.4.1. Synthesis, characterization, and cytotoxicities of the AAEs

2.4.1.1. Synthesis and characterization of the AAEs

We selected several natural, aromatic, aliphatic, sulfur-containing, and acidic amino acids (proline, alanine, aspartic acid, glutamic acid, leucine, methionine, phenylalanine, and tyrosine) that reportedly have low toxicities[10,11], and used them to prepare AAEs (Figure 2.1A, Scheme 2.1a and 2.1b). To investigate the role of cation alkyl chain length in toxicity, we synthesized proline-based AAEs with various alkyl chain lengths (C1–C4) (Figure 2.1A). The synthesized AAEs were clear and colorless liquids at room temperature, and were all water miscible except for L-tyrosine ethyl ester (Figure 2.S1). The purities of all the isolated compounds determined using ^{1}H NMR were ≥ 97.0%[16]. Elemental analysis of the synthesized compounds confirmed the structures of the AAEs.

2.4.1.2. Cytotoxicities of the AAEs

The mammalian cell lines L929 and HeLa were used to investigate the cytotoxicities of the synthesized AAE-based cations (Figure 2.1A). Before comparing the cytotoxicities of the AAEs, we adjusted the pH of the AAEs containing medium to 7.4 using HCl because the pH increased on addition of AAEs, in which the –COOH groups were esterified to –COOR groups

and the amino acids were transformed to basic AAE compounds. In all cases, the IC_{50} values of the AAEs solutions (without pH control) were higher than those with pH control (Figure 2.S2). The lipophilicity of each AAE increased in the solutions with pH control because a higher degree of protonation enhanced the penetration rate into the cell membrane, which disrupted the cell structure[17].

First, we evaluated the effect of the alkyl chain length on cytotoxicity using proline-based cations at pH 7.4. Both cell lines were treated with different doses of proline-based ester cations with methyl (C_1), ethyl (C_2), isopropyl (C_3), and isobutyl (C_4) substituents (Figure 2.S3). The IC_{50} values were calculated by a mathematical logarithm function (Figure 2.2A). The IC_{50} values of L-proline methyl ester, L-proline ethyl ester (ProEt), L-proline isopropyl ester, and L-proline isobutyl ester (ProBu) were 17.6, 18.3, 6.5 and 2.9, respectively, in L929 cells. The corresponding values in HeLa cells were 38.9, 44.8, 33.4 and 15.2 mM. The toxicities of the cations depended on the alkyl chain length in the ester group. The cation toxicity increased with increasing alkyl chain length from C_2 to C_4. Among all the cations in both cell lines, the lowest IC_{50} (highest toxicity) was obtained for ProBu because of the strong interaction between the lipophilic long alkyl chain of ProBu and the plasma cell membrane[18]. This interaction has been proven by an integrated experimental and computational approach[19]. Generally, the hydrophobic or lipophilic nature of an IL increases with increasing alkyl chain length in the cation. High hydrophobicity leads to interaction with the lipid bilayer of biological membranes and enhances the penetration of cations into the cell membrane. Consequently, the lipid bilayer becomes swollen and the cell membrane physiological functions are disrupted, ultimately leading to cell death[2,18,19]. By contrast, ProEt showed low cytotoxicity because of its short alkyl chain, which resulted in weak interactions with the cell membrane and increased mobility of the cation in the medium[20]. L-Proline methyl ester showed relatively high toxicity compared with ProEt. A similar result was found in toxicity studies of L-leucine methyl ester and L-leucine ethyl ester (LeuEt) in Natural killer (NK) cells[21] and sophorolipid derivatives in human pancreatic cancer (HPAC) cells[22]. Further studies are needed to define the precise mechanisms involved. However, our results showed that ethyl ester-based amino acid cations had lower toxicities than cations with other alkyl chain lengths.

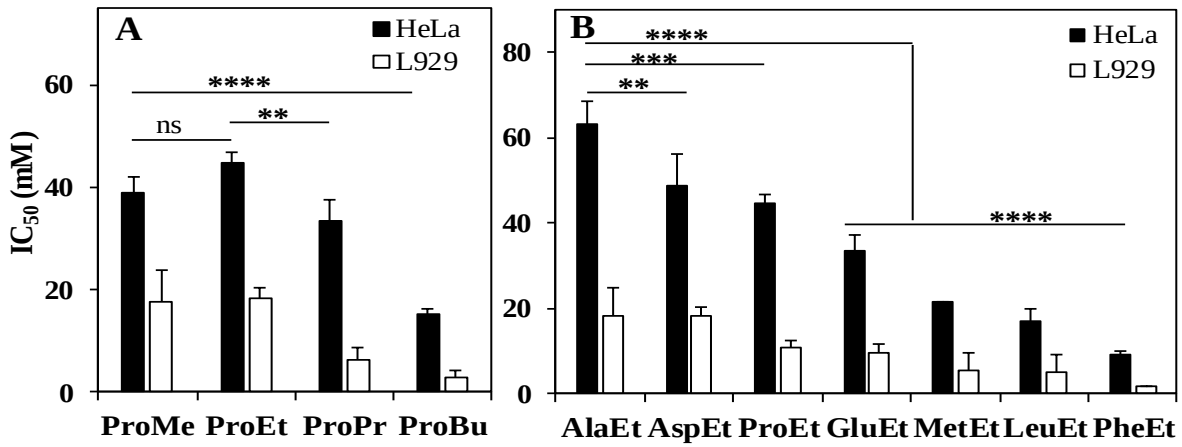

Figure 2.2. Cytotoxicities of AAEs towards L929 and HeLa cell lines at pH 7.4. Effect of (A) alkyl chain length derived from alcohols, and (B) side chains derived from amino acids. n = 3, mean ± SD, ns for non-significant, ** for $P < 0.01$, *** for $P < 0.001$, **** for $P < 0.0001$.

Next, we evaluated the influence of the amino acid side chain on cytotoxicity using ethyl ester-based AAEs (Figure 2.2B and Figure 2.S4). High toxicity was observed when the cation contained sulfur, a long alkyl chain, and an aromatic ring. L-Alanine ethyl ester (AlaEt) showed lower toxicity than the other AAEs in both cell lines because of the short carbon chain in its structure. If the number of carbons increased in the cation structure, the cytotoxicity gradually increased. For example, LeuEt and L-glutamic acid diethyl ester showed higher toxicities than AlaEt and L-aspartic acid diethyl ester (AspEt), respectively. These results are similar to those reported by[10,11]. The hydrophobic/lipophilic nature of ILs in solutions reportedly increases with increasing carbon chain length or the presence of functional groups in the cation core[2,11], and the cytotoxicities of ILs depend on the cation molecular weight[2,23]. ProEt also showed lower toxicity than the other cations. The presence of a cyclic secondary amine in the proline structure could reduce the toxicity because of the higher basicity of the secondary amine compared with that of the primary amine. Among all the AAE cations, L-phenylalanine ethyl ester showed the lowest IC_{50} in both cell lines because of the presence of an aromatic ring in the cation. This high cytotoxicity of PheEt could be attributed to a strong π-π interaction between the cation and the cell membrane, leading to rapid disruption of the cell structure[10].

2.4.2. Synthesis, characterization, and cytotoxicities of the Sal-ILs

2.4.2.1. Synthesis and characterization of the Sal-ILs

AAE-based API-ILs were synthesized by ionization of a poorly water-soluble drug (Sal) and AAEs with relatively low cytotoxicities (AlaEt, ProEt, and AspEt). All API-ILs were clear and

colorless liquids. The results of ^{1}H NMR analysis showed the stoichiometry between the two constituents for the [Sal][ProEt] compounds was 1:1 (Figure 2.3). The acidic proton of Sal (-COOH peak at approximately 10.37 ppm in Figure 2.3B) was absent in the Sal-IL spectra (Figure 2.3C), and a new broad peak was detected at 8.96 ppm, which corresponded to the protonated amine group. These results indicated that all of the Sal and ProEt were converted into [Sal][ProEt].

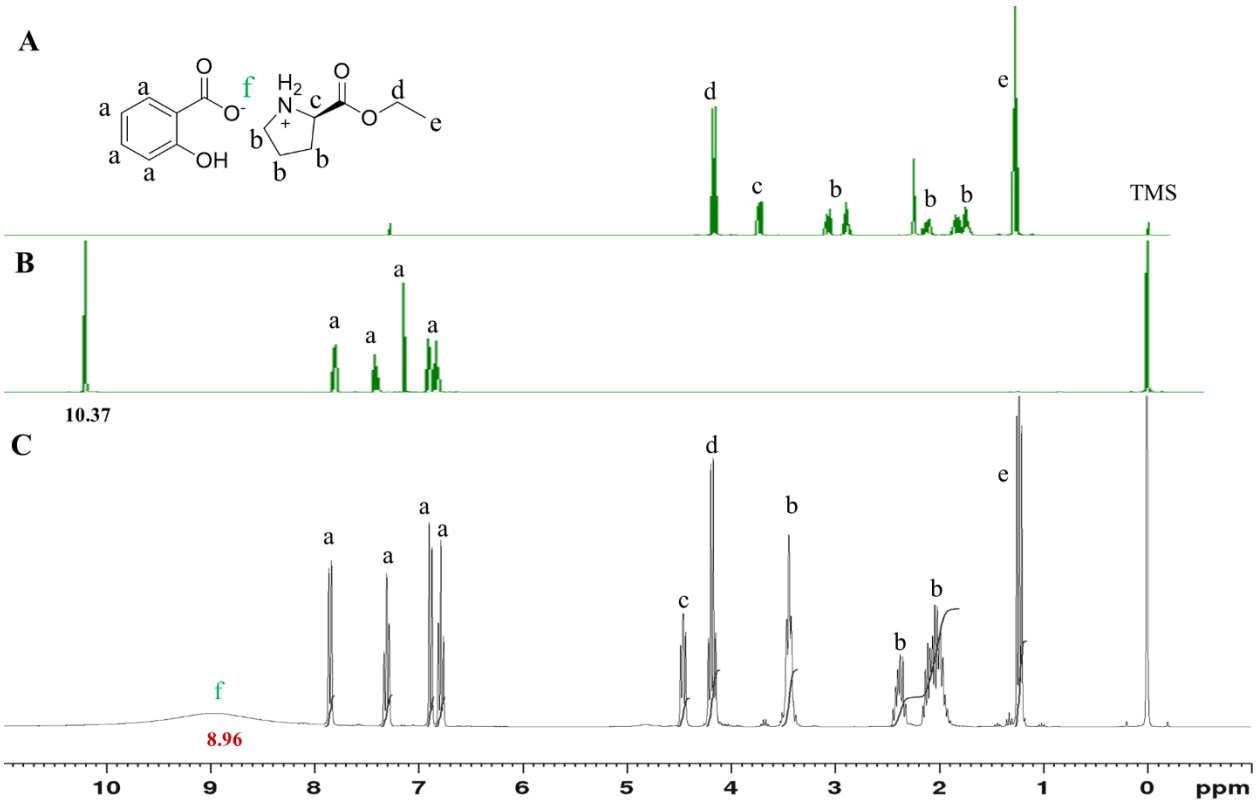

Figure 2.3. ^{1}H NMR spectra of ProEt (A), free Sal (B), and [Sal][ProEt] (C).

To further characterize the Sal-ILs, we obtained a FT-IR spectrum of [Sal][AspEt] and compared it to FT-IR spectra of AspEt, free Sal, and [Sal][Na] (Figure 2.4). In the FT-IR spectrum of [Sal][AspEt], characteristic peaks were observed at 1668 cm^{-1} and 1609 cm^{-1} for C=O stretching of –COOH groups and C=C stretching of the Sal benzene ring, respectively. In the [Sal][Na] spectrum, these peaks shifted slightly to 1650 cm^{-1} and 1615 cm^{-1}. Another characteristic peak was observed at 1731 cm^{-1} for C=O stretching of –COOR groups of AspEt, and this shifted to 1727 cm^{-1} in [AspEt]. An ethyl group C-H stretching peak was observed at 2982 cm^{-1} in the [Sal][AspEt] spectrum and attributed to the ethyl group of AspEt. A broad peak at 3241 cm^{-1} for the –OH group of Sal was not observed in the spectrum of [Sal][AspEt]

or [Sal][Na]. Another characteristic peak at 3384 cm^{-1} for N-H bending of the primary amine in AspEt was absent in the [Sal][AspEt] spectrum. However, a weak shoulder peak appeared at 1592 cm^{-1}, and this could be assigned to C=O and $–NH_2$ stretching. A similar weak shoulder peak at 1582 cm^{-1} was observed in the spectrum of [Sal][Na].

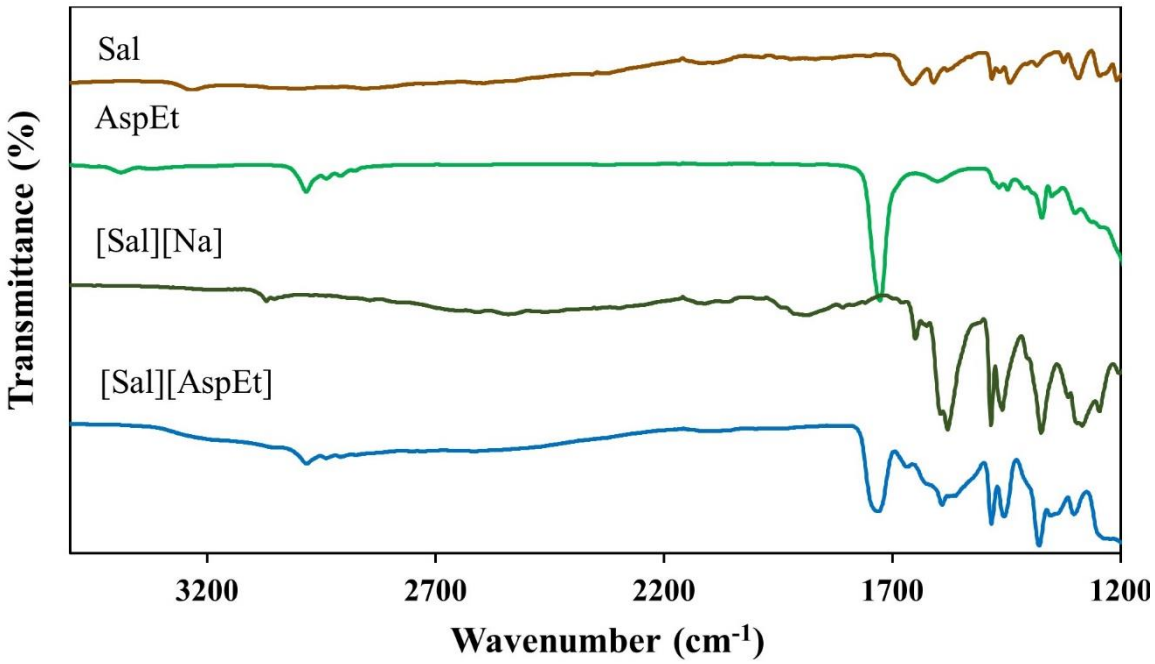

Figure 2.4. FT-IR spectra of free Sal, AspEt, [Sal][AspEt], and [Sal][Na].

Thermal stability is important for ILs and mainly depends on the chemical structure. The thermal stabilities of the synthesized Sal-ILs were investigated by TGA, and we measured the onset ($T_{5\%onset}$) temperatures (Table 2.1 and Figure 2.5). When Sal was used as the anion, the thermal stabilities of the Sal-ILs depended on the cation structures. Thermal decomposition ($T_{5\%\ onset}$) of [Sal][ProEt], [Sal][AlaEt], and [Sal][AspEt] occurred at 125.7 °C, 126.1 °C, and 136.4 °C, respectively, whereas the value previously reported for Sal was 162 °C ($T_{5\%\ onset}$)[16]. Therefore, the synthesized Sal-ILs showed lower thermal stability than free Sal, but all of the compounds decomposed at temperatures above 100 °C. [Sal][AspEt] had higher thermal stability than [Sal][ProEt] and [Sal][AlaEt] because of the high van der Waals forces between the alkyl side chains of [Sal][AspEt][24].

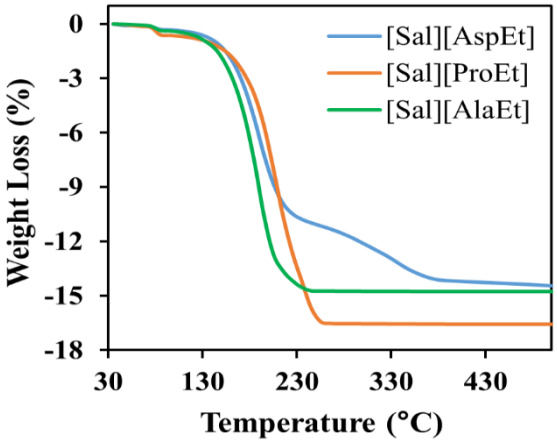

Figure 2.5. Thermogravimetric analysis of [Sal][AspEt], [Sal][ProEt], and [Sal][AlaEt].

However, the solubility of Sal greatly increased in the IL form. The Sal-ILs were miscible with water at any ratio (Table 2.1 and Figure 2.6), whereas free Sal is only slightly water-soluble (2.2 g/L)[25].

Table 2.1. Physical properties and water miscibility of Sal-ILs at room temperature.

Compound	Appearance	$T_{5\%\ onset}$ (°C)	Estimated solubility in water	
			g Sal-IL/ 0.3 mL	g active/ mL
[Sal][ProEt]	Clear colorless liquid	125.7	> 0.722[a]	> 1.130[a]
[Sal][AlaEt]		126.1	> 0.623[a]	>0.967[a]
[Sal][AspEt]		136.4	> 0.708[a]	> 0.958[a]
Sal	Crystalline solid	162[b]	-	0.0022[c]

[a] Estimated lower limit of solubility in water; [b] Data was obtained from[16]; [c] Data was obtained from[25].

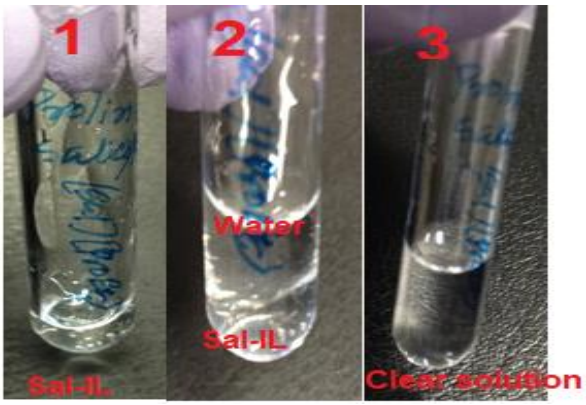

Figure 2.6. Water miscibility of Sal-ILs. 1: Sal-IL viscous sample in transparent glass tube. 2: Added water in Sal-IL sample, 3: Clear solution formed after shaking.

2.4.2.2. Cytotoxicities of the Sal-ILs

We investigated the cytotoxicities of the Sal-ILs synthesized from basic AAE cations and acidic Sal. The Sal in free acid form showed higher toxicity than the Sal-ILs, and the IC_{50} values were similar in both HeLa and L929 cell lines (Table 2.2). The cytotoxicities of the Sal-ILs were much higher than those of the AAEs, because Sal is a cytotoxin with a strong anticancer effect[25]. When cells were treated with Sal-ILs, hydrophilic cations reduced the lipophilicities of Sal-ILs and slightly reduced the toxicities of the Sal-ILs. In both cell lines, [Sal][AlaEt] is low cytotoxicity because of short alkyl chain in the side group on the AlaEt cation. Moreover, The hydrophilicity of [Sal][AlaEt] is higher than that of [Sal][AspEt] or [Sal][ProEt], which could reduce the penetration of Sal through cell membrane by decreasing the lipophilicity of the IL form (log $P_{o/w}$ in Table 2.2). Consequently, the cytotoxicities of the Sal-ILs and Sal were similar (Table 2.2).

Table 2.2. Cytotoxicities of the Sal-ILs towards L929 and HeLa cell lines with partitioning coefficient.

Compound	Log $P_{o/w}$	HeLa ($IC_{50,}$ mM)	L929 ($IC_{50,}$ mM)
[Sal][ProEt]	-0.40	4.2	4.1
[Sal][AlaEt]	-0.60	4.9	6.2
[Sal][AspEt]	-0.19	4.6	3.7
Sal	-	3.2	3.0

2.4.3. Skin permeation studies of Sal-ILs

To evaluate possible medical applications in a transdermal drug delivery, we investigated skin permeation of the Sal-ILs at 32.5 °C using a Franz diffusion cell system with the sodium salt of Sal in a PBS solution as a control. Transport of [Sal][Na] and Sal-ILs in the receiver phase was detected by HPLC analysis at regular intervals. The Sal-ILs easily permeated through the skin, at a speed approximately nine times that of [Sal][Na] (Figure 2.7). After 60 h, the cumulative transport of Sal-IL for [Sal][AspEt] was 0.18 mg/cm^2, whereas the transport of [Sal][Na] was 0.03 mg/cm^2. The differences between the neutral and ionized forms of Sal were similar to data from previous studies, which demonstrated that ionic species cannot easily permeate the skin barrier[16]. This difference in permeation also arises because [Sal][Na] is more hydrophilic (log $P_{o/w}$ of −1.5) than the Sal-ILs (log $P_{o/w}$ in Table 2.2). Therefore, it is difficult for [Sal][Na] to permeate through the skin compared with the Sal-ILs.

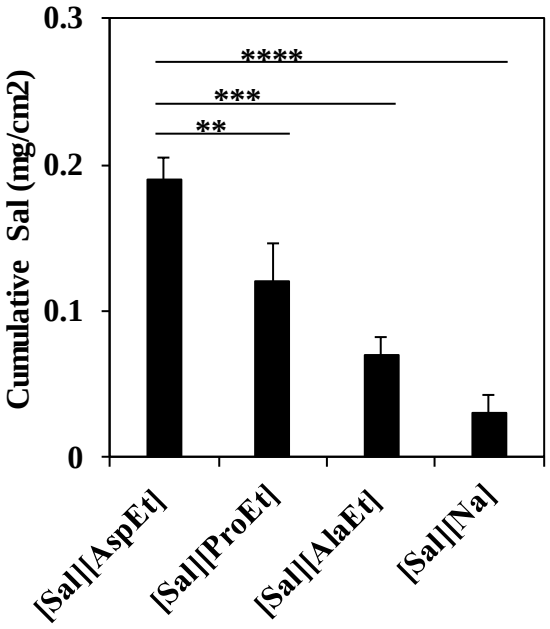

Figure 2.7. Skin permeation of Sal-ILs and [Sal][Na] after 60 h. n = 3, mean ± SD, ** for $P < 0.01$, *** for $P < 0.001$, **** for $P < 0.0001$.

Variation in skin permeation because of strong ion-pairing between a cation and an anionic drug was reported previously for ibuprofen and ProEt cations[24]. In that case, the speed of permeation of [ibuprofen][ProEt] through pig skin was 10 times that of free ibuprofen. However, among the synthesized Sal-ILs, the AspEt cation-based Sal-IL permeated the skin faster than either the ProEt or AlaEt cation-based Sal-IL. The cumulative amount of drug in the receiver phase for [Sal][AspEt] was approximately three times that of [Sal][AlaEt] and 1.5 times that of [Sal][ProEt] after 60 h. The presence of a long alkyl chain in the side group on the cation could enhance skin transport of Sal by increasing the lipophilicity of the IL form (log $P_{o/w}$ in Table 2.2).

2.5. Conclusions

We have demonstrated a new approach to develop API–ILs that are biocompatible and effectively penetration the skin. All synthesized compounds are clear and colorless liquids at room temperature, except for L-tyrosine ethyl ester, with high purities (> 97.0 %). Among the synthesized AAEs, AlaEt, AspEt, and ProEt had low cytotoxicities and were investigated as potential components for synthesis of Sal-ILs with the anionic drug Sal. All synthesized Sal-ILs were fully ionized and had high thermal stabilities. In contrast to Sal, the Sal-ILs show good solubility in aqueous media. When toxic Sal was incorporated into amino acid cations, the cytotoxicity decreased slightly. However, a skin permeation study demonstrated that skin

penetration of the Sal-ILs was approximately nine times faster than that of the sodium salt of Sal. The AspEt formulation showed better transport behavior than ProEt, AlaEt, and [Sal][Na]. We did not use any environmentally unfriendly reagents to increase the solubilities or enhance skin permeation of the Sal-ILs. Therefore, this API-IL technique can be used for effective formulation of poorly water-soluble drugs in an IL form, and it eliminates the use of traditional solvent vehicles for transdermal drug delivery.

2.6. References

[1] M. Rodriguez-Aller, D. Guillarme, J.L. Veuthey, R. Gurny, Strategies for formulating and delivering poorly water-soluble drugs, J. Drug Deliv. Sci. Technol. 30 (2015) 342–351. doi:10.1016/j.jddst.2015.05.009.

[2] K.S. Egorova, E.G. Gordeev, V.P. Ananikov, Biological Activity of Ionic Liquids and Their Application in Pharmaceutics and Medicine, Chem. Rev. 117 (2017) 7132–7189. doi:10.1021/acs.chemrev.6b00562.

[3] C.J. Martínez Rivas, M. Tarhini, W. Badri, K. Miladi, H. Greige-Gerges, Q.A. Nazari, S.A. Galindo Rodríguez, R.Á. Román, H. Fessi, A. Elaissari, Nanoprecipitation process: From encapsulation to drug delivery, Int. J. Pharm. 532 (2017) 66–81. doi:10.1016/j.ijpharm.2017.08.064.

[4] D.E. Peterson, C.B. Boers-Doets, R.J. Bensadoun, J. Herrstedt, Management of oral and gastrointestinal mucosal injury: ESMO Clinical Practice Guidelines for diagnosis, treatment, and follow-up, Ann. Oncol. 26 (2015) v139–v151. doi:10.1093/annonc/mdv202.

[5] M. Lotfi, M. Moniruzzaman, M. Sivapragasam, S. Kandasamy, M.I. Abdul Mutalib, N.B. Alitheen, M. Goto, Solubility of acyclovir in nontoxic and biodegradable ionic liquids: COSMO-RS prediction and experimental verification, J. Mol. Liq. 243 (2017) 124–131. doi:10.1016/j.molliq.2017.08.020.

[6] S. Araki, R. Wakabayashi, M. Moniruzzaman, N. Kamiya, M. Goto, Ionic liquid-mediated transcutaneous protein delivery with solid-in-oil nanodispersions, Medchemcomm. 6 (2015) 2124–2128. doi:10.1039/c5md00378d.

[7] K.S. Egorova, M.M. Seitkalieva, A. V. Posvyatenko, V.P. Ananikov, An unexpected increase of toxicity of amino acid-containing ionic liquids, Toxicol. Res. (Camb). 4 (2015) 152–159. doi:10.1039/C4TX00079J.

[8] M. Moniruzzaman, M. Tamura, Y. Tahara, N. Kamiya, M. Goto, Ionic liquid-in-oil microemulsion as a potential carrier of sparingly soluble drug: Characterization and

cytotoxicity evaluation, Int. J. Pharm. 400 (2010) 243–250. doi:10.1016/j.ijpharm.2010.08.034.

[9] N. Adawiyah, M. Moniruzzaman, S. Hawatulaila, M. Goto, Ionic liquids as a potential tool for drug delivery systems, Med. Chem. Commun. 7 (2016) 1881–1897. doi:10.1039/C6MD00358C.

[10] X.D. Hou, Q.P. Liu, T.J. Smith, N. Li, M.H. Zong, Evaluation of Toxicity and Biodegradability of Cholinium Amino Acids Ionic Liquids, PLoS One. 8 (2013). doi:10.1371/journal.pone.0059145.

[11] A. Yazdani, M. Sivapragasam, J.M. Leveque, M. Moniruzzaman, Microbial Biocompatibility and Biodegradability of Choline-Amino Acid Based Ionic Liquids, J. Microb. Biochem. Technol. 08 (2016) 415–421. doi:10.4172/1948-5948.1000318.

[12] S. Furukawa, G. Hattori, S. Sakai, N. Kamiya, Highly efficient and low toxic skin penetrants composed of amino acid ionic liquids, RSC Adv. 6 (2016) 87753–87755. doi:10.1039/C6RA16926K.

[13] S. a Megwa, S.E. Cross, H. a Benson, M.S. Roberts, Ion-pair formation as a strategy to enhance topical delivery of salicylic acid., J. Pharm. Pharmacol. 52 (2000) 919–928. doi:10.1211/0022357001774804.

[14] S.J. Bashir, F. Dreher, A.L. Chew, H. Zhai, C. Levin, R. Stern, H.I. Maibach, Cutaneous bioassay of salicylic acid as a keratolytic, Int. J. Pharm. 292 (2005) 187–194. doi:10.1016/j.ijpharm.2004.11.032.

[15] H. Magaña, K. Palomino, J.M. Cornejo-Bravo, L. Díaz-Gómez, A. Concheiro, E. Zavala-Lagunes, C. Alvarez-Lorenzo, E. Bucio, Polymeric prodrug–functionalized polypropylene films for sustained release of salicylic acid, Int. J. Pharm. 511 (2016) 579–585. doi:10.1016/j.ijpharm.2016.07.044.

[16] O. Zavgorodnya, J.L. Shamshina, M. Mittenthal, P.D. McCrary, G.P. Rachiero, H.M. Titi, R.D. Rogers, Polyethylene glycol derivatization of the non-active ion in active pharmaceutical ingredient ionic liquids enhances transdermal delivery, New J. Chem. 41 (2017) 1499–1508. doi:10.1039/C6NJ03709G.

[17] M. Kobayashi, T. Kagawa, R. Takano, S. Itagaki, T. Hirano, K. Iseki, Effect of medium pH on the cytotoxicity of hydrophilic statins, J. Pharm. Pharm. Sci. 10 (2007) 332–339.

[18] B. Jing, N. Lan, J. Qiu, Y. Zhu, Interaction of Ionic Liquids with a Lipid Bilayer: A Biophysical Study of Ionic Liquid Cytotoxicity, J. Phys. Chem. B. 120 (2016) 2781–2789. doi:10.1021/acs.jpcb.6b00362.

[19] B. Yoo, B. Jing, S.E. Jones, G.A. Lamberti, Y. Zhu, J.K. Shah, E.J. Maginn, Molecular

mechanisms of ionic liquid cytotoxicity probed by an integrated experimental and computational approach, Sci. Rep. 6 (2016) 2–8. doi:10.1038/srep19889.

[20] L.-S. Wang, L. Wang, L. Wang, G. Wang, Z.-H. Li, J.-J. Wang, Effect of 1-butyl-3-methylimidazolium tetrafluoroborate on the wheat (Triticum aestivum L.) seedlings., Environ. Toxicol. 24 (2009) 296–303. doi:10.1002/tox.

[21] M. Rabinovitch, V. Zilberfarb, C. Ramazeilles, Destruction of Leishmania mexicana amazonensis amastigotes within macrophages by lysosomotropic amino acid esters., J. Exp. Med. 163 (1986) 520–35. doi:10.1084/jem.163.3.520.

[22] S.L. Fu, S.R. Wallner, W.B. Bowne, M.D. Hagler, M.E. Zenilman, R. Gross, M.H. Bluth, Sophorolipids and Their Derivatives Are Lethal Against Human Pancreatic Cancer Cells, J. Surg. Res. 148 (2008) 77–82. doi:10.1016/j.jss.2008.03.005.

[23] B.D. Monnery, M. Wright, R. Cavill, R. Hoogenboom, S. Shaunak, J.H.G. Steinke, M. Thanou, Cytotoxicity of polycations: Relationship of molecular weight and the hydrolytic theory of the mechanism of toxicity, Int. J. Pharm. 521 (2017) 249–258. doi:10.1016/j.ijpharm.2017.02.048.

[24] K. Fukumoto, M. Yoshizawa, H. Ohno, Room temperature ionic liquids from 20 natural amino acids, J. Am. Chem. Soc. 127 (2005) 2398–2399. doi:10.1021/ja043451i.

[25] K.S. Egorova, M.M. Seitkalieva, A. V. Posvyatenko, V.N. Khrustalev, V.P. Ananikov, Cytotoxic Activity of Salicylic Acid-Containing Drug Models with Ionic and Covalent Binding, ACS Med. Chem. Lett. 6 (2015) 1099–1104. doi:10.1021/acsmedchemlett.5b00258.

APPENDIX 2.A- SUPPORTING MATERIALS

1. Photographs of synthesized amino acid esters

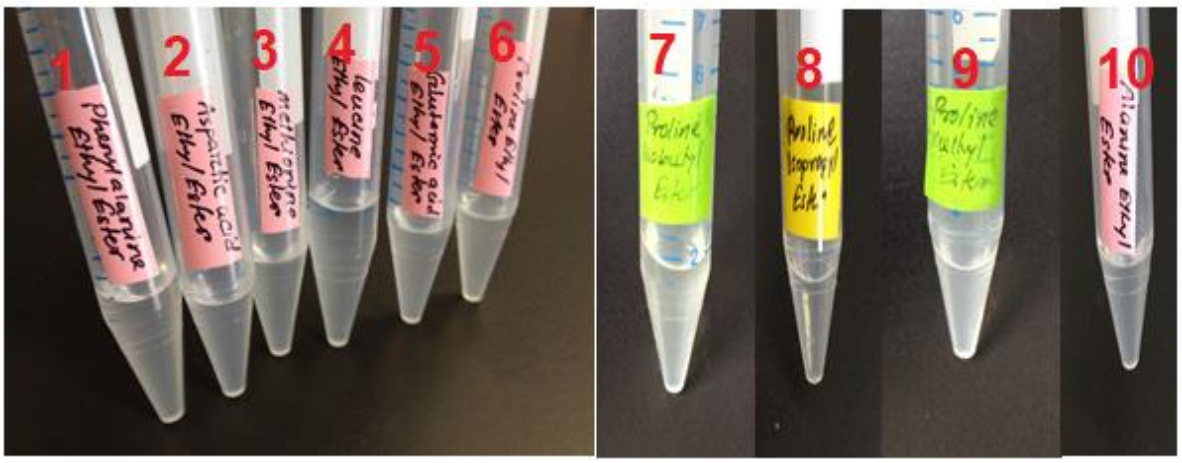

Figure 2.S1. Synthesized amino acid esters: Phenylalanine ethyl ester (1), Aspartic acid diethyl ester (2), Methionine ethyl ester (3), Leucine ethyl ester (4), Glutamic acid diethyl ester (5), Proline ethyl ester (6), Proline Isobutyl ester (7), Proline Isopropyl Ester (8), Proline methyl ester (9) and Alanine ethyl ester (10).

2. Effect of pH on cytotoxicity

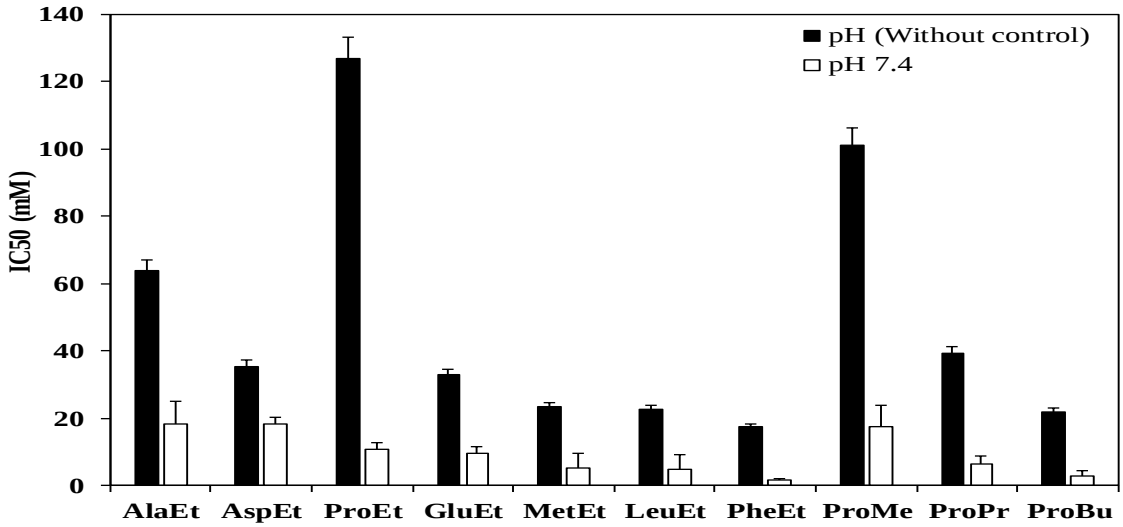

	AAEt									
	AlaEt	AspEt	ProEt	GluEt	MetEt	LeuEt	PheEt	ProMe	ProPr	ProBu
pH	8.9	9.0	9.8	8.7	8.5	9.0	8.1	9.8	9.7	9.5

Figure 2.S2. Cytotoxicity of AAE cations on L929 at with and without control pH 7.4. n = 3, mean ± SD.

3. Effect of alkyl chain length on cytotoxicity

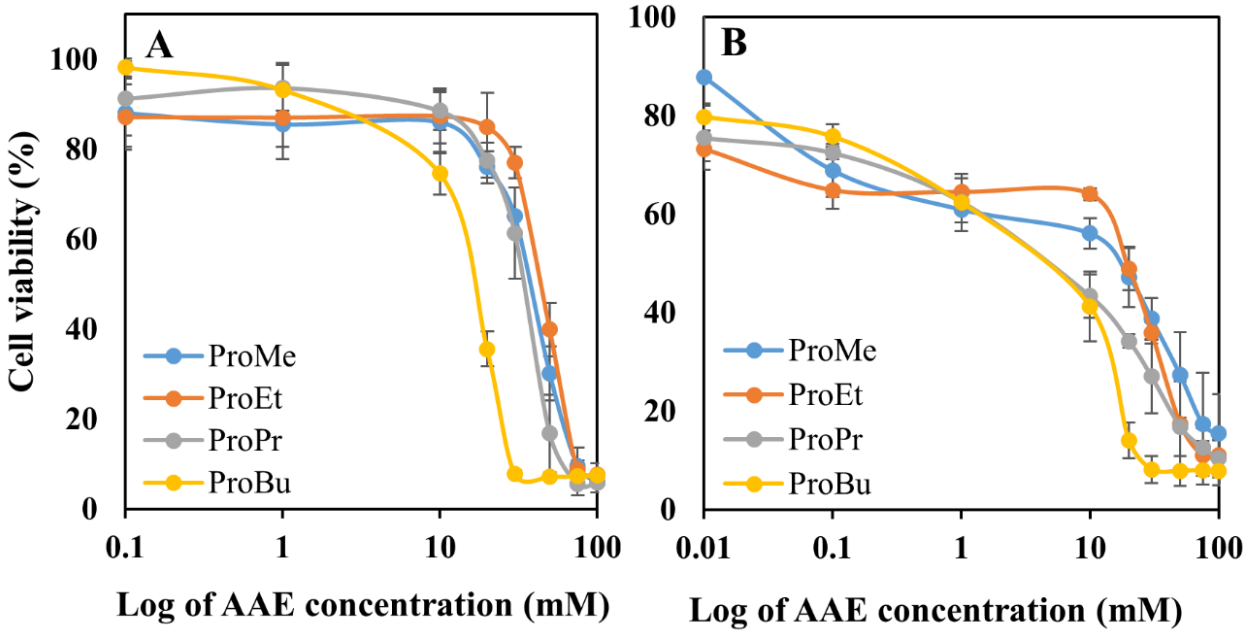

Figure 2.S3. Cytotoxicity of proline-based AAE cations on mammalian cell lines (A) HeLa and (B) L929. n = 3, mean ± SD.

4. Effect of amino acid side chains on cytotoxicity

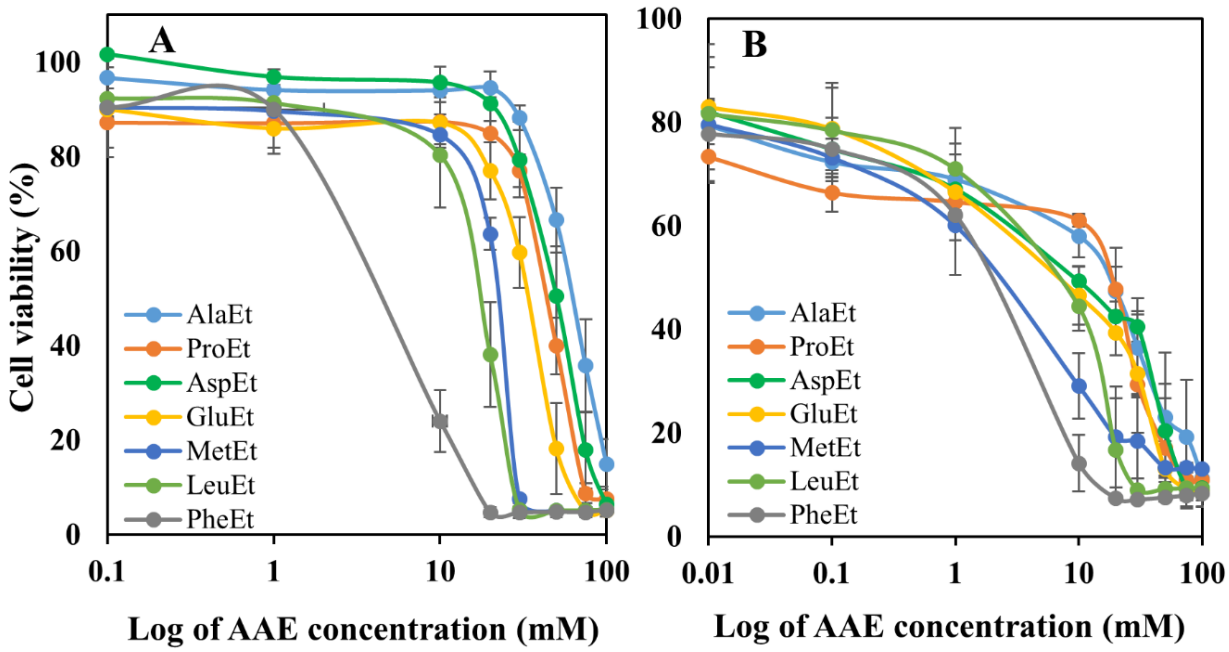

Figure 2.S4. Cytotoxicity of AAE cations on mammalian cell lines (A) HeLa and (B) L929. n = 3, mean ± SD.

CHAPTER 3: IONIC LIQUIDS WITH METHOTREXATE MOIETIES AS A POTENTIAL ANTICANCER DRUG: SYNTHESIS, CHARACTERIZATION AND SOLUBILITY EVALUATION

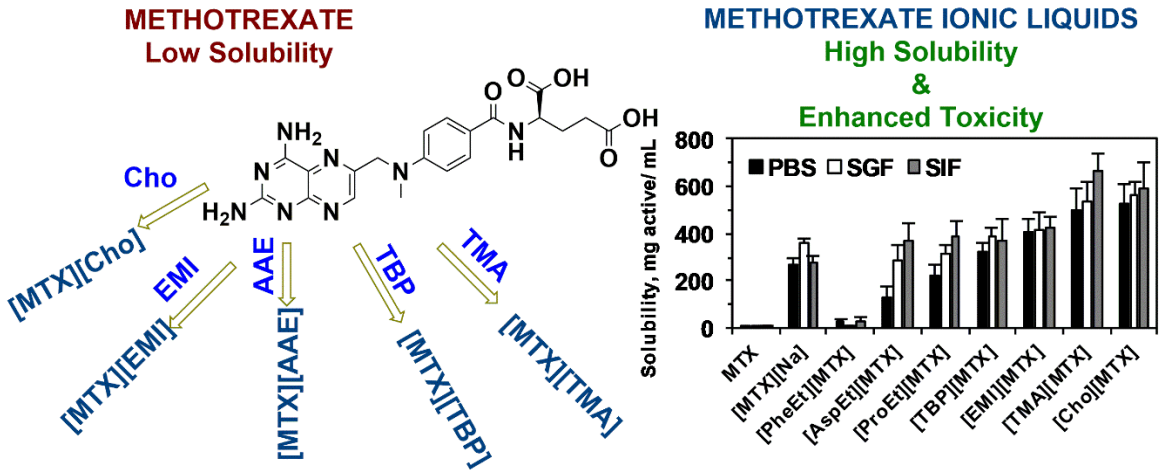

This chapter was partially published in Journal of Molecular Liquids 278 (**2019**) 226–233; https://doi.org/10.1016/j.molliq.2019.01.063 with permission of Elsevier.

3.1. Abstract

The technological utility of active pharmaceutical ingredients (APIs) is enormously improved when they are converted into ionic liquids (ILs). API-ILs possess better aqueous solubility and thermal stability than that of solid-state salt or crystalline drugs. However, many such API-ILs are not biocompatible or biodegradable. In the current study, we synthesized a series of IL-APIs using methotrexate (MTX), a potential anticancer drug, and biocompatible IL-forming cations (choline and amino acid esters). The MTX-IL moieties were characterized through ^{1}HNMR, FTIR, p-XRD, DSC and thermogravimetric analysis. The solubility of the MTX-ILs was evaluated in simulated body fluids (phosphate-buffered saline, simulated gastric, and simulated intestinal fluids). An assessment of the in vitro antitumor activity of the MTX-ILs in a mammalian cell line (HeLa cells) was used to evaluate their cytotoxicity. The MTX-ILs showed aqueous solubility at least 5000 times higher than that of free MTX and two orders of magnitude higher compared with that of a sodium salt of MTX in both water and simulated body fluids. Importantly, a proline ethyl ester MTX drug showed similar solubility as the MTX sodium salt but it provided improved in vitro antitumor activity. In pharmacokinetic study through oral administration, the MTX-ILs showed significantly higher pharmacokinetic parameters than that of sodium salt of MTX especially amino acid esters based ILs (AAE-MTX). The bioavailability of AAE-MTXs showed at least six times higher than that of sodium MTX. These results clearly suggest that the newly synthesized API-ILs represent promising potential drug formulations.

3.2. Introduction

The development of smart drug delivery systems for anticancer drugs has been a challenging task for pharmaceutical researchers because of their polymorphisms, lower solubility and bioavailability [1–4]. Currently, new anticancer drugs are developed to achieve maximum therapeutic efficacy with minimal possible side-effects through oral or parenteral administration [3]. However, most chemotherapeutic agents exhibit undesirable physico-chemical properties such as low water solubility, low permeability (barriers to drug delivery), a narrow therapeutic window and a short half-life, along with systemic side-effects [5]. To avoid severe adverse effects, pharmaceutical scientists are trying to design drug delivery formulations specifically to kill tumor cells only, with little or no adverse effects on healthy tissues or cells. Methotrexate (MTX) is a biopharmaceutical classification systems class IV drug and has been approved by the USA Food and Drug Administration (FDA) as a chemotherapeutic agent. MTX possesses low permeability (C log P = 0.53), poor aqueous

solubility (0.1 mg/mL) and poor bioavailability (only 18% for doses >40 mg/m^2) [6,7]. MTX is used clinically for the treatment of different types of cancer, rheumatoid arthritis, psoriasis, and other autoimmune diseases, and the induction of abortion (along with misoprostol) [6–9]. In general, MTX is absorbed by the gastrointestinal tract (GIT). The rate of absorption mainly depends on the drug dose [10]. For example, the therapeutic and toxic plasma concentration of MTX varies from low-dose therapy (0.005 and 0.001 µg/mL, respectively) to high-dose therapy (2.27 and 4.54 µg/mL, respectively) [11]. On the basis of this erratic GIT absorption, it has been suggested that high-dose therapy (>25 mg) should be administered orally or parenterally [7]. Although MTX tablets and injections were FDA approved in 1980, high-dose oral therapy could increase the risk of adverse effects, such as GI toxicity [12,13], because of poor MTX solubility and bioavailability [7]. The therapeutic effect of MTX is largely influenced by its low tumor cell uptake and therapeutic doses can cause severe side effects such as diarrhea and ulcerative stomatitis [13].

To address these limitations, an ionic liquid (IL) formulation of active pharmaceutical ingredients (APIs), such as MTX, is a promising technique to deliver drugs. Recently, ILs have been used extensively to form IL-API because they provide many advantages over solid or crystalline forms of drugs [14–16]. IL-APIs can also address the issue of polymorphisms, a significant problem in drug delivery. The combination of poorly water-soluble APIs with specific counter-ions is an excellent approach to upgrade conventional pharmaceuticals using an IL-based strategy [16]. This prodrug technique can eliminate the effect of drug polymorphisms or crystallinity, which is often responsible for reducing therapeutic efficiency, bioavailability and thermal stability [15–17]. Recently, Rogers groups demonstrated the successful application of an IL formulation to deliver the poorly soluble drug sulfasalazine and reported that solubility increased 4000 times and bioavailability was 2.5-fold higher compared with that of free drug [18]. Yoshiura et al. [19] described an IL-based microemulsion for the delivery of MTX and demonstrated that MTX penetration through pig skin increased dramatically. Moniruzzaman el al. [20] reported a novel imidazolium-based IL-in-oil microemulsion, in which MTX dissolved more efficiently than in water. However, an MTX-based API-IL, either as an anion or as a cation, has not previously been reported.

In the present study, we explored the use of the IL-API approach to solve the deficiencies of the solid drug MTX, by creating an MTX anion-based IL, and report the synthesis, characterization, solubility (both in aqueous and physiological fluids) and in vitro antitumor activity of the MTX-IL moieties.

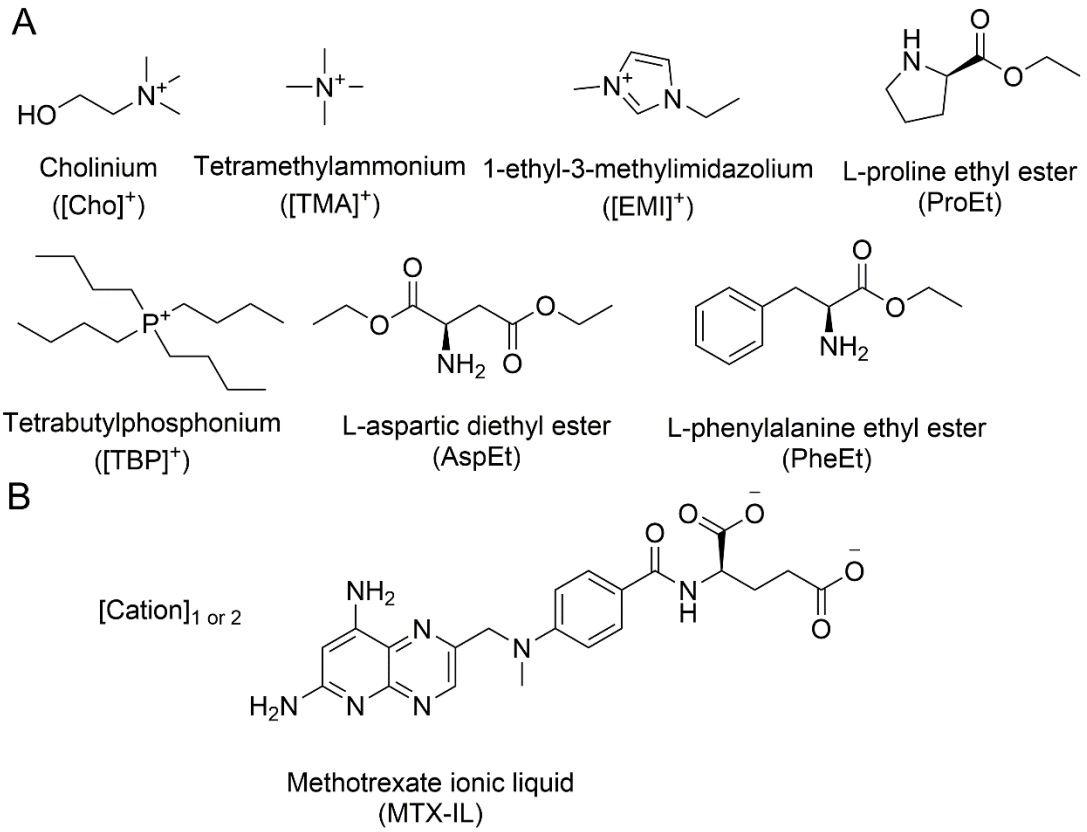

Figure 3.1. Structures, names, and abbreviations for the (A) IL-forming cations and (B) MTX-ILs used in this study.

3.3. Experimental

3.3.1. Materials

MTX (anhydrous, >98% purity) was purchased from Wako Chemicals Ltd. (Osaka, Japan). L-proline, L-aspartic acid, tetramethylammonium hydroxide (15% in water), and tetrabutyl-phosphonium hydroxide (40% in water) were obtained from Wako Chemicals Ltd. (Osaka, Japan). L-phenylalanine with a high level of purity (>98.0%) was purchased from Kishida Chemical Co. Ltd. (Osaka, Japan), and 1-ethyl-3-methylimidazolium chloride was purchased from TCI America (Tokyo, Japan). The concentrations of ammonium, phosphonium, choline and imidazolium were determined via titration. All other reagents, solvents and materials were of analytical grade and were used without any further purification. Gibco minimum essential media (MEM), Opti-MEM, fetal bovine serum, and antibiotic-antimycotic were purchased from Thermo Fisher Scientific (Waltham, MA, USA). Dulbecco's phosphate buffered saline (PBS) and 0.25% trypsin/1 mM ethylenediamine tetraacetic acid were obtained from Nacalai Tesque (Kyoto, Japan). A WST-8 (2-(2-methoxy-4-nitrophenyl)-3-(4-nitrophenyl)-5-(2,4-disulfophenyl)-2H-tetrazolium monosodium salt) cell counting kit was obtained from Dojindo

Molecular Technologies, Inc. (Kumamoto, Japan). The HeLa cell line was provided by the RIKEN cell bank (Tsukuba, Japan).

3.3.2. Animal models

Female C57BL/6NJc1 (C57BL/6) mice (7-9 weeks old, 19 ± 4 g) have been considered as a suitable model for evaluating the oral absorption of drug. Mice were purchased from CLEA Japan, Inc. and housed in our specific pathogen-free facility at natural light/dark conditions (Temp.: 25 ±2 °C & RH: 60 ± 10%) with free access to food and water. The mice are cared and handle according to the approved protocol by the Animal Ethics Committee of Kyushu University, Japan.

3.3.3. General synthetic procedure for cations

ProEt, AspEt and PheEt cations were synthesized according to previously reported procedure[2]. Briefly, 3.0 g of amino acid was suspended in 20 ml anhydrous ethanol and then thionyl chloride (mole ratio of thionyl chloride: amino acid = 1.5:1) was added dropwise to the slurry. The resultant mixture was kept on ice for 1 h and, then 24 h at room temperature under constant stirring. The excess solvent was evaporated under reduced pressure to yield the AAE hydrochloride salt. Then, distilled water was added to dissolve the salt and neutralized with ammonia solution (mole ratio of ammonia: AAE salt = 2:1). The organic layer was extracted using diethyl ether as solvent concentrated under reduced pressure to yield the AAE.

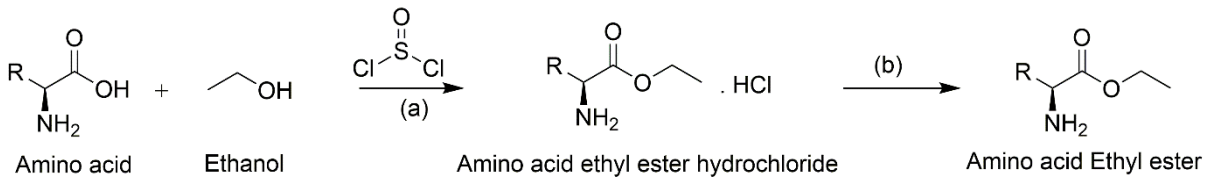

Scheme 3.1. General synthetic procedure for amino acid ethyl ester. (a) Thionyl chloride-interceded esterification in ethanol on ice for 1 h, and then at room temperature for 24 h; (b) ammonia solution and diethyl ether at room temperature for 2 h.

Choline hydroxide and 1-ethyl-3-methylimidazolium hydroxide cations were synthesized using the protocol of earlier published literature[21]. In briefly, two gram of chloride salts was added in 50 ml water and stirred vigorously. Then, equimolar of silver oxide was added to the mixture and kept for 2 h at room temperature. The resultant solution was filtered using whatman filter (grade 41) and evaporated the filtrate under reduced pressure to yield the respect cations.

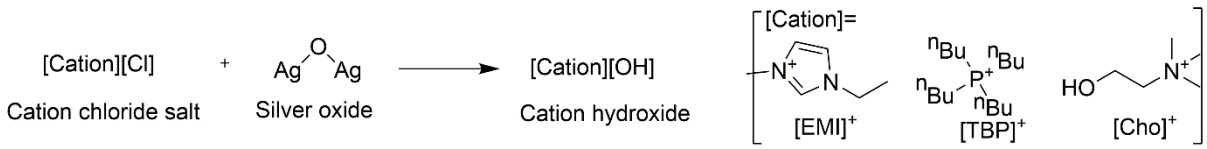

Scheme 3.2. General synthetic procedure for IL forming cation. Silver chloride was precipitated in water at room temperature for 2 h.

3.3.4. Synthesis of MTX-IL moieties

Finally, MTX anion-containing IL-API moieties were synthesized as shown in Scheme S3, through the ionization of a hydrophobic MTX hydrate and hydroxide salts of the desired cations in methanol at 40°C for 2 h. A clear solution was obtained and then evaporated the methanol under reduced pressure. The obtained compounds were further dried using high vacuum.

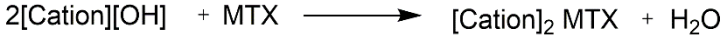

Scheme 3.3. Synthesize of MTX-ILs.

3.3.5. Measurements

The ^{1}H NMR spectra were recorded using a JEOL ECZ400S 400 MHz spectrometer (Tokyo, Japan) in deuterated dimethyl sulfoxide (2.5 ppm)/ methanol (3.3 ppm). The NMR solvents were obtained from Wako Pure Chemical Industries Ltd. The coupling constants (J) are reported in Hertz (Hz). The DeltaV software package (version 5.0.5.1, JEOL) was used to process the spectra. The purities of the synthesized sample moieties were determined using the following equation:

Purity (%) = [Σ I (product)/Σ I (total)] × 100……. (3.1)

where, I represents the relative area of each signal [22].

The Fourier transform infrared (FT-IR) spectra of the samples were recorded using a Perkin Elmer spectrometer (Frontier FT/IR, Waltham, MA) in the range 400–4000 cm^{-1} with an accumulation of 20 scans. Thermogravimetric and derivative thermogravimetric analysis (TGA/DTG) was performed using a Hitachi High-Technologies TG/DTA 7300 (Tokyo, Japan) under a flow of nitrogen. Samples weighing approximately 10 to 20 mg were analyzed in an aluminum crucible and were heated from 30 to 550°C using a constant heating rate of 5°C min^{-1} with a 30 min isothermal step at 70°C. Differential scanning calorimetric (DSC) measurements were carried out using a Hitachi High-Technologies DSC X7000 (Tokyo, Japan) to characterize the thermal behavior of the drug moieties. Standard aluminum pans containing 4–6 mg samples were crimped with an aluminum lid using a press (T Zero sample press), and

heated from −50 to 300°C at a rate of 10°C/min under constant nitrogen at 30 mL/min. An empty pan, sealed in the same way as the sample, was used as a reference. For structural analysis, p-XRD analyses were performed using a high-resolution X-ray diffractometer (Rigaku, Smartlab 9 kW, Tokyo, Japan) with monochromatized and Ni-filtered Cu Kα radiation (λ = 1.5418 Å), operating at 40 kV and 30 mA. The data were collected using the 2θ range of 5–50° with a scanning speed of 2°/min with 0.02°.

Characterization of free MTX

Crystalline powder. ^{1}H-NMR (400 MHz, DMSO-D6, TMS) δ ppm: 2.08-1.89 (m, 2H), 2.32 (t, J = 7.3 Hz, 2H), 3.19 (q, J = 15.1 Hz, 3H), 4.38-4.32 (m, 1H), 4.79 (s, 2H), 6.83 (d, J = 8.7 Hz, 2H), 7.73 (d, J = 9.1 Hz, 3H), 8.20 (d, J = 7.8 Hz, 1H), 8.58 (s, 1H).

Characterization of [Cho][MTX]

Cho cation: Yield 74.3%. Purity 98.5%. A light brown liquid. ^{1}H-NMR (400 MHz, Methanol-D4, TMS) δ ppm: 3.20 (s, 9H), 3.44-3.42 (m, 2H), 4.04-4.00 (m, 2H). Water (5.1-5.2 ppm). *[Cho][MTX] IL:* Yield 99.4%. Purity 98.8%. ^{1}H-NMR (400 MHz, DMSO-D6, TMS) δ ppm: 2.01-1.82 (m, 4H), 3.17-3.05 (m, 22H), 3.42 (dd, J = 5.7, 3.9 Hz, 4H), 3.93-3.83 (m, 5H), 4.75 (s, 2H), 6.80 (d, J = 8.7 Hz, 2H), 7.65 (d, J = 9.1 Hz, 2H), 8.38 (t, J = 6.2 Hz, 1H), 8.58 (d, J = 8.2 Hz, 1H).

Characterization of [TMA][MTX]

TMA cation: Purity 98.3%. A clear colorless liquid. ^{1}H-NMR (400 MHz, Methanol-D4, TMS) δ ppm: 3.23 (s, 12H). Water (5.1ppm). *[TMA][MTX] IL:* Yield 94.6%. Purity 96.4%. A solid powder. ^{1}H-NMR (400 MHz, Methanol-D4, TMS) δ ppm: 2.42-2.16 (m, 4H), 3.24-3.13 (m, 27H), 4.41 (q, J = 4.1 Hz, 1H), 4.78 (s, 2H), 6.79 (d, J = 9.1 Hz, 2H), 7.76 (d, J = 9.1 Hz, 2H), 8.52 (s, 1H). Water (5.0 ppm).

Characterization of [EMI][MTX]

EMI cation: Yield 62.7%. Purity 98.2%. ^{1}H-NMR (400 MHz, Methanol-D4, TMS) δ ppm: 1.55 (t, J = 7.3 Hz, 3H), 4.01 (d, J = 15.1 Hz, 3H), 4.33 (q, J = 7.3 Hz, 2H), 7.70 (dd, J = 33.8, 1.8 Hz, 2H), 9.12 (s, 1H). Water (4.8ppm). *[EMI][MTX] IL:* Yield 86.1%. Purity 98.6%. A wax. ^{1}H-NMR (400 MHz, DMSO-D6, TMS) δ ppm: 1.38 (td, J = 7.3, 1.8 Hz, 6H), 2.03-1.80 (m, 4H), 3.16 (d, J = 2.7 Hz, 4H), 3.96-3.81 (m, 7H), 4.21-4.13 (m, 4H), 4.75 (s, 2H), 6.81 (d, J = 9.1 Hz, 2H), 7.79-7.44 (m, 6H), 8.57 (s, 1H), 9.59 (s, 1H).

Characterization of [TBP][MTX]

TBP cation: Purity 98.9%. ^{1}H-NMR (400 MHz, Methanol-D4, TMS) δ ppm: 1.00 (t, J = 7.1 Hz, 12H), 1.54-1.50 (m, 16H), 2.24-2.17 (m, 8H). Water (5.0-5.2 ppm). *[TBP][MTX] IL:* Yield 98.0%. Purity 98.9%. A wax. ^{1}H-NMR (400 MHz, Methanol-D4, TMS) δ ppm: 0.94 (q, J =

7.3 Hz, 24H), 1.56-1.42 (m, 32H), 2.41-2.13 (m, 20H), 3.20 (s, 3H), 4.47 (q, J = 4.0 Hz, 1H), 4.78 (s, 2H), 6.78 (d, J = 9.1 Hz, 2H), 7.74 (d, J = 8.7 Hz, 2H), 8.52 (s, 1H). Water (5.0 ppm).

Characterization of [AspEt][MTX]

AspEt cation: Yield 80.5%. Purity 97.6%. Clear colorless liquid. ^{1}H-NMR (400 MHz, Chloroform-D, TMS) δ ppm: 1.27 (td, J = 7.2, 4.4 Hz, 6H), 2.82-2.66 (m, 2H), 3.81 (dd, J = 7.3, 4.6 Hz, 1H), 4.24-4.14 (m, 4H). *[AspEt][MTX] IL:* Yield 99.1%. Purity 98.1%. Solid powder. ^{1}H-NMR (400 MHz, DMSO-D6, TMS) δ ppm: δ 1.19 (td, J = 7.1, 3.5 Hz, 6H), 2.12-1.91 (m, 2H), 2.33 (t, J = 7.5 Hz, 2H), 2.76-2.61 (m, 4H), 3.69-3.62 (m, 3H), 3.84-3.78 (m, 2H), 4.17-4.05 (m, 4H), 4.36 (dd, J = 13.5, 8.0 Hz, 1H), 4.80 (s, 2H), 6.84 (d, J = 9.1 Hz, 2H), 7.75 (d, J = 8.7 Hz, 2H), 8.10 (d, J = 7.3 Hz, 1H), 8.60 (s, 1H). Water (3.2 ppm).

Characterization of [ProEt][MTX]

ProEt cation: Yield 52.4 %. Purity 98.3%. Clear colorless liquid. ^{1}H-NMR (400 MHz, Chloroform-D, TMS) δ ppm: 1.28 (t, J = 7.1 Hz, 3H), 1.89-1.71 (m, 3H), 2.18-2.09 (m, 1H), 2.93-2.88 (m, 1H), 3.12-3.06 (m, 1H), 3.74 (dd, J = 8.5, 5.7 Hz, 1H), 4.19 (q, J = 7.0 Hz, 2H). *[ProEt][MTX] IL:* Yield 96.6%. Purity 97.0%. Solid powder. ^{1}H-NMR (400 MHz, DMSO-D6, TMS) δ ppm: 1.20 (td, J = 14.8, 7.3 Hz, 3H), 2.07-1.64 (m, 4H), 2.34-2.23 (m, 2H), 3.03-2.82 (m, 4H), 3.24-3.14 (m, 4H), 3.84-3.80 (m, 2H), 4.13-4.03 (m, 1H), 4.30-4.25 (m, 2H), 4.78 (s, 2H), 6.88-6.82 (m, 2H), 7.71 (d, J = 9.1 Hz, 2H), 8.00 (d, J = 7.3 Hz, 1H), 8.56 (d, J = 15.1 Hz, 1H). Water (3.6 ppm).

Characterization of [PheEt][MTX]

PheEt cation: Yield 87.6%. Purity 98.5%. Clear colorless liquid. ^{1}H-NMR (400 MHz, Chloroform-D, TMS) δ ppm: 1.24 (t, J = 7.1 Hz, 3H), 2.86 (dd, J = 13.5, 8.0 Hz, 1H), 3.08 (dd, J = 13.5, 5.3 Hz, 1H), 3.71 (dd, J = 7.8, 5.5 Hz, 1H), 4.16 (q, J = 7.2 Hz, 2H), 7.32-7.19 (m, 5H). *[PhEt][MTX] IL:* Yield 96.7%. Purity 98.3%. Solid powder. ^{1}H-NMR (400 MHz, DMSO-D6, TMS) δ ppm: 1.12-1.05 (m, 3H), 2.05-1.89 (m, 2H), 2.33-2.30 (m, 2H), 2.91-2.82 (m, 2H), 3.17 (s, 3H), 3.68-3.58 (m, 2H), 4.03 (q, J = 7.2 Hz, 2H), 4.33 (dd, J = 13.3, 8.7 Hz, 1H), 4.78 (s, 2H), 6.83 (d, J = 9.1 Hz, 2H), 7.30-7.18 (m, 5H), 7.72 (d, J = 9.1 Hz, 3H), 8.14 (d, J = 7.3 Hz, 1H), 8.57 (s, 1H). Water (3.2 ppm).

3.3.6. Partitioning coefficient determination

Approximately 2–3 mg of free MTX-ILs were added to a mixture of 5 mL of mili-q-water and 5 ml of octanol. The mixtures were allowed to mix overnight at room temperature with constant shaking in the dark. Then, the solution was centrifuged at 10,000 g for 60 min to separate the layers. The concentration of free MTX in each layer was quantified through UV spectroscopy

(JASCO V-750, Japan) using known concentrations of a standard at 302 nm. The partition coefficient, log Po/w, was determined using the following equation:

$\log Po/w = \log (Solute_{octanol}/Solute_{water})$ ..... (3.2)

where, $Solute_{octanol}$ and $Solute_{water}$ represent the amount of free MTX in octanol and water, respectively.

3.3.7. Media for solubility studies

Mill-q-water, PBS, simulated intestinal fluid (SIF) and simulated gastric fluid (SGF) were used as dissolution media to perform a solubility study of the MTX-IL moieties. PBS (pH = 7.4) was purchased from Nacalai tesque INC. (Kyoto, Japan). SIF (pH = 6.8, without pancreatic enzyme) and SGF (pH = 1.2, without pepsin enzyme) were prepared following United States Pharmacopeia guidelines. Briefly, SIF buffer was prepared by dissolving 0.0896 g of NaOH and 0.6805 g of KH_2PO_4 in 100 mL of water in a volumetric flask. SGF was prepared by dissolving 0.200 g of NaCl and 0.7 mL of concentrated HCl (to adjust the pH to 1.2) in a 100 mL volumetric flask and diluting the solution using water.

3.3.8. Solubility of the MTX-IL moieties

To determine the aqueous solubility of the MTX-IL moieties, equilibrium solubility was determined using a "shake-flask" method. Briefly, an excess amount of MTX-ILs was mixed in 0.5 mL of water or physiological fluids (PBS, SIF, or SFG), and the mixtures were stirred thoroughly for 24 h at 20°C. Then, each solution was centrifuged at 10,000 g for 60 min to separate the solid-liquid phases. The liquid phase was filtered using a 0.2 µm syringe filter to remove the remaining solid particles. The filtrate was analyzed using UV-vis spectroscopy, with quartz cells at a wavelength of 302 nm, which is the wavelength of the maximum absorbance of MTX. Duplicate samples were measured. A predetermined calibration curve was used to determine the amount of drug in the dissolution media (for all curves R^2>0.9957), which was constructed using different solutions with known concentrations of the corresponding MTX-ILs.

3.3.9. In vitro antitumor activity

To evaluate the antitumor activity of the MTX-ILs and sodium salt of MTX, a WST cell viability assay was conducted using the HeLa mammalian cell line, as described in the literature [2]. Briefly, the cells were cultured in MEM containing 10% fetal bovine serum and 1% antibiotic-antimycotic. The cells were seeded into 96-well flat-bottomed plates at 5000

cells/well and, then incubated for 24 h at 37°C under a 5% CO_2 atmosphere. Samples were prepared in Opti-MEM at varying concentrations in the range 0.01–50 mM. A total of 100 µL of each sample solution was replaced in each well, and the plates were incubated for 24 h. After incubation, the solution was removed through washing with PBS and 100 µL of the WST cell counting kit solution in Opti-MEM was added to each well to measure the mitochondrial activity of the cells. After a further 3 h incubation at 37°C in a CO_2 incubator, the absorbance of the supernatant ($A_{treated}$) was measured at 450 nm using a microplate spectrophotometer (Bio-Rad, Tokyo, Japan). The cell viability compared with untreated cells ($A_{control}$) was calculated using the following equation:

Cell viability (%) = $(A_{treated}/A_{control}) \times 100$ …… (3.3)

All tests were performed in triplicate and the average values are reported. Microsoft Excel 2016 (Microsoft, Washington, USA) was used to perform the statistical analysis. Data are presented as the mean with the standard deviation.

3.3.10. Chromatographic conditions

The concentration of free MTX in both sodium salt and ILs of MTX was determined using HPLC (reverse phase) analysis consisting an auto sampler injector (AS-4050, JASCO, Japan), a chromatographic pump (PU-4180, JASCO, Japan) fitted with photo diode array detector (MD-4010, JASCO, Japan) and column oven controller (CO-4060, JASCO, Japan) with an interface box (LC-NetII/ADC). The mobile phase was composed of 10 % acetonitrile and 90% solution A, which prepared by the mixture of 63 % aqueous 0.2M dibasic sodium phosphate and 37% 0.1M citric acid. The pH of solution A was adjusted at 6.0 using 0.2M dibasic sodium phosphate. A reversed-phase Inertsil ODS C18 column (250 × 4.6 mm, 5 µm) (GL Sciences Inc., Shinjuku-ku, Tokyo, 163-1130, Japan) with a Guard column (10 × 4.6 mm, micelle size 5 µm) was used for HPLC analysis at a wavelength of 303 nm. The samples were injected at 10 µL and delivered the flow rate at1.0 mL/min. Under these conditions, the sample was recorded for 20 min in where the MTX was eluted at 11.0 min and, the concentration of MTX in unknown solutions were calculated using a calibration curve derived from known concentration of standards.

3.3.11. Pharmacokinetics studies

The pharmacokinetic study of sodium salt and ILs of MTX ([ProEt][MTX], [AspEt][MTX], [TMA][MTX], [TBP][MTX] and [Cho][MTX]) were carried out using C57BL/6 mice, which were randomly divided into six groups each consisting of three mice. All of the mice were

fasted for six hours before starting the experiments. After mild isoflurane anesthetization, single oral dose (equivalent to 30 mg/kg of MTX) of [Na][MTX] and MTX-ILs were administrated through oral gavage needle. Subsequently, blood sample (50 µl) was collected at 30, 60, 90, 120, 180, 300 and 480 min of post injection. The distilled water was used in the same way as a control. The blood sample were processed for HPLC analysis by adding equal volume (w/w) of mobile phase and vortexed properly. After 30 min sonication, the blood samples were then centrifuged for 45 min at 15000 rpm and filtered the supernatant through a 0.22 µm membrane filter. Finally, the filtrate was injected for analysis using HPLC-system.

3.3.12. Statistical Analysis

Statistical analysis was performed using GraphPad Prism version 6 software (GraphPad Software, Inc., La Jolla, CA). Statistical significance was evaluated through a one-way analysis of variance (ANOVA) followed by Tukey's post-hoc test for multiple comparisons.

3.4. Results and Discussion

3.4.1. Synthesis and characterization of MTX-IL moieties

API-IL prodrugs represent a highly promising approach to turn crystalline drugs into a liquid form to improve their physiochemical or biological activity. To synthesize IL-APIs (Figure 3.1B), the hydrophobic crystalline drug MTX is considered an anion which possesses two acidic protons (pK_a = 2.9 and 4.6) and a nitrogen basic site (pK_a = 6.6) in its structure [23].

Several types of cation, such as AAE, cholinium, imidazolium, quaternary ammonium and quaternary phosphonium, are described in Figure 3.1A. They reportedly have low toxicities or additional biological activity among their corresponding groups, and they were chosen as a counterion for use during MTX-IL moiety synthesis [2,24–28]. The rationale for the choice of these cations is their potential to improve aqueous solubility and skin permeability when combined with free drugs [18]. However, MTX anion-containing IL-API moieties were synthesized through ionization of hydrophobic hydrate MTX and AAEs or hydroxide salts of the desired cations in methanol. The results of the ^{1}H NMR spectroscopy analysis show that the stoichiometry between the two constituents for the [Cho][MTX] compounds was 1:2 (Figure 3.2). In the case of the MTX-AAEs, the stoichiometry ratio was 1:1 because of the lower pKb value of AAE cations (the pKb value of AspEt is 6.6). However, all the MTX-IL moieties demonstrated high yields and were present as solids except [Cho][MTX],

[EMI][MTX] and [TBP][MTX]. The purities of all the synthetic compounds determined using ^{1}H NMR were ≥97.0%.

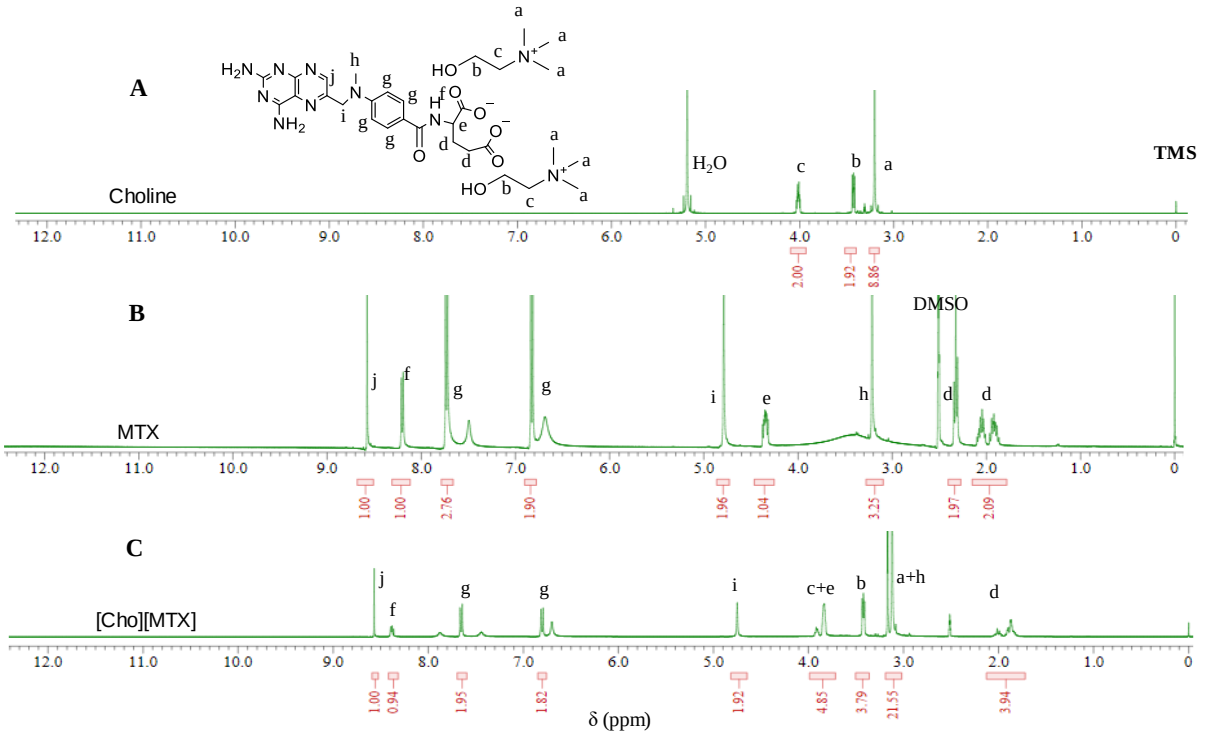

Figure 3.2. ^{1}H NMR spectra of (A) the Cho cation, (B) free MTX and (C) [Cho][MTX].

While the stoichiometry ratio of the MTX-ILs was assessed using ^{1}HNMR, the assessment of fully ionization of the moieties was performed using FT-IR. FT-IR measurements were performed to further understand the interaction between MTX and the cations and then compare the moieties with a fully ionized sodium salt of MTX. In the FT-IR spectrum of free MTX, characteristic peaks were observed at 1678 cm^{-1}, 1640 cm^{-1} and 1606 cm^{-1} for C=O stretching of the –COOH groups, C=C stretching of the MTX benzene ring and the MTX amide, respectively. The spectrum of the [ProEt][MTX] moieties was confirmed to contain characteristic peaks at 1616 cm^{-1} and 1590 cm^{-1} for C=C stretching of the MTX benzene ring and MTX amide, respectively (Figure 3.3). These peaks were also observed in the [Na][MTX] spectrum. Characteristic peaks for C=O stretching of the –COOR groups of ProEt were observed at nearly 1731 cm^{-1} and this shifted to ca. 1726 cm^{-1} in the ProEt cation [2]. The characteristic peaks for C-H stretching of the ethyl group were observed at ca. 2981 cm^{-1} in the [ProEt][MTX] spectrum and were attributed to the ethyl group of ProEt. Similarly, characteristic peaks for other cations were observed in their respective MTX-IL sprectra. For all spectra of the MTX-IL moieties, the characteristic peaks for C=O stretching of –COOH groups at 1678 cm^{-1}, as seen in free MTX, were not observed (Figure 3.S1–3.S3). However, a

new weak shoulder peak appeared at ca. 1602 cm^{-1}, which has been attributed to hydrogen bonding between carbonyl groups and respective cations (i.e. amine/ ammonium/ phosphonium groups of cations). These similar weak shoulder peaks were observed at 1602 cm^{-1} in the [Na][MTX] spectrum (Figure 3.3).

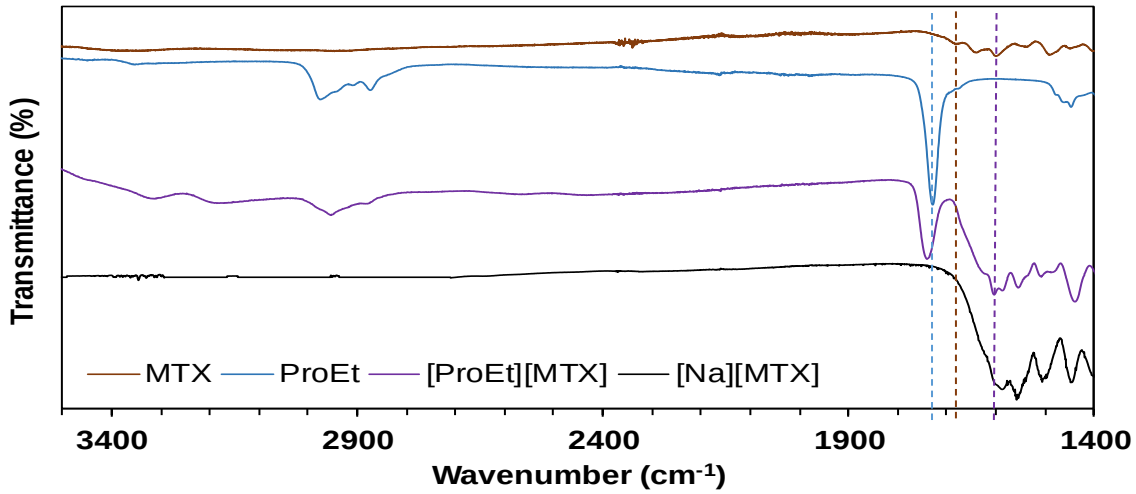

Figure 3.3. FT-IR spectra of free MTX, ProEt, [ProEt][MTX] and [Na][MTX].

The amorphous structure of API-ILs is the important parameter to achieve maximum therapeutic efficacy. It has been reported that amorphous APIs have higher solubility, higher dissolution rate and reduced polymorphism than corresponding crystals[29]. It reveals a great ability to stick together during tableting and reduce the amount of additives, which simplify the formulation procedure[30]. The XRD pattern shown in Figure 3.4 confirmed the amorphous phase of the MTX-ILs while the free MTX was crystalline in nature. Several characteristic sharp peaks were observed in the X-ray diffractogram of free MTX between the 2θ of 5° and 30°. The most promising peaks of MTX were identified at 9.3, 11.4, 12.8, 14.3, 15.9, 17.6, 19.4, 21.4, 24.2, 25.4, 26.9 and 27.8 (2θ scattered angles), which clearly indicated the crystalline nature of the free MTX [31]. All sharp crystalline peaks were diffused in the diffractogram of the MTX-ILs, as shown in Figure 3.4, which is indicative of the amorphous nature of the MTX-IL moieties. Therefore, these results indicate that free MTX was encapsulated or homogeneously distributed in the cationic matrix and then dispersed molecularly (Figure 3.S4).

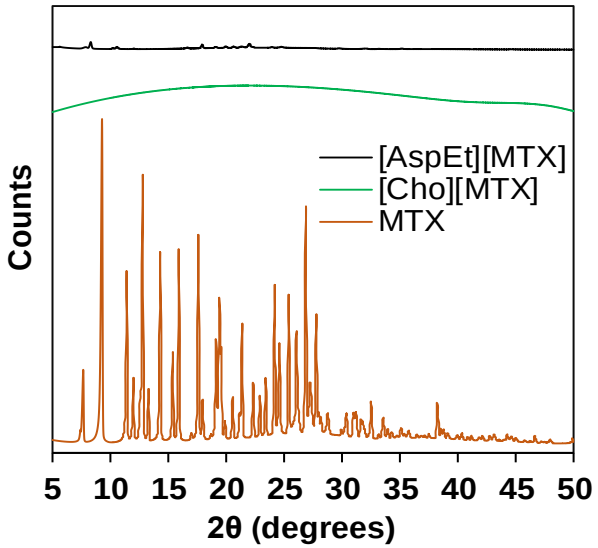

Figure 3.4. The XRD spectra of [AspEt][MTX], [Cho][MTX] and free MTX.

3.4.2. Thermophysical studies of MTX-IL moieties

The thermal behavior of all synthetic MTX-IL compounds was investigated using thermoanalytic methods, as well as DSC, TGA and DTG, to provide evidence on the possible thermal interaction between free drug and various cations. Initially, we evaluated the thermal stabilities of the synthesized MTX-IL moieties through TGA and measured the onset ($T_{5\%onset}$) temperatures (Table 3.1 and Figure 3.5). The MTX-ILs showed similar or lower thermal stabilities than that of the free hydrate MTX (Table 3.1). In the TGA and DTG thermograms of free MTX and [Cho][MTX], the free hydrate MTX thermogram showed a three step decomposition with 37.26% loss of its initial mass on heating to 550°C, which was clearly seen in the DTG thermogram. The first decomposition step occurred from 40°C to 75°C, and was attributed to removal of volatile materials and surface adsorbed water molecules with a ca. 8% loss of mass. The second decomposition step corresponds to a 2% dehydration of drug from 75°C to 120°C, which is required to remove structural water. This value of mass loss is in good agreement with the theoretical percentage of water contained in the free drug (ca. 10%). After the removal of the water, anhydrous MTX is formed and shows good thermal stability in a 120–228°C temperature range. The actual thermal decomposition of free anhydrous MTX takes place from 232°C to 550°C with a mass loss of ca. 52.7% of its initial mass. The $T_{5\%onset}$ of the free hydrate MTX is approximately 246°C. These results are in agreement with previous findings [32].

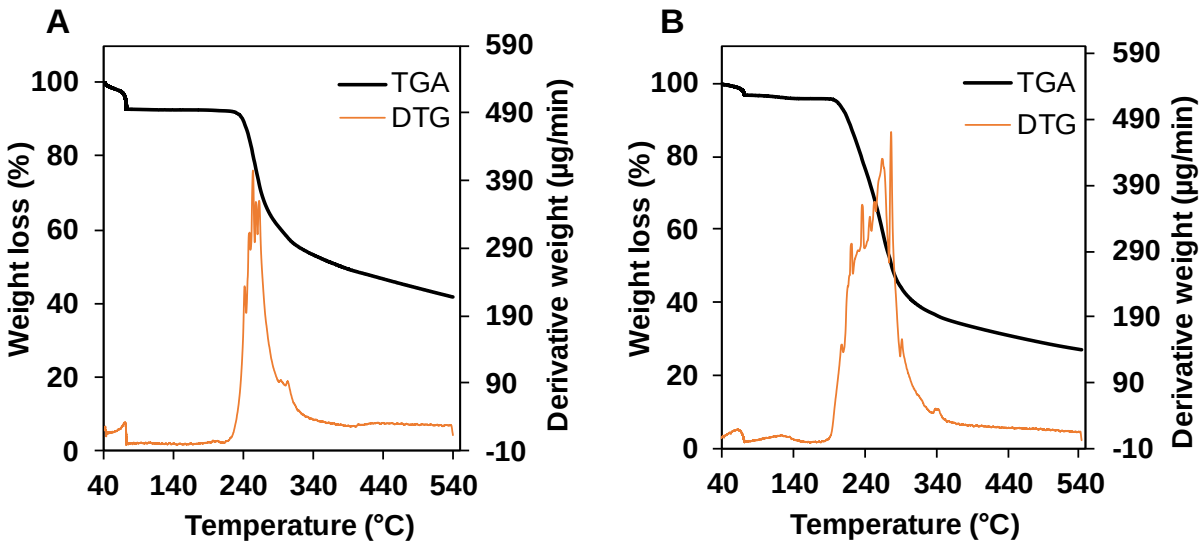

Figure 3.5. TGA and DTG thermograms of (A) free hydrate MTX and (B) [Cho][MTX] measured in a nitrogen atmosphere with a heating rate of 10°C min^{-1}.

The MTX-IL moieties exhibited slightly different results compared with the free hydrate MTX. For example, [Cho][MTX] demonstrated three main thermal phenomena. The first and second weight losses of 3.72% and 1% at 30–75°C and 75–150°C, respectively, were attributed to the removal of volatile materials and surface adsorbed water, and structural water molecules. Similar decomposition steps were also found for all MTX-IL moieties (Figure 3.S5). It was found that the MTX-IL moieties demonstrated good thermal stability up to 200°C except [AAEs][MTX]. The $T_{5\%onset}$ temperatures of decomposition for the MTX-IL moieties are shown in Table 3.1.

Table 3.1. Physicothermal properties of the free hydrate MTX and MTX-IL moieties.

Compound	Log P (o/w)	DSC		TGA
		T_g (°C)	T_m (°C)	$T_{5\%\ onset}$ (°C)
Methotrexate	-1.98	114	154	246
[Cho][MTX]	-3.62	27	143	200
[TMA][MTX]	-3.99	46	141	208
[EMI][MTX]	-3.83	45	112	251
[TBP][MTX]	-1.17	17	137	296
[ProEt][MTX]	-2.82	93	120	171
[AspEt][MTX]	-2.56	104	164	142
[PheEt][MTX]	-1.91	103	142	175

To further investigate the physical properties such as the melting points and/or phase transitions of the MTX-ILs, we carried out DSC analyses. The DSC thermograms are shown in Figure 3.6. The free MTX exhibited a characteristic sharp endothermic peak at 154°C with an enthalpy of relaxation of 8 mW, which corresponds to its melting point. It has been reported that the thermogram of choline exhibits no endothermic peak during the complete heating procedure (20°C–300°C) [33]. However, in the thermogram of [Cho][MTX] the characteristic sharp endothermic peak shifted to 143°C, which is an indication of a significant change in the physical state from crystalline to amorphous.

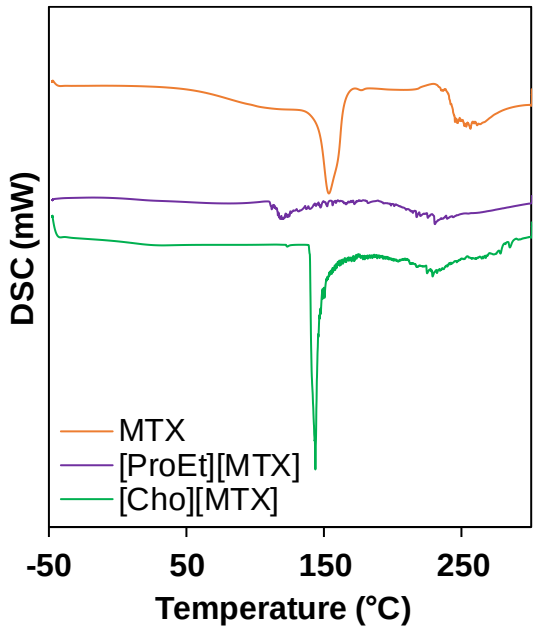

Figure 3.6. DSC thermograms of free MTX, [ProEt][MTX] and [Cho][MTX].

Similarly, IL moieties of MTX with different cations ([ProEt][MTX]) showed variable characteristic sharp endothermic peaks at different temperatures without any phase transformation (Figure 3.6 and Figure 3.S6–3.S8). These results confirmed that there was a strong physicochemical interaction between free drug and cations.

3.4.3. Solubility study of the MTX-IL moieties

Solubility and bioavailability of a drug molecule is essential physicochemical parameters in order to predict their mode of release mechanisms and possible in vivo behavior into the human body. The pharmacokinetic and pharmacodynamics parameters of drug molecules were limited due to their insufficient aqueous solubility and permeability in the simulated body fluids following oral administration. To determine if we had achieved our goal of increased solubility, we carried out an equilibrium solubility analysis (undissolved solid MTX-IL remains in

equilibrium within a saturated aqueous solution) of MTX-ILs in various physiological fluids at room temperature and atmospheric pressure. All MTX-IL compounds showed higher solubility than free MTX in both water (Figure 3.S9) and buffers (Figure 3.7). As expected, [Cho][MTX] showed higher aqueous solubility than the other MTX-ILs, and this was 5280 times higher than that of free MTX (0.15 mg/mL) or two times higher than that of an MTX sodium salt in PBS (pH = 7.4). The presence of hydroxyl groups in the alkyl chains of the cholinium cation, which enhance the hydrogen bonding capacity and polarity of a cation, increases its aqueous solubility. These results are similar to previously reported data, in which choline-based drugs showed higher aqueous solubility than free drugs. For example, choline naproxen and choline tolmetin showed a 6700- and 8000-fold higher aqueous solubility than their corresponding free drugs, respectively [34].

The aqueous solubility of MTX-ILs in PBS decreases in accordance with the following sequence: [PheEt][MTX] < [AspEt][MTX] < [ProEt][MTX] < [TBP][MTX] < [EMI][MTX] < [TMA][MTX] < [Cho][MTX]. This depends on the chemical structure of cations such as ammonium, imidazolium, phosphonium, choline and AAEs (Figure 3.7). Table 3.1 shows the Log P of the MTX-ILs. [Cho][MTX] (Log P = −3.62) showed the highest solubility in PBS among the MTX-ILs, free MTX and an MTX sodium salt, because of its high hydrophilicity. The relative aqueous solubility of the MTX-ILs mainly depends on the hydrophilicity of the cations. However, although the hydrophilicity of [ProEt][MTX] (Log P = −2.82) is higher than that of [TBP][MTX] (Log P = −1.17), the aqueous solubility of [ProEt][MTX] is lower than that of [TBP][MTX], yet that of both MTX-ILs is higher than that of free MTX.

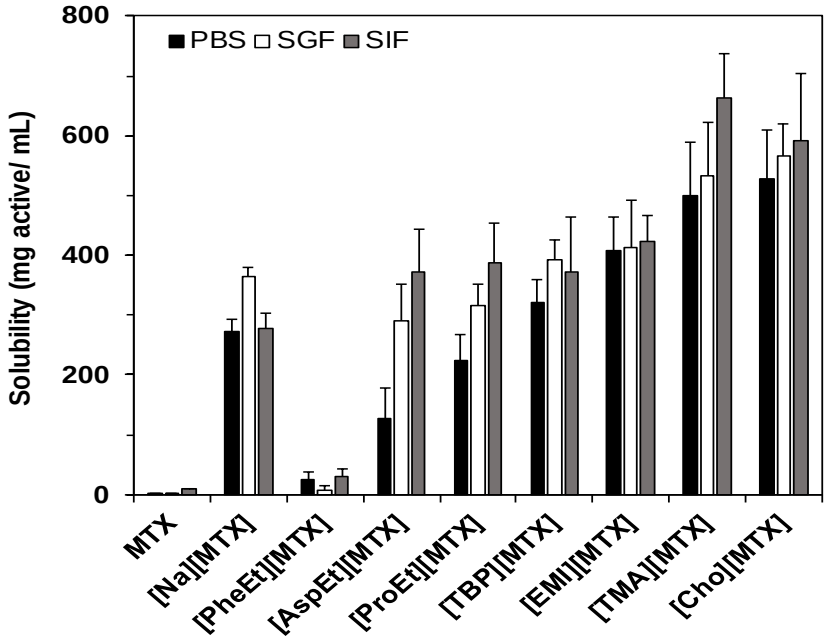

Figure 3.7. Solubility of MTX-IL moieties in buffers (SIF, SGF and PBS).

Next, we evaluated the solubility of the MTX-ILs in different simulated physiological body fluids such as SGF (pH 1.2), and SIF (pH 6.8). The solubility of the MTX-ILs was much higher compared with that of free MTX in all physiological media. In SGF, [Cho][MTX] showed the highest solubility because of an increase in the hydrophilicity of the cholinium cation produced by the presence of hydrophilic hydroxyl groups in the alkyl chains. However, [TMA][MTX] showed a slightly higher solubility than [Cho][MTX] in SIF, because of its high hydrophilicity at neutral pH. The solubility of [TMA][MTX] in PBS or SGF was lower than that of [Cho][MTX] because of the effect of the low pH and ionic strength of the testing media. In all cases, [PheEt][MTX] showed the lowest solubility in water and the three simulated body fluids (PBS, SGF and SIF). The PheEt cation increased the hydrophobicity of the MTX-ILs because of the presence of a hydrophobic benzene ring in its side chains.

3.4.4. In vitro antitumor activity of the MTX-ILs

Finally, the in vitro antitumor activity of the MTX-ILs was evaluated using a HeLa mammalian cancer cell line, and compared with that of MTX sodium salt. Before comparing the antitumor activity of the MTX-IL moieties, we evaluated the cytotoxicity of the cations (Figure 3.8A). Among the cations, TBP showed the lowest IC_{50} because of the presence of a long alkyl chain in the cation. In the AAEs, the high cytotoxicity of PheEt could be attributed to a strong π-π interaction between the cation and the cell membrane, leading to a rapid disruption of the cell structure. ProEt showed lower toxicity than the other cations because of the presence of a cyclic secondary amine in its structure[2]. Both ProEt and AspEt demonstrated relatively low toxicity because of their higher hydrophilicity (Table 3.1).

The in vitro antitumor activity of the MTX-ILs mainly depends on the toxic nature of the relevant cations (Figure 3.8B). Among all the MTX-IL moieties, [TBP][MTX] was the most toxic in HeLa cells because of the presence of a highly cytotoxic cation (Figure 3.8A), which enhanced the penetration of MTX into the cell membrane and disrupted its physiological functions, ultimately leading to cell death. A similar result was obtained in [PheEt][MTX] and [EMI][MTX] because of the presence of a benzene or pyridine ring, which is attributed to a strong π-π interaction between the hydrophobic or liphophilic cations and the plasma membrane of cells, leading to rapid disruption of the cell structure. These results are in agreement with published work showing that higher hydrophobicity or long alkyl chains leads to high toxicity [1,2].

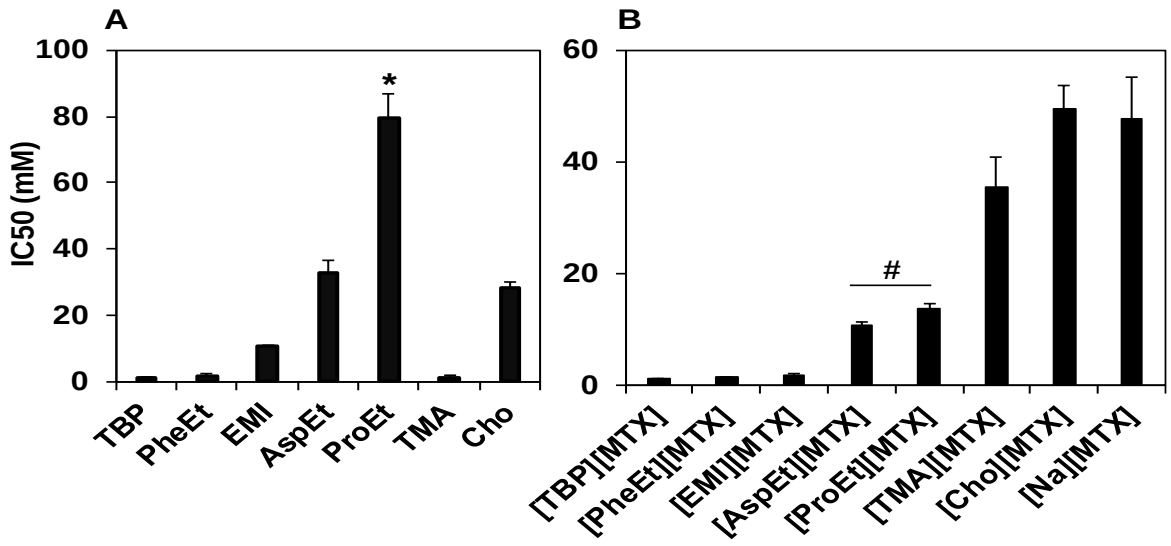

Figure 3.8. In vitro antitumor activity of MTX-IL moieties in HeLa cells. Effect of (A) cations derived from IL-forming cationic salts, and (B) MTX-IL moieties. Statistical significance was evaluated by one-way ANOVA followed by Tukey's post-hoc test for multiple comparisons. **P* < 0.05 versus all the other cations, #*P* < 0.05 versus all the other MTX-ILs. Data are expressed as mean ± SD, n = 3.

Ammonium-based IL moieties such as [TMA][MTX] and [Cho][MTX] showed the least toxicity whereas the AAE- and imidazolium-based MTX-ILs showed relatively high antitumor activity. These cations could be partially attributed to their high aqueous solubility and partition coefficient (Table 3.1), which reduced their interaction with the lipid bilayer of the cell membrane. The higher hydrophilicity of MTX-ILs could reduce the penetration of MTX through cell membrane by decreasing the lipophilicity of the IL form. Interestingly, the ProEt and AspEt cations were not toxic when administered alone (Figure 3.8A). However, the AAE-based MTX-ILs with low toxicity ([ProEt][MTX] and [AspEt][MTX]) showed enhanced toxicity compared with a sodium salt of MTX because of their lower hydrophilicity. The ProEt cation-based MTX-IL showed lower toxicity than either the AspEt or PheEt cation-based MTX-IL because of the higher hydrophilicity of [ProEt][MTX] (Table 3.1). Therefore, the enhanced cytotoxic activity in a cancer cell line of these cations compared with their sodium analogs can be related to their greater lipophilicity.

3.4.5. Pharmacokinetics analysis

Pharmacokinetic parameters of MTX-ILs and sodium salts of MTX were determined to compare to assess the effect of ionic liquid on the oral bioavailability of MTX. The

concentration of MTX in mice blood plasma was calculated by HPLC analysis, which has been calibrated with known standards concentration in the range of 1.04 µg/mL to 10.4 mg/mL of MTX and regression coefficient over this concentration range was 1. The plasma concentration over time profiles of MTX in mice blood plasma after oral administration of MTX-ILs and sodium salt of MTX were illustrated in Figure 3.9, and the mean pharmacokinetic parameters of MTX were summarized in Table 3.2. All the pharmacokinetic parameters (nine parameters were calculated) of MTX-ILs showed significantly higher than that of sodium salt of MTX especially amino acid esters based ILs (AEEs-MTX). The proline ethyl ester MTX ([ProEt][MTX]) showed about 1.6-fold increase in C_{max}, 11.0-fold increase in $T_{1/2}$, 5.2-fold increase in $AUC_{0-\infty}$, 17.9-fold increase in $AUMC_{0-\infty}$, 3.4-fold increase in $MRT_{0-\infty}$ and 5.3-fold reduce in Cl as compared to sodium salt of MTX. The C_{max} of sodium MTX showed at 1.0 h; after that the MTX concentration in blood plasma was rapidly decreased and reached almost zero after 5 h, indicating rapid metabolism of the sodium MTX whereas MTX-ILs showed reasonably amount of drugs in blood plasma. The quaternary phosphonium MTX showed maximum C_{max} (6.88±1.01) among all drugs due to the presence of hydrophobic counterions of MTX, which enhance the MTX absorption through GI track of stomachs.

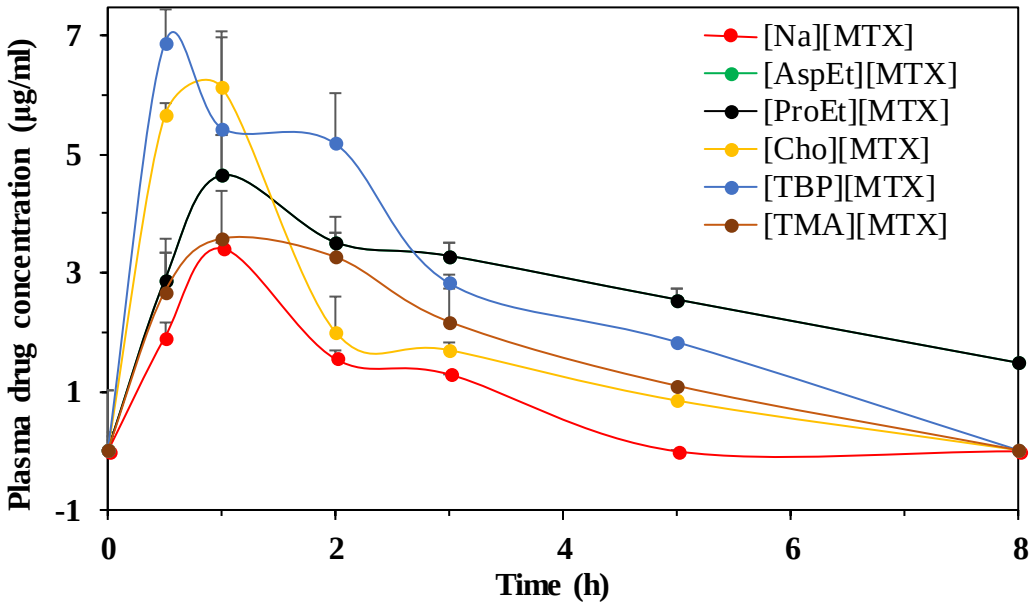

Figure 3.9. Time-dependent plasma drug concentration of MTX-ILs and sodium salt of MTX in C57BL/6 mice at single oral administration (at 30 mg kg^{-1} of MTX drug). Data are expressed as mean ± SD, n = 3.

However, the AEEs-MTX showed sustantial drug release in mice blood plasma even after 8 h of administration. The significant increase of $T_{1/2}$ and reduction of Cl in AEEs-MTX were

attributed to long residence time of MTX drug in mice body. The significant increase of AUC and F_R of the MTX in AAEs-MTX (5.66±1.11 and 5.25 or 35.76±2.25 and 5.09 of [ProEt][MTX] or [AspEt][MTX], respectively) than sodium MTX distinctly indicates the improved bioavailability of MTX. High absorptions by GIT track, sustaintial drug releases and drug protection against enzymatic barriers could be responsible for improved bioavailability of AAEs-MTX. However, cholinium MTX showed enhanced relative bioavailability (F_R = 2.0 in Table 3.2) as compared with sodium MTX which is almost similar reported by Rogers groups for cholinium sulfasalazine after oral administration. Although, [Cho][MTX] showed higher solubility in water or physiological body fluids due to the presence of hydrophilic hydroxyl groups.

Table 3.2. Pharmacokinetic parameters of MTX-ILs and sodium salt of MTX in mice after oral administration at a dose of 30 mg/kg. Drug solutions was administrated at 100 µL per mice.

PK	**MTX-ILs**					
	[Na][MTX]	**[Cho][MTX]**	**[ProEt][MTX]**	**[AspEt][MTX]**	**[TBP][MTX]**	**[TMA][MTX]**
C_{max}	3.42±0.26	6.34±0.07	5.40±0.70	4.64±0.46	6.88±1.01	4.02±0.28
T_{max}	1.00±0.0	0.75±0.35	1.0±0.0	1.00±0.0	1.25±1.1	1.5±0.71
$T_{1/2}$	0.51±0.01	1.16±0.19	5.66±1.11	6.57±1.14	0.85±0.11	0.93±0.05
$AUC_{0-\infty}$	7.03±0.32	14.08±1.10	36.9±2.33	35.76±2.25	21.50±0.18	13.25±0.44
$AUMC_{0-\infty}$	7.04±0.32	14.09±1.11	125.74±35.3	134.07±6.07	21.51±0.19	13.25±0.44
$MRT_{0-\infty}$	1.00±0.0	1.00±0.0	3.38±0.74	3.75±0.07	1.00±0.0	1.00±0.0
Cl	4.27±0.19	2.14±0.17	0.81±0.05	0.84±0.05	1.40±0.01	2.27±0.08
K_{el}	1.36±0.04	0.61±0.10	0.12±0.02	0.11±0.02	0.82±0.11	0.75±0.04
F_R	-	2	5.25	5.09	3.06	1.88

Parameters with units: maximal concentration (C_{max}, µg/mL), time of maximual concentration (T_{max}, h), elimination half-life ($T_{1/2}$, H), area under the plasma concentration–time curve from 0 h to ∞ ($AUC_{0-\infty}$, µg/mL.h), area under the moment curve ($AUMC_{0-\infty}$, µg/mL.h^2), mean retention time ($MRT_{0-\infty}$, h), total body clearance (Cl, L/h/g), Elimination rate constant (K_{el}, h^{-1}) and relative bioavailability (F_R).

3.5. Conclusions

The current study reported a new series of IL-APIs consisting of MTX as an anion and biocompatible ILs, such as choline and AAEs, as a cation. Characterization studies (including NMR, FTIR, DSC and TGA) showed the successful synthesis of IL-MTX APIs with excellent API properties. The solubility of the MTX-IL moieties in simulated body fluids improved significantly compared with MTX and MTX sodium salts. Importantly, the [AspEt][MTX] and [ProEt][MTX] showed enhanced in vitro antitumor activity compared with that of MTX sodium salt. The bioavailability of AAE-MTXs showed at least six times higher than that of sodium MTX. The antitumor efficacy of MTX-ILs and sodium MTX are presently under investigation. The results reported here could play a significant role in the development of MTX-IL-assisted drug delivery systems that take advantage of the various attractive properties of ILs.

3.6. References

[1] A.M.O. Azevedo, S.P.F. Costa, A.F.V. Dias, A.H.O. Marques, P.C.A.G. Pinto, K. Bica, A.K. Ressmann, M.L.C. Passos, A.R.T.S. Araújo, S. Reis, M.L.M.F.S. Saraiva, Anti-inflammatory choline based ionic liquids: Insights into their lipophilicity, solubility and toxicity parameters, J. Mol. Liq. 232 (2017) 20–26. doi:10.1016/j.molliq.2017.02.027.

[2] R.M. Moshikur, M.R. Chowdhury, R. Wakabayashi, Y. Tahara, M. Moniruzzaman, M. Goto, Characterization and cytotoxicity evaluation of biocompatible amino acid esters used to convert salicylic acid into ionic liquids, Int. J. Pharm. 546 (2018) 31–38. doi:10.1016/j.ijpharm.2018.05.021.

[3] S. Kalepu, V. Nekkanti, Insoluble drug delivery strategies: Review of recent advances and business prospects, Acta Pharm. Sin. B. 5 (2015) 442–453. doi:10.1016/j.apsb.2015.07.003.

[4] M. Lotfi, M. Moniruzzaman, M. Sivapragasam, S. Kandasamy, M.I. Abdul Mutalib, N.B. Alitheen, M. Goto, Solubility of acyclovir in nontoxic and biodegradable ionic liquids: COSMO-RS prediction and experimental verification, J. Mol. Liq. 243 (2017) 124–131. doi:10.1016/j.molliq.2017.08.020.

[5] I. Ali, M.N. Lone, Z.A. Alothman, A. Alwarthan, Insights into the pharmacology of new heterocycles embedded with oxopyrrolidine rings: DNA binding, molecular docking, and anticancer studies, J. Mol. Liq. 234 (2017) 391–402. doi:10.1016/j.molliq.2017.03.112.

[6] J. Chen, L. Huang, H. Lai, C. Lu, M. Fang, Q. Zhang, X. Luo, Methotrexate-loaded

PEGylated chitosan nanoparticles: Synthesis, characterization, and in vitro and in vivo antitumoral activity, Mol. Pharm. 11 (2014) 2213–2223. doi:10.1021/mp400269z.

[7] Z.A. Khan, R. Tripathi, B. Mishra, Methotrexate: a detailed review on drug delivery and clinical aspects, Expert Opin. Drug Deliv. 9 (2012) 151–169. doi:10.1517/17425247.2012.642362.

[8] R. Tondwal, M. Singh, Effect of increasing alkyl chain of 1st tier dendrimers on binding and release activities of methotrexate drug: An in vitro study, J. Mol. Liq. 211 (2015) 466–475. doi:10.1016/j.molliq.2015.07.033.

[9] F. Yang, N. Kamiya, M. Goto, Transdermal delivery of the anti-rheumatic agent methotrexate using a solid-in-oil nanocarrier, Eur. J. Pharm. Biopharm. 82 (2012) 158–163. doi:10.1016/j.ejpb.2012.05.016.

[10] R.M. Bremnes, L. Slørdal, J. Aarbakke, E. Wist, Dose-dependent Pharmacokinetics of Methotrexate and 7-Hydroxymethotrexate in the Rat in Vivo, Cancer Res. 49 (1989) 6359–6364. doi:2804982.

[11] R. Regenthal, M. Krueger, C. Koeppel, R. Preiss, Drug levels: therapeutic and toxic serum/plasma concentrations of common drugs., J. Clin. Monit. Comput. 15 (1999) 529–544. doi:10.1023/A:1009935116877.

[12] C.Z. Yang, C.Y. Liang, D. Zhang, Y.J. Hu, Deciphering the interaction of methotrexate with DNA: Spectroscopic and molecular docking study, J. Mol. Liq. 248 (2017) 1–6. doi:10.1016/j.molliq.2017.10.017.

[13] Effects of vehicles and penetration enhances on the.pdf, (n.d.).

[14] S. Furukawa, G. Hattori, S. Sakai, N. Kamiya, Highly efficient and low toxic skin penetrants composed of amino acid ionic liquids, RSC Adv. 6 (2016) 87753–87755. doi:10.1039/C6RA16926K.

[15] R. Ferraz, L.C. Branco, C. Prudêncio, J.P. Noronha, Ž. Petrovski, Ionic liquids as active pharmaceutical ingredients, ChemMedChem. 6 (2011) 975–985. doi:10.1002/cmdc.201100082.

[16] J.L. Shamshina, R.D. Rogers, Overcoming the problems of solid state drug formulations with ionic liquids., Ther. Deliv. 5 (2014) 489–91. doi:10.4155/tde.14.28.

[17] Z. Yan, L. Ma, S. Shen, J. Li, Studies on the interactions of some small biomolecules with antibacterial drug benzethonium chloride and its active pharmaceutical ingredient ionic liquid (API-IL) benzethonium L-proline at varying temperatures, J. Mol. Liq. 255 (2018) 530–540. doi:10.1016/j.molliq.2018.02.007.

[18] M. Shadid, G. Gurau, J.L. Shamshina, B.-C. Chuang, S. Hailu, E. Guan, S.K.

Chowdhury, J.-T. Wu, S.A.A. Rizvi, R.J. Griffin, R.D. Rogers, Sulfasalazine in ionic liquid form with improved solubility and exposure, Med. Chem. Commun. 6 (2015) 1837–1841. doi:10.1039/C5MD00290G.

[19] H. Yoshiura, M. Tamura, M. Aso, N. Kamiya, M. Goto, Ionic liquid-in-oil microemulsions as potential carriers for the transdermal delivery of Methotrexate, J. Chem. Eng. Japan. 46 (2013) 794–796. doi:10.1252/jcej.13we009.

[20] M. Moniruzzaman, N. Kamiya, M. Goto, Ionic liquid based microemulsion with pharmaceutically accepted components: Formulation and potential applications, J. Colloid Interface Sci. 352 (2010) 136–142. doi:10.1016/j.jcis.2010.08.035.

[21] C.M. Raihan, R.M. Moshikur, R. Wakabayashi, Y. Tahara, N. Kamiya, M. Moniruzzaman, M. Goto, Ionic-Liquid-Based Paclitaxel Preparation: A New Potential Formulation for Cancer Treatment, Mol. Pharm. 15 (2018) 2484–2488. doi:10.1021/acs.molpharmaceut.8b00305.

[22] O. Zavgorodnya, J.L. Shamshina, M. Mittenthal, P.D. McCrary, G.P. Rachiero, H.M. Titi, R.D. Rogers, Polyethylene glycol derivatization of the non-active ion in active pharmaceutical ingredient ionic liquids enhances transdermal delivery, New J. Chem. 41 (2017) 1499–1508. doi:10.1039/C6NJ03709G.

[23] K. Mioduszewska, J. Dołżonek, D. Wyrzykowski, Ł. Kubik, P. Wiczling, C. Sikorska, M. Tański, Z. Kaczyński, P. Stepnowski, A. Białk-Bielińska, Overview of experimental and computational methods for the determination of the pKa values of 5-fluorouracil, cyclophosphamide, ifosfamide, imatinib and methotrexate, TrAC - Trends Anal. Chem. 97 (2017) 283–296. doi:10.1016/j.trac.2017.09.009.

[24] Y. Ohta, Y. Kondo, K. Kawada, T. Teranaka, N. Yoshino, Synthesis and antibacterial activity of quaternary ammonium salt-type antibacterial agents with a phosphate group., J. Oleo Sci. 57 (2008) 445–52. doi:10.5650/jos.57.445.

[25] A. Foulet, O. Ben Ghanem, M. El-Harbawi, J.M. Lévêque, M.I.A. Mutalib, C.Y. Yin, Understanding the physical properties, toxicities and anti-microbial activities of choline-amino acid-based salts: Low-toxic variants of ionic liquids, J. Mol. Liq. 221 (2016) 133–138. doi:10.1016/j.molliq.2016.05.046.

[26] A. Yazdani, M. Sivapragasam, J.M. Leveque, M. Moniruzzaman, Microbial Biocompatibility and Biodegradability of Choline-Amino Acid Based Ionic Liquids, J. Microb. Biochem. Technol. 08 (2016) 415–421. doi:10.4172/1948-5948.1000318.

[27] S. Wu, L. Zeng, C. Wang, Y. Yang, W. Zhou, F. Li, Z. Tan, Assessment of the cytotoxicity of ionic liquids on Spodoptera frugiperda 9 (Sf-9) cell lines via in vitro

assays, J. Hazard. Mater. 348 (2018) 1–9. doi:10.1016/j.jhazmat.2018.01.028.

[28] A.A. Elgharbawy, F.A. Riyadi, M.Z. Alam, M. Moniruzzaman, Ionic liquids as a potential solvent for lipase-catalysed reactions: A review, J. Mol. Liq. 251 (2018) 150–166. doi:10.1016/j.molliq.2017.12.050.

[29] L. Yu, <Amorphous pharmaceutical solids preparation, characterization.pdf>, 48 (2001) 27–42. doi:10.1016/S0169-409X(01)00098-9.

[30] Z. Wojnarowska, J. Knapik, M. Rams-Baron, A. Jedrzejowska, M. Paczkowska, A. Krause, J. Cielecka-Piontek, M. Jaworska, P. Lodowski, M. Paluch, Amorphous Protic Ionic Systems as Promising Active Pharmaceutical Ingredients: The Case of the Sumatriptan Succinate Drug, Mol. Pharm. 13 (2016) 1111–1122. doi:10.1021/acs.molpharmaceut.5b00911.

[31] C. Agatemor, K.N. Ibsen, E.E.L. Tanner, S. Mitragotri, Ionic liquids for addressing unmet needs in healthcare, Bioeng. Transl. Med. (2018) 7–25. doi:10.1002/btm2.10083.

[32] M. Dhanka, C. Shetty, R. Srivastava, Methotrexate loaded gellan gum microparticles for drug delivery, Int. J. Biol. Macromol. 110 (2018) 346–356. doi:10.1016/j.ijbiomac.2017.12.026.

[33] X. Han, W. Qi, W. Dong, M. Guo, P. Ma, J. Wang, Preparation, optimization and in vitro–in vivo investigation for capsules of the choline salt of febuxostat, Asian J. Pharm. Sci. 11 (2016) 715–721. doi:10.1016/j.ajps.2016.05.009.

[34] 7. Drug Formulation.pdf, (n.d.).

APPENDIX 3.A. SUPPORTING MATERIALS

1. Fourier Transform Infra-Red Spectroscopy (FT-IR) of MTX-ILs

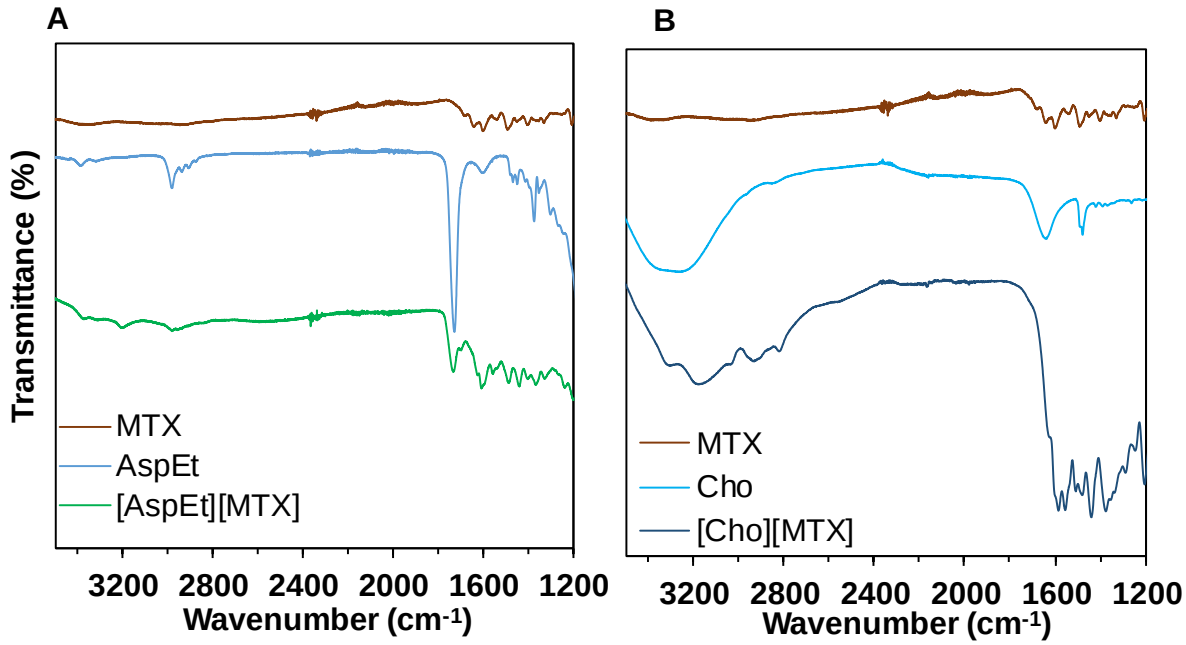

Figure 3.S1. FT-IR spectra of (A) free MTX, AspEt cation and [AspEt][MTX], (B) Free MTX, choline cation and [Cho][MTX].

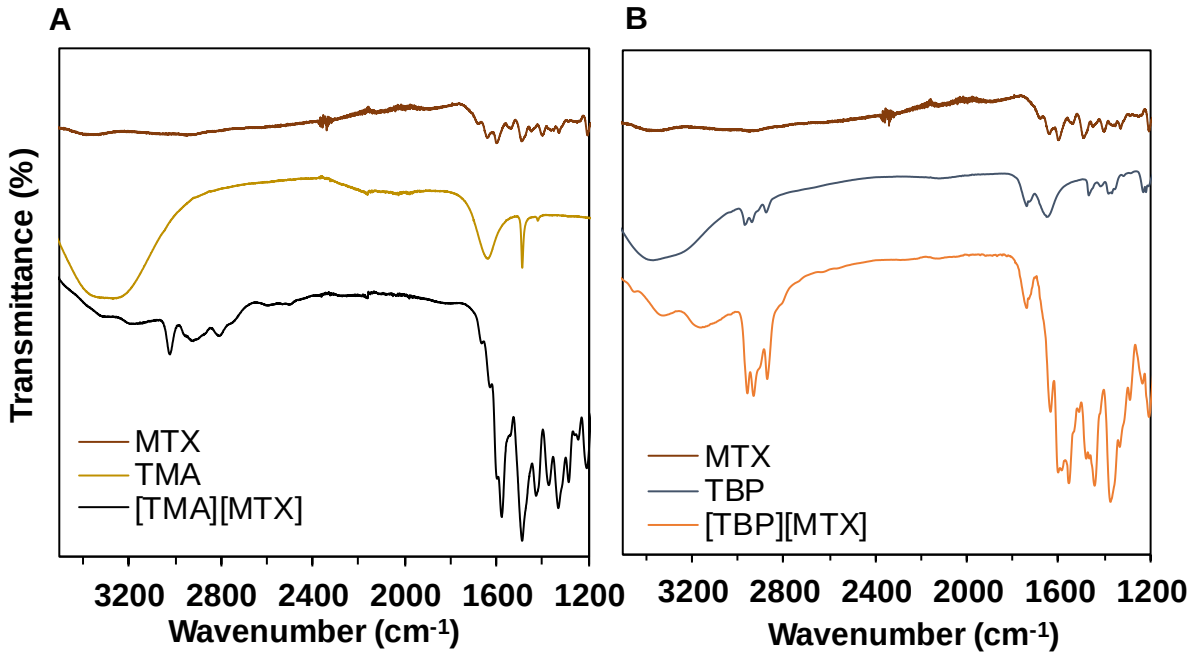

Figure 3.S2. FT-IR spectra of (A) free MTX, TMA cation and [TMA][MTX], (B) Free MTX, TBP cation and [TBP][MTX].

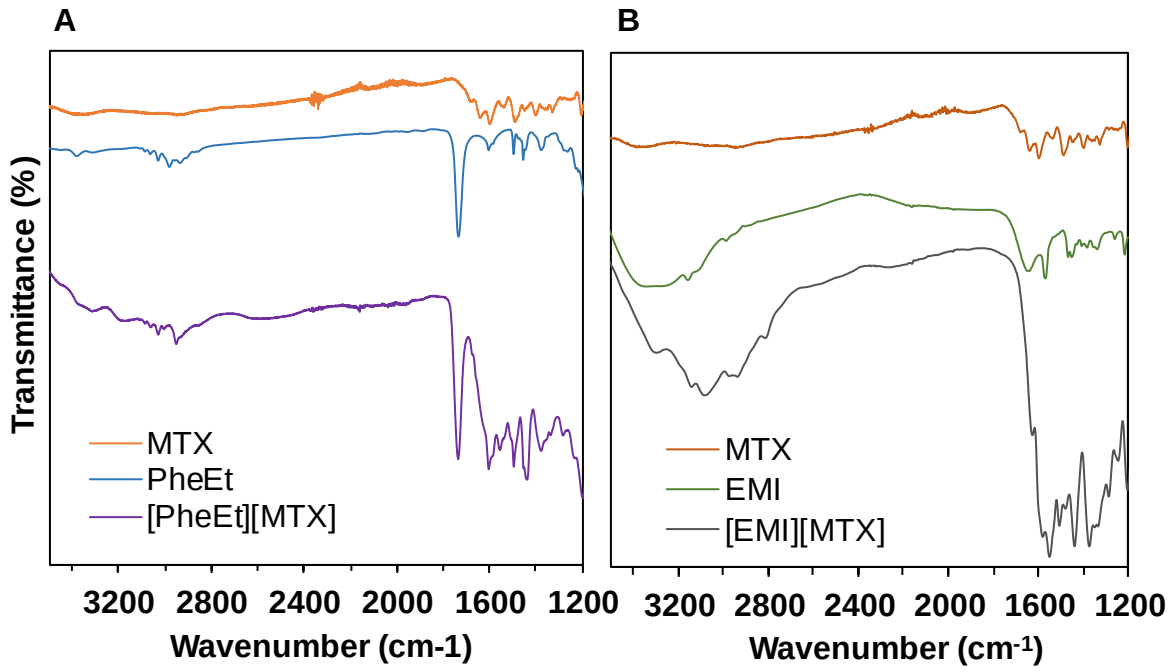

Figure 3.S3. FT-IR spectra of (A) free MTX, PheEt and [PheEt][MTX], (B) Free MTX, EMI cation and [EMI][MTX].

2. Powder X-Ray Diffraction (p-XRD) of MTX-ILs

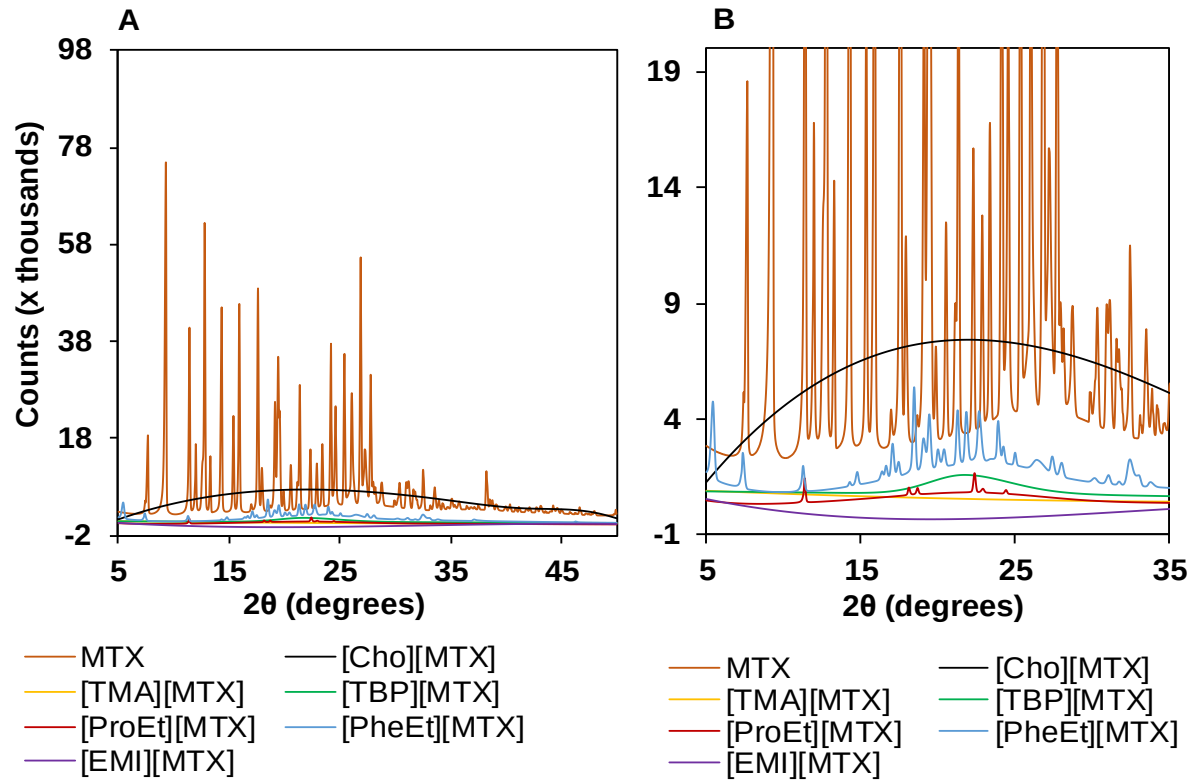

Figure 3.S4. XRD diffractograms of free MTX and MTX-ILs. A) Full spectrum and B) expanded regions of free MTX and MTX-ILs.

3. Thermal Gravimetric Analysis (TGA) of MTX-ILs

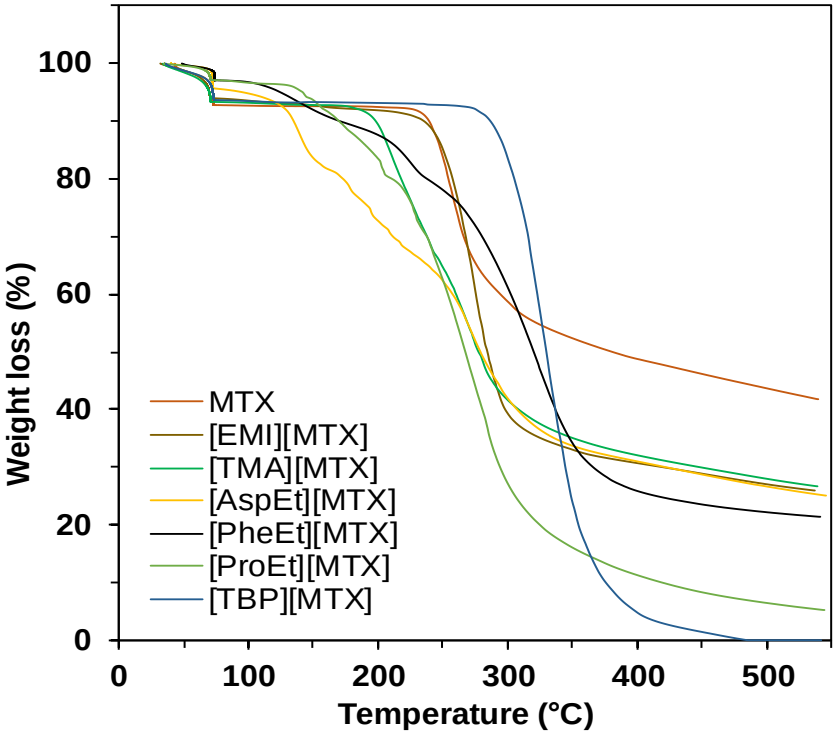

Figure 3.S5. TGA thermograms of free MTX (orange), [EMI][MTX] (tan), [TMA][MTX] (green), [AspEt][MTX] (mustard), [PheEt][MTX] (black), [ProEt][MTX] (pal green) and [TBP][MTX] (blue).

4. Differential Scanning Calorimetry (DSC) of MTX-ILs

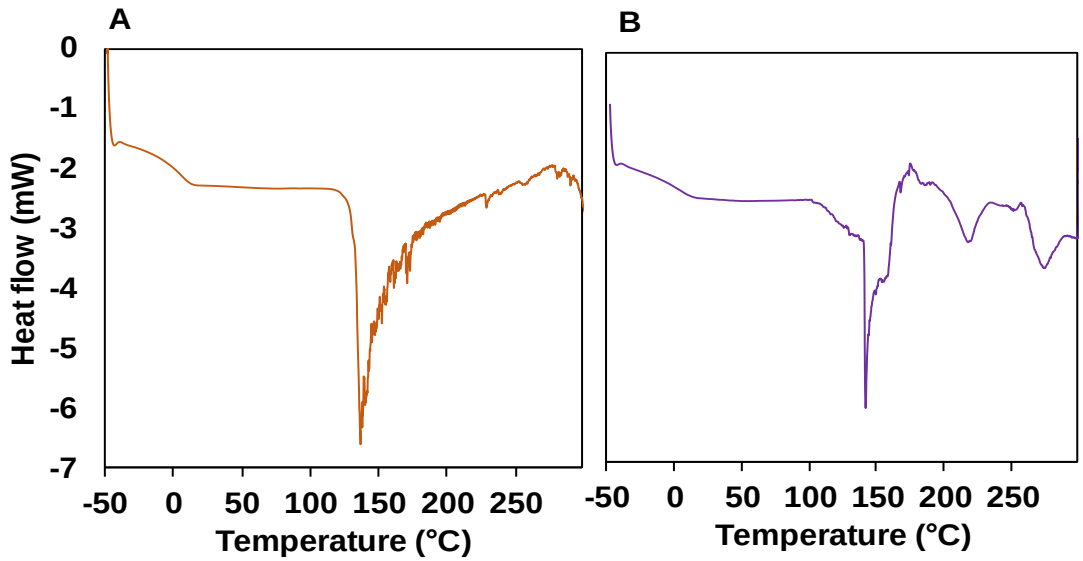

Figure 3.S6. DSC thermograms of A) [TBP][MTX] and B) [PheEt][MTX]

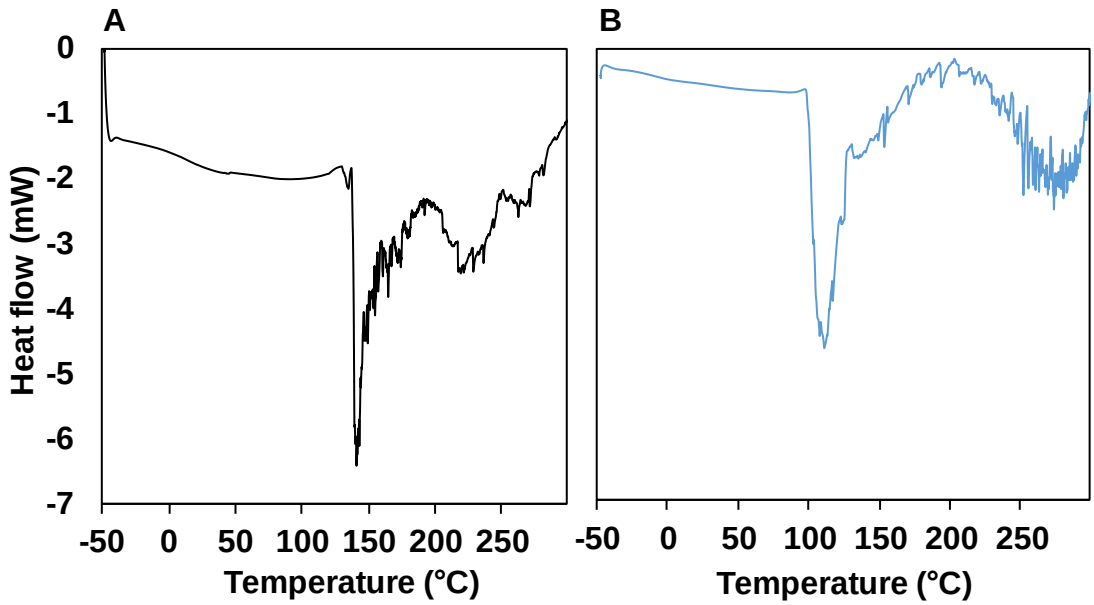

Figure 3.S7. DSC thermograms of A) [TMA][MTX] and B) [EMI][MTX].

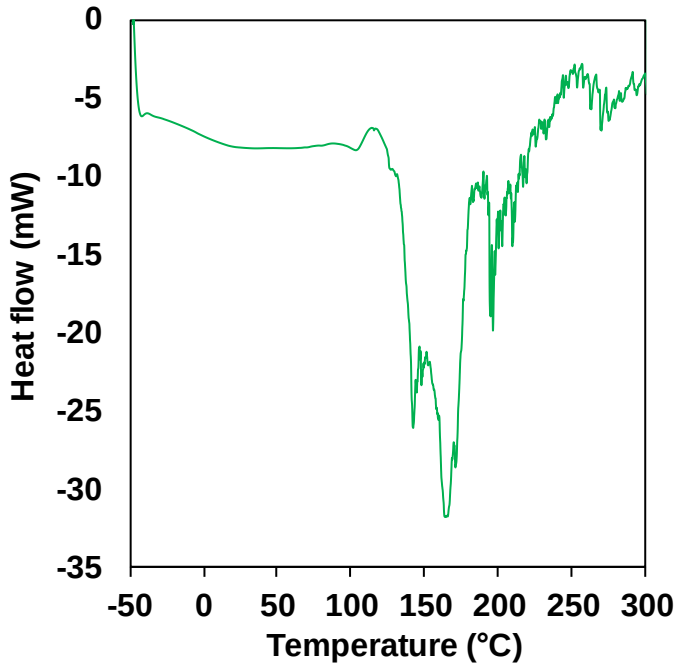

Figure 3.S8. DSC thermograms of [AspEt][MTX].

5. Solubilities of MTX-ILs in water

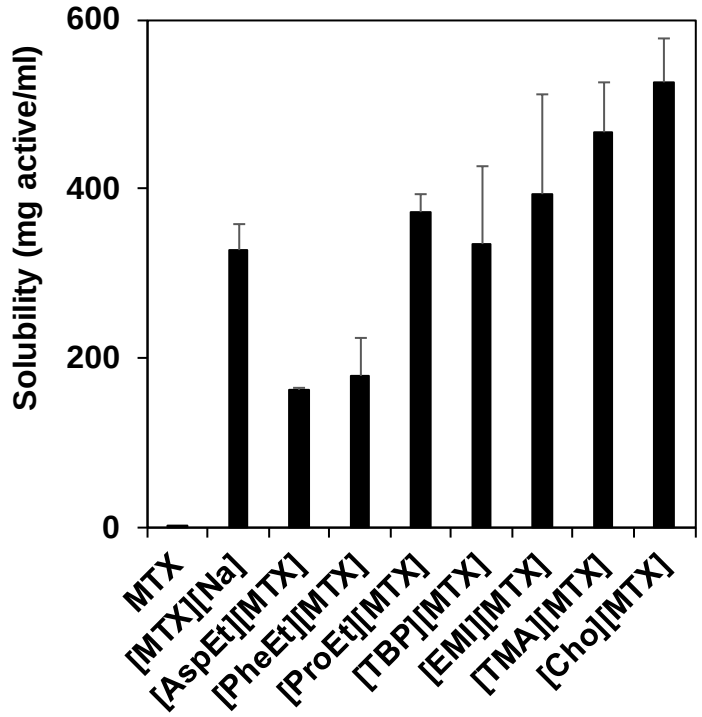

Figure 3.S9. Solubilities of MTX-IL moieties in water.

CHAPTER 4: *N*-METHYL-2-PYRROLIDONE-BASED IONIC LIQUID AS AN ENHANCER FOR TOPICAL DRUG DELIVERY: SYNTHESIS, CHARACTERIZATION, AND SKIN-PENETRATION EVALUATION

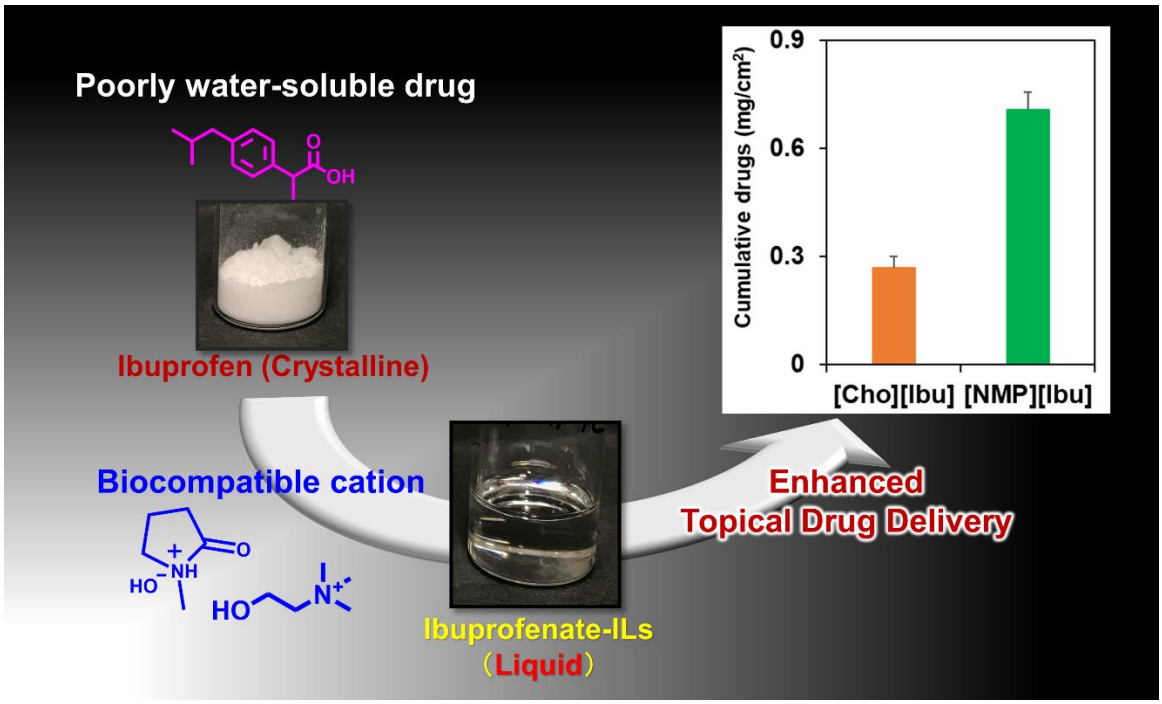

4.1. Abstract

The pharmacological properties of the active pharmaceutical ingredients (APIs) can be significantly enhanced when they are synthesized in ionic liquids (ILs) form. IL-APIs provide better physico-chemical and thermal properties than that of crystalline or solid-state salts drugs. However, the toxicological aspects of IL-APIs is the foremost concern for their effective applications in drug delivery. In this study, we introduced *N*-Methyl-2-pyrrolidone (NMP) as a potent biocompatible counter ion to prepare ionic liquefied drugs for topical drug delivery. The cytotoxicity of NMP cation was investigated using mammalian cell lines (NIH3T3 and L929 cells) and showed lower cytotoxicity than that of conventional counter cations. The synthesized NMP-based ionic liquid (NMP-IL) was characterized using ^{1}H & ^{13}C-NMR, FT-IR, DSC and TGA. NMP-IL showed better physico-thermal stability, enhanced skin penetration, and enriched drug accumulation 2.6 times higher than that of IL [Cho][Ibu] in the target tissue. These results suggested that NMP cation based API-IL can be an effective biocompatible formulation for topical drug delivery by accumulating active drugs in the skin.

4.2. Introduction

The development of effective drug delivery methods to target specific pharmacological responses is difficult for crystalline active pharmaceutical ingredients (APIs) because of their polymorphism and low aqueous solubility and bioavailability[1–3]. To address these limitations, the use of API ionic liquids (API-ILs; generally prepared by an equimolar pairing of an ionizable drug with an appropriate counter-ion[4,5]) has appeared as a promising approach to modify the physicochemical and biopharmaceutical properties of drug molecules to improve the solubility, skin permeability, stability, and bioavailability[5–8]. In addition, the effective design and choice of the counter ion can improve the synergetic action of the API-ILs[3]. For example, API-ILs of ibuprofen, ampicillin, nalidixic acid, and salicylic acid have been combined with different counter-ions that provided better skin permeability, antibacterial, or antifungal activity with improved solubility and thermal stability compared with the commercially used salts[5,9,10]. The biological activity of API-ILs also depends on the structure of the cations[6,11,12]. It has been reported that the antibacterial activity of the API-ILs was influenced greatly by the cations, when antibacterial agents (benzalkonium or didecyldimethylammonium) were combined with an artificial sweetener (acesulfame or saccharinate)[11].

Despite considerable progress in designing and preparing API-ILs, biocompatible API-ILs for topical or transdermal and oral drug delivery are limited[4]. In fact, the biocompatibility of

API-ILs is highly dependent on the cations, which also play an important role during dermal drug delivery. Generally, solid API salts penetrate poorly through skin compared with the neutral analogs[13]. When a poorly water-soluble API is combined with a counter-cation and the IL form is generated, the skin or membrane transport can be enhanced by the appropriate choice of cation. For example, transdermal delivery of salicylate triethylene glycol monomethyl ether tributylammonium was shown to be ~2.5-fold faster than using choline or 1-methylpyrrolidinium cations[14]. In another study, transdermal delivery of salicylate proline ethyl ester was shown to be three times faster than salicylate alanine ethyl ester[5]. Although API-ILs using various cations, including ammonium-, phosphonium-, imidazolium- and pyridinium-based API-ILs exhibit enhanced solubility and permeability, many of these compounds are not biocompatible. Recently, the biocompatible choline cation has been paired with Biopharmaceutics Classification System (BCS) class 4 drugs, such as sulfasalazine, resulting in improved solubility and bioavailability of the API-ILs[7]. Cholinium geranate has been used to deliver antibiotics through dermal delivery and showed excellent biocompatibility and multi-functional properties[15]. It is therefore desirable to synthesize API-ILs with cations that are not only effective in dermal delivery, but are also biocompatible, to further increase the potential applications of API-ILs.

The aim of this study was to synthesize a new API-IL with a biocompatible cation from neutral *N*-methyl-2-pyrrolidone (NMP) solvent. NMP was chosen because NMP is a biodegradable, the Food and Drug Administration (FDA)-approved enlisted as generally recognized as safe solvent with low toxicity, which is known to enhance the absorption of topically applied drugs[16–18]. NMP hydroxide was used as a potential biocompatible counter cation to convert the non-steroidal anti-inflammatory drug ibuprofen, as a model API, into the IL form. A penetration study of this API-IL was then performed using pig skin.

4.3. Experimental

4.3.1. Materials

Ibuprofen (anhydrous, >98% purity) was obtained from Tokyo Chemical Industry Co., Ltd (Tokyo, Japan). Hydrochloric acid, silver oxide, diethyl ether and N-Methyl-2-pyrrolidone (NMP) were purchased from Wako Chemicals Ltd. (Osaka, Japan). No purification was done for any analytical reagents, which were used in this study.

Gibco minimal essential medium (MEM), Dulbecco's phosphate buffered saline (PBS), Opti-MEM, fetal bovine serum, and antibiotic–antimycotic were also purchased from Thermo Fisher Scientific (Waltham, MA, USA). The WST-8 cell counting kit was obtained from Dojindo

Molecular Technologies, Inc. (Kumamoto, Japan). NIH3T3 and L929 were obtained from the RIKEN cell bank (Tsukuba, Japan).

4.3.2. General synthetic procedure for cations

The typical synthetic procedure of NMP cation is described briefly as follows[19]. 1.0 mol of NMP commercial solvent was weighted and added in 20 ml water and then 1.0 mol of hydrochloric acid was added dropwise to the solution. The resultant mixture was kept on ice for 1 h and, then 24 h at room temperature under constant stirring. The excess water was evaporated under reduced pressure to yield the NMP hydrochloride salt. Then, the salt was dissolved in distilled and neutralized with silver oxide (mole ratio of silver oxide: NMP salt = 2:1) for 2 h at room temperature. The resultant solution was filtered using whatman filter (grade 41) and evaporated the filtrate under reduced pressure to yield the NMP hydroxide. The synthesized cation was characterized by proton nuclear magnetic resonance spectroscopy (^{1}H & ^{13}C NMR).

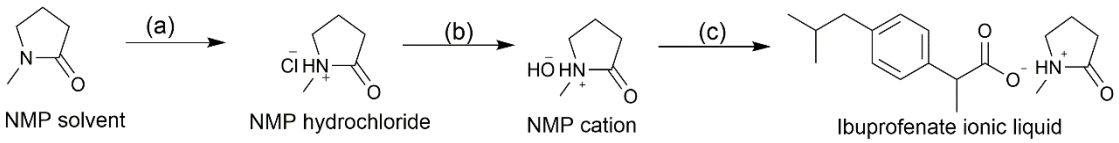

Scheme 4.1. Synthetic scheme for the NMP-based IL. (a) Hydrochloric acid in water on ice for 1 h, and then at room temperature for 24 h; (b) silver oxide in water at room temperature for 2 h; (c) ibuprofen powder at 40 °C for 2 h.

Choline hydroxide cation was synthesized using according to the previously published protocol[2]. In briefly, two gram of choline chloride salts was dissolved in 50 ml water and, then added equimolar of silver oxide under constant stirring. The mixture was kept for 2 h at room temperature. The resultant solution was filtered using whatman filter (grade 41) and evaporated the filtrate under reduced pressure to yield the choline hydroxide cation.

4.3.3. General synthetic procedure for Ibu-ILs

Ibu-ILs were synthesized using the neutralization method, according to the procedure of previously published literature[5]. In briefly, an equimolar amount of ibuprofen free drug and respective cation were stirred thoroughly in dark for 2 h at 40 °C. A clear and colorless solution was obtained and then purities of API-ILs were determined using ^{1}HNMR.

4.3.4. Measurements

The ^{1}H and ^{13}C NMR spectra of API-ILs were carried out in deuterated DMSO/ methanol/ chloroform with tetramethylsilane as the internal standard using a JEOL ECZ400S 400 MHz spectrometer (Tokyo, Japan) at room temperature. The unit of coupling constants (J) are in Hertz (Hz). The obtained spectra were analyzed usin DeltaV software package (version 5.0.5.1, JEOL). The purities of the synthesized compounds were calculated by using following equation:

Purity (%) = [ΣI (product)/ΣI (total)] × 100 …..……. (4.1)

where I represent the relative area of each signal.

The FT-IR spectra of NMP cation and API-ILs were measured by using Perkin Elmer (Frontier FT/IR, MA) featuring a lessened whole reflection sampler equipped with diamond crystal. All spectra were recorded by collection of 20 scans in the wavenumber range 400–4000 cm^{-1}. Differential scanning calorimetric (DSC) data were recorded on a Hitachi High-Technologies DSC X7000 (Tokyo, Japan). Approximately 5–6 mg of samples were taken in standard aluminum pans and sealed an aluminum lid using a press (T Zero sample press). Scans were conducted under constant nitrogen at 30 mL/min with a heating range from −60 to 250°C at a rate of 10°C/min. The reference was used as an empty pan. Thermogravimetric and derivative thermogravimetric analysis (TGA/DTG) data were recorded on a Hitachi High-Technologies TG/DTA 7300 (Tokyo, Japan). Approximately 5–10 mg of samples were heated from 30 to 400 °C at rate of 5 °C min^{-1} in an aluminum crucible under constant nitrogen at 30 mL/min. An isothermal was conducted for 30 min to remove volatile solvents at 70 °C.

Characterization of NMP cation

^{1}H-NMR (400 MHz, Methanol-D4, TMS) δ ppm: 2.07-1.99 (m, 2H), 2.35 (t, J = 8.2 Hz, 2H), 2.82 (s, 3H), 3.44 (t, J = 7.1 Hz, 2H). water (4.8ppm). ^{13}C-NMR (400 MHz, DMSO-D6, TMS) δ ppm: 17.74, 29.45, 30.60, 39.41, 39.62, 39.83, 40.03, 40.24, 40.45, 40.66, 49.00, 174.28.

Characterization of Ibuprofen

^{1}H-NMR (400 MHz, DMSO-D6, TMS) δ ppm: 0.85 (d, J = 6.4 Hz, 6H), 1.34 (d, J = 6.9 Hz, 3H), 1.84-1.77 (m, 1H), 2.41 (d, J = 7.3 Hz, 2H), 3.62 (q, J = 7.0 Hz, 1H), 7.14 (dd, J = 38.0, 7.8 Hz, 4H), 12.22 (s, 1H). ^{13}C-NMR (400 MHz, CHLOROFORM-D, TMS) δ ppm: 18.19, 22.51, 30.29, 45.15, 45.18, 76.83, 77.15, 77.47, 127.42, 129.51, 137.09, 140.96, 181.45.

Characterization of [NMP][Ibu] IL

^{1}H-NMR (400 MHz, *DMSO-D6*, TMS) δ ppm: 0.83 (dd, J = 15.1, 6.4 Hz, 6H), 1.33 (t, J = 7.5 Hz, 3H), 1.93-1.77 (m, 3H), 2.20-2.16 (m, 2H), 2.41 (d, J = 7.3 Hz, 2H), 2.68 (d, J = 14.6 Hz, 3H), 3.31-3.28 (m, 2H), 3.62 (q, J = 7.2 Hz, 1H), 7.20-7.08 (m, 4H). ^{1}H-NMR (400 MHz,

CHLOROFORM-D, TMS) δ ppm: 0.94-0.88 (m, 6H), 1.53-1.47 (m, 3H), 2.03-1.79 (m, 3H), 2.44-2.36 (m, 4H), 2.82 (t, J = 15.1 Hz, 3H), 3.38-3.35 (m, 2H), 3.69 (q, J = 7.2 Hz, 1H), 7.28-7.07 (m, 4H), 8.52 (s, 1H). ^{13}C-NMR (400 MHz, DMSO-D6, TMS) δ ppm: 17.74, 19.03, 22.65, 29.47, 30.14, 30.62, 39.36, 39.57, 39.77, 39.98, 40.19, 40.40, 40.62, 44.77, 44.86, 49.02, 127.60, 129.45, 139.03, 140.06, 174.32, 175.98.

Characterization of physical mixture (NMP solvent and Ibu)

^{1}H-NMR (400 MHz, DMSO-D6, TMS) δ ppm: 0.90-0.81 (m, 6H), 1.39-1.34 (m, 3H), 1.93-1.76 (m, 3H), 2.18 (t, J = 8.0 Hz, 2H), 2.41 (d, J = 7.3 Hz, 2H), 2.70 (t, J = 15.1 Hz, 3H), 3.35-3.28 (m, 2H), 3.62 (q, J = 7.2 Hz, 1H), 7.14 (dd, J = 36.9, 8.3 Hz, 4H), 12.23 (s, 1H). ^{1}H-NMR (400 MHz, CHLOROFORM-D, TMS) δ ppm: 0.89 (d, J = 6.9 Hz, 6H), 1.49 (d, J = 7.3 Hz, 3H), 2.05-1.80 (m, 3H), 2.45-2.37 (m, 4H), 2.86 (d, J = 15.1 Hz, 3H), 3.38 (t, J = 7.1 Hz, 2H), 3.70 (q, J = 7.2 Hz, 1H), 7.27-7.08 (m, 4H).

Characterization of [Cho][Ibu] IL

^{1}H-NMR (400 MHz, DMSO-D6, TMS) δ ppm: 0.85 (d, J = 6.4 Hz, 6H), 1.25 (d, J = 6.9 Hz, 3H), 1.80 (q, J = 6.7 Hz, 1H), 2.38 (d, J = 6.9 Hz, 2H), 3.09 (d, J = 13.3 Hz, 9H), 3.39-3.33 (m, 3H), 3.81 (d, J = 4.6 Hz, 2H), 7.09 (dd, J = 75.0, 7.8 Hz, 4H). ^{1}H-NMR (400 MHz, CHLOROFORM-D, TMS) δ ppm: 0.87 (d, J = 6.9 Hz, 6H), 1.36 (d, J = 6.9 Hz, 3H), 1.83-1.76 (m, 1H), 2.39 (d, J = 7.3 Hz, 2H), 2.86 (d, J = 15.1 Hz, 9H), 3.18-3.16 (m, 2H), 3.52 (q, J = 7.0 Hz, 1H), 3.77 (q, J = 2.1 Hz, 2H), 7.01 (d, J = 8.2 Hz, 2H), 7.27-7.22 (m, 2H).

4.3.5. Stratum corneum (SC) studies using FT-IR

SC studies were carried out according to the procedure reported by Mitragotri S. groups[15]. Briefly, YMP pig skin was heated for 10 min in a 60 °C hot plate with raping an aluminum foil to separate the SC containing epidermis layer from dermis of skin. The SC layer was soaked in trypsin to digest the epidermis from SC. The SC layer was washed in water and dried under fume hood for 24 h at room temperature. SC pieces (1.5 cm x 1.5 cm) were incubated with 0.3 ml of test samples for 24 h at 32.5 °C. The following day, SC samples were rinsed by soaking in water and dried for 24 h under fume hood at room temperature.

A Fourier Transform Infra-Red (FT-IR) spectrum was obtained from each sample using Perkin Elmer spectrometer (Frontier FT/IR, Waltham, MA) with an accumulation of 20 scans in the range 500–4000 cm^{-1}.

4.3.6. Partitioning co-efficient

The log P value of the synthesized API-ILs were measured by using octanol and water system.

About 3 mg free API containing API-ILs were added into the equivolume mixtures of octanol (5ml) and milli-q water (5ml). The resultants were permitted to mix overnight in the dark at room temperature with constant shaking. Then, the mixture was centrifuged to separate the layers at 10,000 rpm for 45 min. Quantifications of free ibuprofen in each layer was performed with known concentrations of standard at 230 nm through UV spectroscopy (JASCO V-750), Japan. The following formula was used to determine the partioning co-efficient (log $P_{o/w}$) of synthesized API-ILs.

$\log P_{o/w} = \log (Solute_{octanol} / Solute_{water})$……..……..(4.2)

4.3.7. Skin penetration study

The skin permeation test was performed using a female Yucatan micro pig (Charles River Japan Inc.,Tokyo, Japan) in Franz-type diffusion cell. The fat layer of skin was carefully removed and cut into small pieces. The skin was positioned into the Franz diffusion cell with inner skin facing to receptor phase. The receptor phase was filled with 5 mL of equivolume of phosphate solution and ethanol with constant stirring at 32.5 °C. Then, 0.3 mL of API-IL solutions were drawn on the outer side of skin (donor phase) and covered with parafilm to minimize the atmosphere absorption. Aliquots (0.1 mL) of the receiving phases were withdrawn at fixed intervals for 96 h and quantified the concentration of ibuprofen by HPLC analysis. The quantification was carried out by using a 250 x 4.6 mm ODS L-column with mobile phase consisted of 60 % acetonitrile and 40% water (adjusted to pH to 3.0 with phosphoric acid). The eluted ibuprofen was calculated by calibrating with known concentrations of standard at 230 nm.

4.3.8. In vitro cytotoxicity evaluation

Viability evaluation of the WST-8 cell was performed using mouse fibroblast cell lines NIH3T3 and L929 by a previously reported method with some modifications[5]. The cells were cultivated on a cell culture dish and trypsinized to collect the cells from the dish. The target cells were matured at 5000 cells/well in a 96-well flat-bottomed plate system and cultured for 24 h in MEM (containing 10% fetal bovine serum and 1% antibiotic–antimycotic) at 37 °C in a CO_2 incubator. The samples were prepared in Opti-MEM with concentrations in the range 0.01–200 mM. The medium of each well was then replaced by 100 µL of each sample solution and the plates were kept in an incubator for 24 h. The wells were then washed twice with phosphate-buffered saline after the solution was removed from each well. The mitochondrial activities of the cells were measured using 100 µL of Opti-MEM containing 10 µL of the WST

assay reagent. After 3 h incubation at 37 °C in a CO_2 incubator, the absorbance of the supernatant ($A_{treated}$) was measured at 450 nm with a microplate spectrophotometer (Bio-Rad, Tokyo, Japan). A control ($A_{control}$) was prepared by dilution of the cell in Opti-MEM without a sample. The relative cell viability indicates the cytotoxicity, which was determined by the following equation:

Cell viability (%) = $(A_{treated}/A_{control}) \times 100$…….…… (4.3)

The average values of three repeated measurements are reported. Microsoft Excel 2016 (Microsoft, Washington, USA) was used for statistical analysis of the data. The half maximal inhibitory concentration (IC_{50}) of each sample was calculated. The results are given as the mean and standard deviation.

4.3.9. Statistical Analysis

Statistical analysis was evaluated using GraphPad Prism version 6 software (GraphPad Software, Inc., La Jolla, CA). Statistical significance was calculated through a one-way analysis of variance (ANOVA) followed by Tukey's post-hoc test for multiple comparisons.

4.4. Results & discussion

4.4.1. Synthesis and characterization of NMP-based ionic liquid

API-IL techniques are considered as promising approaches to transform the poorly water-soluble drugs into a liquid form to increase their pharmacological responses in targeted sites. The NMP-based API-IL was synthesized by neutralization of the hydrophobic crystalline drug ibuprofen as the free acid with NMP hydroxide as a base (Scheme 4.1). The NMP cation was synthesized by adding an equimolar amount of silver oxide with the chloride salt of NMP, which was prepared by the reaction between commercially available NMP solvent and hydrochloric acid in water[20]. The resulting product, *N*-methyl-2-pyrrolidone ibuprofenate ([NMP][Ibu]), formed as a clear and colorless liquid (Figure 4.1).

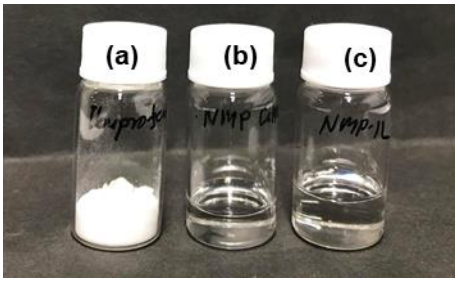

Figure 4.1. Photographs of free ibuprofen powder (a), NMP cation (b), and IL [NMP][Ibu] (c).

It was found that the sparingly soluble solid ibuprofen was fully converted into ionic liquefied ibuprofen as a room temperature IL. The yield of the synthesized NMP cation was 65.3%. The purity of the cation as determined by NMR was >99.0%.

The stoichiometric ratio (1:1) between the two constituents of API-IL ([NMP][Ibu]) was confirmed by ^{1}H NMR[4,21]. The peak from the –COOH hydrogen of free ibuprofen was detected at 12.2 ppm in DMSO (Figure 4.2A and Figure 4.S1), but no clear peak was observed for the –COOH hydrogen of IL [NMP][Ibu] in DMSO (Figure 4.2C and Figure 4.S4). Interestingly, a new singlet peak was detected at 8.5 ppm in $CDCl_3$ as the NMR solvent (Figure 4.2D and Figure 4.S5), indicating full ionization by proton transfer between NMP hydroxide and ibuprofen had occurred. In the physical mixture of ibuprofen and NMP (an equimolar amount of free ibuprofen and neutral NMP), a singlet peak was detected at 12.2 ppm in DMSO (Figure 4.2E and Figure 4.S6) indicating that no ionization by proton transfer between ibuprofen and NMP had occurred (Figure 4.2F and Figure 4.S7). These results suggested that only the NMP cation was able to transfer the proton from the acidic drug and form an IL.

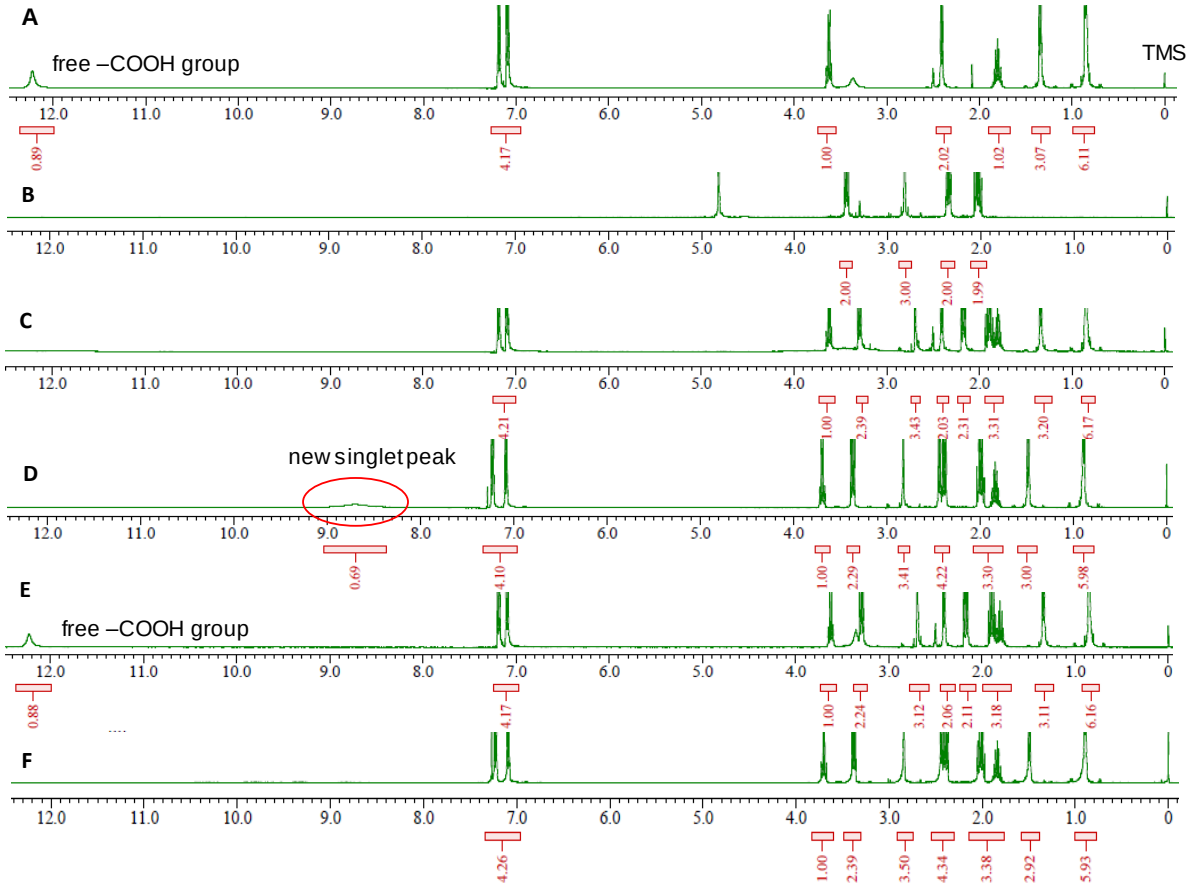

Figure 4.2. ^{1}H NMR spectra of free ibuprofen in DMSO (A), NMP hydroxide in CD_3OD (B), IL [NMP][Ibu] in DMSO (C), IL [NMP][Ibu] in $CDCl_3$ (D), physical mixture of ibuprofen and NMP in DMSO (E), and in $CDCl_3$ (F).

To further confirm the structure of the API-IL, FT-IR spectroscopy was used to assess the ionization of free ibuprofen, the NMP cation, and IL [NMP][Ibu] (Figure 4.3). In the FT-IR spectra of IL [NMP][Ibu], the characteristic peaks for the C=O stretching of ibuprofen at 1712 cm^{-1} and the C=O vibration of the NMP cation at 1685 cm^{-1} were slightly shifted to higher frequencies at 1735 and 1691 cm^{-1}, respectively[9,22]. A new broad peak was detected at 1650 cm^{-1} in the FT-IR spectra of IL [NMP][Ibu], indicating a strong hydrogen-bonding interaction between ibuprofen and the NMP cation.

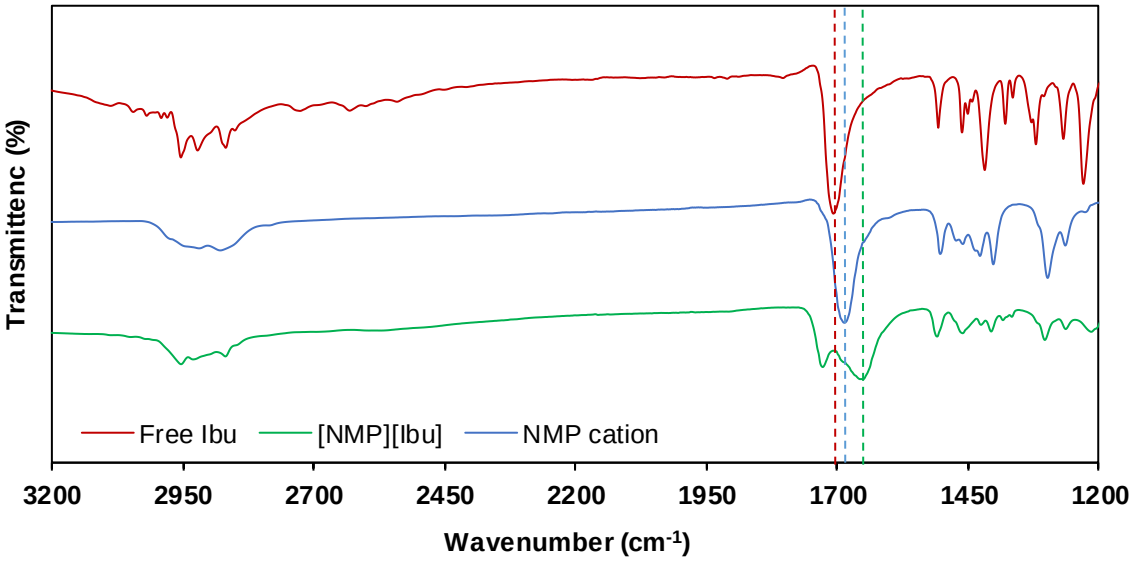

Figure 4.3. FT-IR spectra of free ibuprofen (Ibu), NMP cation and IL [NMP][Ibu].

The storage stability of the synthesized API-IL ([NMP][Ibu]) at room temperature was evaluated by ^{1}H NMR for up to 6 months. No color changes or hydrolysis was observed. The IL retained drug efficacy during the examined period, as quantified by HPLC. Therefore, IL [NMP][Ibu] had good stability at room temperature.

4.4.2. Thermophysical studies of NMP-based ionic liquid

The thermoanalytic methods, Differential scanning calorimetric (DSC) and Thermogravimetric/ derivative thermogravimetric analysis (TGA/DTG), were used to confirm a possible thermal interaction between free ibuprofen and the NMP cation. In the DSC thermogram of free ibuprofen, a characteristic sharp endothermal peak was observed at 76.6 °C, which corresponds to the melting point of ibuprofen (Figure 4.4). This peak had disappeared in the thermogram of IL [NMP][Ibu], indicating no crystallization or polymorphism was present, which is a considerable advantage for pharmaceutical formulation and stability[10,23].

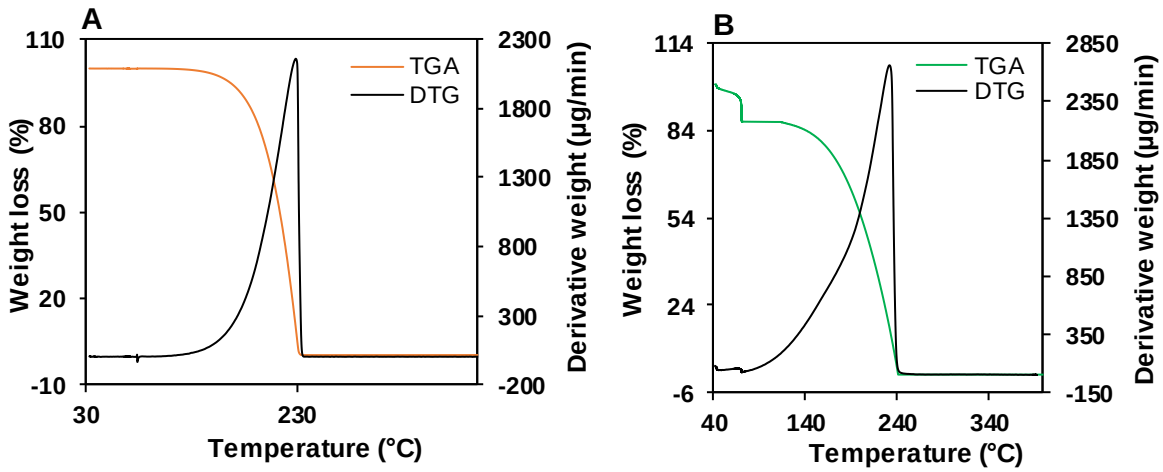

Figure 4.4. TGA and DTG thermograms of A) free ibuprofen (Ibu) and B) IL [NMP][Ibu].

To further investigate the thermal stability of IL [NMP][Ibu], we also carried out TGA and calculated the onset ($T_{5\%\ onset}$) temperature. The thermal decomposition of free ibuprofen and IL [NMP][Ibu] were showed in the TGA and DTG thermograms (Figure 4.5). The initial decomposition of IL [NMP][Ibu] occurred from 40 °C to 75 °C with ca.10% loss of initial mass due to removal of volatile molecules (Figure 4.5B), whereas the free ibuprofen was ca. 2% loss of initial mass from 40 °C to 140 °C (Figure 4.5A). The actual decomposition of IL [NMP][Ibu] started from 110 °C to 240 °C with 100% loss of initial mass. The $T_{5\%\ onset}$ of IL [NMP][Ibu] indicated good thermal stability up to 110 °C.

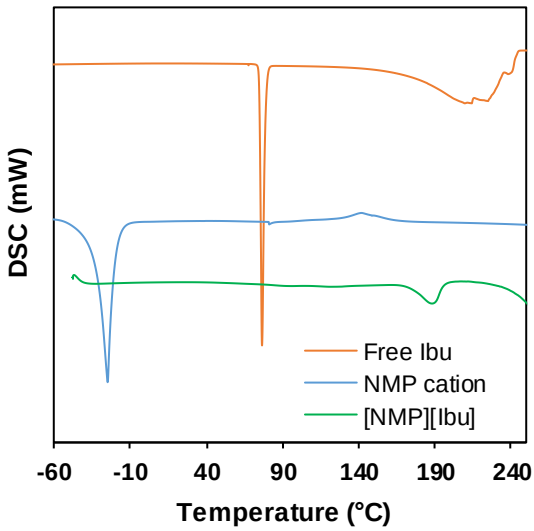

Figure 4.5. DSC thermograms of free ibuprofen (Ibu), [NMP][OH] cation and IL [NMP][IBU].

4.4.3. Effect of NMP-based ionic liquid on stratum corneum structure

The skin permeation profile of IL [NMP][Ibu] was investigated to evaluate possible pharmaceutical application for dermal delivery, using a Franz diffusion cell system according

to our previous study[5]. The efficiency of IL [NMP][Ibu] as a skin-penetration enhancer was compared with choline ibuprofenate (IL [Cho][Ibu]), which is a known biodegradable API-IL with low toxicity[2,3,12]. FT-IR studies were performed to evaluate the effect of NMP and choline cations on the structure of the stratum corneum (SC) using pig skin[15,24]. Generally, extraction and/ or fluidization of the lipids from SC bilayers increases with increasing drug penetration through the skin[15,25]. As shown in Fig. 4.6A, characteristic peaks for lipids were observed between 2800 and 3000 cm^{-1} in the FT-IR spectra and the peak heights indicated the lipid content in the SC samples[15]. A trend for reduced peak heights for the CH_2 symmetric stretching at 2850 cm^{-1} and/ or the CH_2 asymmetric stretching at 2922 cm^{-1} were observed in both incubated IL samples, but all the peak heights were significantly reduced for IL [NMP][Ibu] (NMP may conjugate with the lipophilic lipid molecules, then partition the lipids by weakening the inter-lipid interactions and extract the lipids into the NMP reservoir on the skin surface)[17,26]. This peak reduction suggests that NMP acts as a lipid extractor to increase the penetration of ibuprofen into the skin. Moreover, the peak heights at 2850 and 2922 cm^{-1} decreased with increasing hydrophobicity of the incubated ILs (the partition coefficients of IL [Cho][Ibu] and IL [NMP][Ibu] are –0.56 and 2.26, respectively), suggesting increased lipid removal from the SC with increasing hydrophobicity[24].

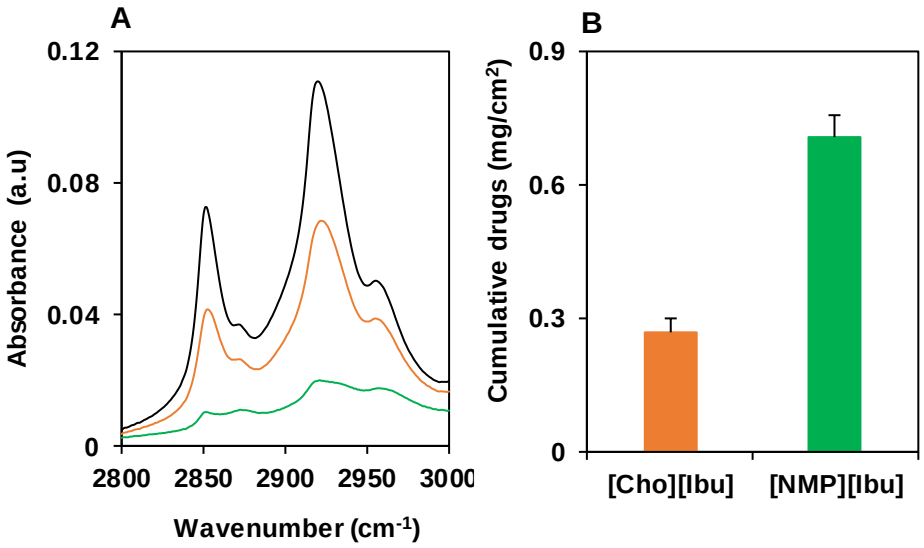

Figure 4.6. *In vitro* skin penetration profile of ibuprofenate ILs. A) FT-IR spectra of the lipid content for SC control sample (black line), IL [Cho][Ibu] (orange line), and IL [NMP][Ibu] (green line) as measured by the peak heights of the CH_2 asymmetric and symmetric stretching bands. B) Drug retention in the skin (epidermis and dermis) after 1 h. Data are expressed as mean ± SD, n = 3.

4.4.4. In vitro skin permeation/ retention of NMP-based ionic liquid

After the liquefied API-ILs were applied on pig skin (5 month-old female Yucatan micro pig; purchased from Charles River Laboratories International, Inc., MA, USA), the amount of ibuprofen was detected into the skin and the receiver phase by HPLC analysis at regular intervals. After one hour, the cumulative amount of ibuprofen into the skin for IL [NMP][Ibu] was 0.71 mg/cm^2, which was 2.6 times higher than that for IL [Cho][Ibu] (Figure 4.6B). There was no detectable amount of the drug in the receiver phase after one hour. This retention of ibuprofen into the skin can be attributed to the molecular interactions between NMP, skin lipids, and the drug[27] (via π interactions, van der Waals interactions, and hydrogen bonding)[28,29]. NMP has known solubilizing properties, so NMP may be able to solubilize the drug in the tissue. As a result, the thermodynamic activity (the driving force for the permeation process) of the drug molecules is reduced and the drug is retained for a prolonged period[30].

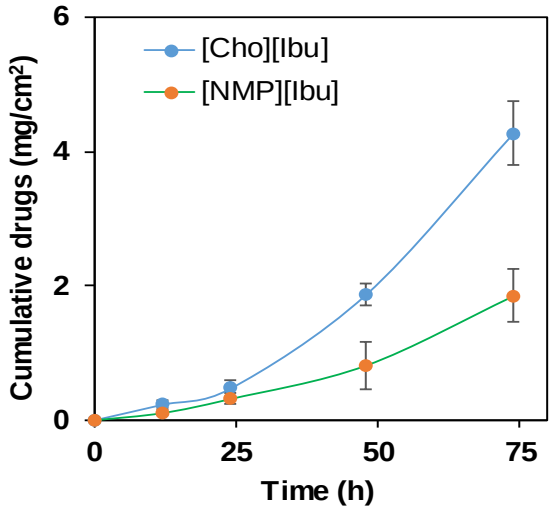

Figure 4.7. Skin permeation of [NMP][Ibu] IL and [Cho][Ibu] IL. . Data are expressed as mean ± SD, n = 3.

However, the cumulative amount of ibuprofen for both API-ILs in the receiver phase was significantly increased with increasing application times (Figure 4.7). The IL [Cho][Ibu] permeated faster through the skin than IL [NMP][Ibu] over a prolonged period. After 74 h, the cumulative transport of ibuprofen from IL [Cho][Ibu] was 4.3 mg/cm^2, whereas the transport of ibuprofen from IL[NMP][Ibu] was 1.9 mg/cm^2 (Figure 4.7). This difference may be caused by NMP for altering the solvent surrounding the skin membrane and creating reservoirs in the skin membrane, which gave a sustained release of the drug over a prolonged period[17]. If the affinity between the drug molecules and the skin lipids is high, NMP could cause the penetration of the drug to slow down. However, further studies are needed to determine the

specific mechanisms involved. These results clearly suggested that an API-IL based on the NMP cation can be an effective formulation for accumulating active drugs in the skin as a target tissue.

4.4.5. In vitro cytotoxicity of the synthesized NMP cation wilt ILs

To evaluate the biocompatibility of the synthesized NMP cation, mammalian cell lines NIH3T3 and L929 were used to investigate the cytotoxicity and the results were then compared with those of the cations, which were previously reported as a well-known biocompatible cation. It has been reported that proline ethyl ester (ProEt) or choline hydroxide showed lower toxicity on HeLa or L929 cell among the previously reported conventional cations such as 1-ethyl-3-methylimidazolium hydroxide, tetrabutylphosphonium hydroxide, etramethylammonium hydroxide, triethanolamine, etc. Moreover, NMP solvent is a biodegradable, FDA-approved solvent with low toxicity and used as a skin enhancer in pharmaceutical applications. However, the mathematical logarithm function was used to calculate the IC_{50} values (Figure 4.8). The IC_{50} of synthesized NMP cation showed almost similar toxicity with NMP solvent or ProEt cation in both cell lines, even though these values higher when compared with biocompatible choline hydroxide (Figure 4.8A). The IC_{50} values of NMP cation, NMP solvent, choline hydroxide and ProEt are 113.1, 120.3, 85.2 and 122.7 on NIH3T3 or 57.8, 62.6, 50.7 and 97.6 mM on L929 cell, respectively. Although, choline hydroxide cation is well-known biocompatible cation that showed higher toxicity as compared with NMP solvent or cation because of the ethanolic structure of choline hydroxide.

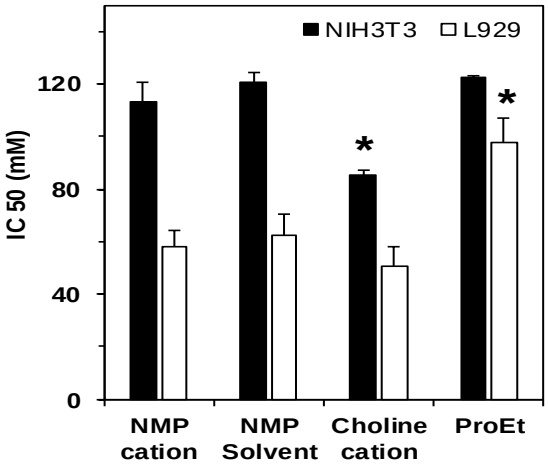

Figure 4.8. *In vitro* cytotoxicities of IL-forming cations with neutral NMP solvent in NIH3T3 and L929 cell lines. Statistical significance was estimated by one-way ANOVA followed by Tukey's post-hoc test for multiple comparisons. *P<0.05 versus all the other cations. Data are expressed as mean ± SD, n = 3.

These results clearly demonstrated that NMP cation is a new biocompatible counterion in the development of new ionic liquid drug formulations for topical or transdermal drug delivery.

4.4.6. Conclusions

We have developed the NMP cation as a promising biocompatible counter ion to form ILs with poorly- water insoluble drugs for topical drug delivery. The synthesized NMP cation is clear and colorless liquid at room temperature with high purity. NMP cation shows lower toxicity than that of conventional counter cations, indicating as a biocompatible and safe counter ion of API-ILs. When NMP cation combined with a model drug (ibuprofen), NMP-based API-ILs have potential advantages, including high physico-thermal stability, enhanced penetration through the SC, and ability to accumulate a drug in the target tissue of pig skin. This study provides information for the future development of API-IL formulations for the topical treatment of skin diseases.

4.5. References

[1] N. Adawiyah, M. Moniruzzaman, S. Hawatulaila, M. Goto, Ionic liquids as a potential tool for drug delivery systems, Med. Chem. Commun. 7 (2016) 1881–1897. doi:10.1039/C6MD00358C.

[2] C.M. Raihan, R.M. Moshikur, R. Wakabayashi, Y. Tahara, N. Kamiya, M. Moniruzzaman, M. Goto, Ionic-Liquid-Based Paclitaxel Preparation: A New Potential Formulation for Cancer Treatment, Mol. Pharm. 15 (2018) 2484–2488. doi:10.1021/acs.molpharmaceut.8b00305.

[3] J.M.M. Araújo, C. Florindo, A.B. Pereiro, N.S.M. Vieira, A.A. Matias, C.M.M. Duarte, L.P.N. Rebelo, I.M. Marrucho, Cholinium-based ionic liquids with pharmaceutically active anions, RSC Adv. 4 (2014) 28126–28132. doi:10.1039/c3ra47615d.

[4] S. Furukawa, G. Hattori, S. Sakai, N. Kamiya, Highly efficient and low toxic skin penetrants composed of amino acid ionic liquids, RSC Adv. 6 (2016) 87753–87755. doi:10.1039/C6RA16926K.

[5] R.M. Moshikur, M.R. Chowdhury, R. Wakabayashi, Y. Tahara, M. Moniruzzaman, M. Goto, Characterization and cytotoxicity evaluation of biocompatible amino acid esters used to convert salicylic acid into ionic liquids, Int. J. Pharm. 546 (2018) 31–38. doi:10.1016/j.ijpharm.2018.05.021.

[6] R. Ferraz, V. Teixeira, D. Rodrigues, R. Fernandes, C. Prudêncio, J.P. Noronha, Ž. Petrovski, L.C. Branco, Antibacterial activity of Ionic Liquids based on ampicillin

against resistant bacteria, RSC Adv. 4 (2014) 4301–4307. doi:10.1039/c3ra44286a.

[7] M. Shadid, G. Gurau, J.L. Shamshina, B.-C. Chuang, S. Hailu, E. Guan, S.K. Chowdhury, J.-T. Wu, S.A.A. Rizvi, R.J. Griffin, R.D. Rogers, Sulfasalazine in ionic liquid form with improved solubility and exposure, Med. Chem. Commun. 6 (2015) 1837–1841. doi:10.1039/C5MD00290G.

[8] H.D. Williams, L. Ford, S. Lim, S. Han, J. Baumann, H. Sullivan, D. Vodak, A. Igonin, H. Benameur, C.W. Pouton, P.J. Scammells, C.J.H. Porter, Transformation of Biopharmaceutical Classification System Class I and III Drugs Into Ionic Liquids and Lipophilic Salts for Enhanced Developability Using Lipid Formulations, J. Pharm. Sci. 107 (2018) 203–216. doi:10.1016/j.xphs.2017.05.019.

[9] S. Govardhana Rao, T. Madhu Mohan, T. Vijaya Krishna, K. Narendra, B. Subba Rao, Thermophysical properties of 1-butyl-3-methylimidazolium tetrafluoroborate and N-methyl-2-pyrrolidinone as a function of temperature, J. Mol. Liq. 211 (2015) 1009–1017. doi:10.1016/j.molliq.2015.08.019.

[10] M.T. Viciosa, G. Santos, A. Costa, F. Danède, L.C. Branco, N. Jordão, N.T. Correia, M. Dionísio, Dipolar motions and ionic conduction in an ibuprofen derived ionic liquid, Phys. Chem. Chem. Phys. 17 (2015) 24108–24120. doi:10.1039/c5cp03715h.

[11] W.L. Hough-Troutman, M. Smiglak, S. Griffin, W. Matthew Reichert, I. Mirska, J. Jodynis-Liebert, T. Adamska, J. Nawrot, M. Stasiewicz, R.D. Rogers, J. Pernak, Ionic liquids with dual biological function: Sweet and anti-microbial, hydrophobic quaternary ammonium-based salts, New J. Chem. 33 (2009) 26–33. doi:10.1039/b813213p.

[12] A. Yazdani, M. Sivapragasam, J.M. Leveque, M. Moniruzzaman, Microbial Biocompatibility and Biodegradability of Choline-Amino Acid Based Ionic Liquids, J. Microb. Biochem. Technol. 08 (2016) 415–421. doi:10.4172/1948-5948.1000318.

[13] M. Moniruzzaman, M. Tamura, Y. Tahara, N. Kamiya, M. Goto, Ionic liquid-in-oil microemulsion as a potential carrier of sparingly soluble drug: Characterization and cytotoxicity evaluation, Int. J. Pharm. 400 (2010) 243–250. doi:10.1016/j.ijpharm.2010.08.034.

[14] O. Zavgorodnya, J.L. Shamshina, M. Mittenthal, P.D. McCrary, G.P. Rachiero, H.M. Titi, R.D. Rogers, Polyethylene glycol derivatization of the non-active ion in active pharmaceutical ingredient ionic liquids enhances transdermal delivery, New J. Chem. 41 (2017) 1499–1508. doi:10.1039/C6NJ03709G.

[15] A. Banerjee, K. Ibsen, Y. Iwao, M. Zakrewsky, S. Mitragotri, Transdermal Protein Delivery Using Choline and Geranate (CAGE) Deep Eutectic Solvent, Adv. Healthc.

Mater. 6 (2017) 1–11. doi:10.1002/adhm.201601411.

[16] P.J. Lee, R. Langer, V.P. Shastri, Role of n-methyl pyrrolidone in the enhancement of aqueous phase transdermal transport, J. Pharm. Sci. 94 (2005) 912–917. doi:10.1002/jps.20291.

[17] H. Hamishehkar, M. Khoshbakht, A. Jouyban, S. Ghanbarzadeh, The relationship between solubility and transdermal absorption of tadalafil, Adv. Pharm. Bull. 5 (2015) 411–417. doi:10.15171/apb.2015.056.

[18] W.I. Higuchi, S.K. Li, Mechanistic Studies of the 1-Alkyl-2-pyrrolidones as Skin Permeation Enhancers, 84 (1995) 2–7.

[19] F.T. Li, B. Wu, R.H. Liu, X.J. Wang, L.J. Chen, D.S. Zhao, An inexpensive N-methyl-2-pyrrolidone-based ionic liquid as efficient extractant and catalyst for desulfurization of dibenzothiophene, Chem. Eng. J. 274 (2015) 192–199. doi:10.1016/j.cej.2015.04.027.

[20] X. Wang, M. Han, H. Wan, C. Yang, G. Guan, Study on extraction of thiophene from model gasoline with brønsted acidic ionic liquids, Front. Chem. Eng. China. 5 (2011) 107–112. doi:10.1007/s11705-010-0539-0.

[21] R.M. Moshikur, M.R. Chowdhury, R. Wakabayashi, Y. Tahara, M. Moniruzzaman, M. Goto, Ionic liquids with methotrexate moieties as a potential anticancer prodrug: Synthesis, characterization and solubility evaluation, J. Mol. Liq. 278 (2019) 226–233. doi:10.1016/j.molliq.2019.01.063.

[22] N. Carreras, V. Acuña, M. Martí, M.J. Lis, Drug release system of ibuprofen in PCL-microspheres, Colloid Polym. Sci. 291 (2013) 157–165. doi:10.1007/s00396-012-2768-x.

[23] Y. Miwa, H. Hamamoto, T. Ishida, Lidocaine self-sacrificially improves the skin permeation of the acidic and poorly water-soluble drug etodolac via its transformation into an ionic liquid, Eur. J. Pharm. Biopharm. 102 (2016) 92–100. doi:10.1016/j.ejpb.2016.03.003.

[24] E.E.L. Tanner, K.N. Ibsen, S. Mitragotri, Transdermal insulin delivery using choline-based ionic liquids (CAGE), J. Control. Release. 286 (2018) 137–144. doi:10.1016/j.jconrel.2018.07.029.

[25] S. Araki, R. Wakabayashi, M. Moniruzzaman, N. Kamiya, M. Goto, Ionic liquid-mediated transcutaneous protein delivery with solid-in-oil nanodispersions, Medchemcomm. 6 (2015) 2124–2128. doi:10.1039/c5md00378d.

[26] P.J. Lee, N. Ahmad, R. Langer, S. Mitragotri, V. Prasad Shastri, Evaluation of chemical enhancers in the transdermal delivery of lidocaine, Int. J. Pharm. 308 (2006) 33–39.

doi:10.1016/j.ijpharm.2005.10.027.

[27] M.F. Peralta, M.L. Guzmán, A.P. Pérez, G.A. Apezteguia, M.L. Fórmica, E.L. Romero, M.E. Olivera, D.C. Carrer, Liposomes can both enhance or reduce drugs penetration through the skin, Sci. Rep. 8 (2018) 1–11. doi:10.1038/s41598-018-31693-y.

[28] N. He, K.S. Warner, D. Chantasart, D.S. Shaker, W.I. Higuchi, S.K. Li, Mechanistic Study of Chemical Skin Permeation Enhancers with Different Polar and Lipophilic Functional Groups, 93 (2004) 1415–1430.

[29] K.S. Warner, S.K. Li, W.I. Higuchi, In ¯ uences of Alkyl Group Chain Length and Polar Head Group on Chemical Skin Permeation Enhancement, 90 (2001) 1143–1153.

[30] L. Montenegro, C. Bucolo, G. Puglisi, Enhancer effects on in vitro corneal permeation of timolol and acyclovir, Pharmazie. 58 (2003) 497–501.

CHAPTER 5. GENERAL CONCLUSIONS AND FUTURE WORK

5.1. General Conclusions

The pharmaceutical industry is facing unparalleled challenges to develop the effective drug delivery systems for achieving targeted pharmacological response of many drugs because of their polymorphism, limited solubility, permeability and bioavailability. To address these limitations, an IL based formulation of APIs is a promising approach to design the smart delivery of drugs. Recently, ILs have been extensively used to convert the crystalline drugs into API-IL form because they provide improved aqueous solubility, enhanced absorption, desired dissolution rate and even targeting ability. API-ILs also would solve the problem of polymorphism, a significant challenge in drug delivery. In this thesis, we mainly focused on the synthesis and characterization of IL-forming cations as well as API-ILs and evaluated their feasibility for drug delivery systems.

In the **second chapter**, we concentrated on the synthesis and characterization of biocompatible amino acid esters (AAEs) based cations for transforming the crystalline salicylic acid (Sal) into liquid forms. A series of amino acids such as proline alanine, aspartic acid, glutamic acid, leucine, methionine, tyrosine and phenylalanine were selected to convert AAE cations by considering their reportedly low toxicities and physico-chemical activities. To investigate the biological activity of AAE cations in mammalian cell lines (L929 and HeLa), we synthesized proline-based AAE cations with various alkyl chain lengths (C_1–C_4) and found that the cytotoxicity of AAE cations mainly depends on the alkyl chain length in the ester group. The AAE cations toxicity increased with increasing the alkyl chain length from C_2 to C_4 and ethyl ester-based AAE cation showed comparatively lower toxicity among the other alkyl chain lengths. All synthesized amino acid ethyl esters (AAEt) cations were clear, colorless room temperature liquids and miscible in water except for L-tyrosine ethyl ester, with high purities (> 97.0%). The AAEt cations were characterized using ^{1}H and ^{13}C NMR, FTIR, elemental, and thermogravimetric analyses. However, the toxicities of the AAEt cations greatly increased with inclusion of long alkyl chains, sulfur, and aromatic rings in the side groups of the cations. Among the synthesized AAEt's, AlaEt, AspEt, and ProEt had low cytotoxicities and were investigated as potential components for synthesis of salicylate ionic liquids (Sal-ILs) with the anionic Sal drug. All synthesized Sal-ILs were fully ionized and had high thermal stabilities. In contrast to free Sal, Sa-ILs were miscible with water at any ratio. The cytotoxicities of the Sal-ILs drastically increased compared with the AAEt's on incorporation of Sal into the cations,

and were comparable to that of free Sal. In view of transdermal application, skin permeation studies were performed using a female Yucatan micro pig skin with temperature controlled Franz diffusion cell and demonstrated that the Sal-ILs ([Sal][AspEt]) penetrated through skin approximately nine times faster than that of the Sal sodium salt.

In the **third chapter**, we have dedicated our attention for evaluating the effect of cations in API-ILs on *in vitro* solubility and antitumor activity, and then *In vivo* biocompatibility, pharmacokinetics and antitumor efficacy studies. For these purpose, we selected several types of IL-forming cations from amino acids, cholinium, imidazolium, ammonium, phosphonium groups by considering their reportedly lower toxicities among their corresponding groups and were synthesized for converting the poorly water-soluble methotrexate into IL forms (MTX-ILs). All the synthesized MTX-ILs were solids except [Cho][MTX], [EMI][MTX] and [TBP][MTX], with high purities (> 97.0%). The synthesized MTX-ILs were characterized through ^{1}H NMR, FTIR, p-XRD, DSC and thermogravimetric analysis. The stoichiometry ratio and the fully ionization of MTX-ILs between MTX and the cations were clearly assessed by using ^{1}H NMR and FTIR, respectively, and confirmed by comparing with fully ionized sodium salt of MTX. The p-XRD spectra of MTX-ILs were confirmed the amorphous phase of the MTX-ILs while the free MTX was crystalline in nature. In thermophysical study, the MTX-ILs showed almost similar thermal stabilities than that of the free hydrate MTX. The DSC thermogram of free MTX exhibited a characteristic sharp endothermic peak at 154 °C, whereas the characteristic sharp endothermic peak of MTX-ILs were shifted lower from 154 °C, indicating a significant changes in their physical state from crystalline to amorphous. The solubility of the MTX-ILs was evaluated in both water and simulated body fluids (phosphate-buffered saline, simulated gastric, and simulated intestinal fluids). The MTX-ILs showed aqueous solubility at least 5000 times higher than that of free MTX and two orders of magnitude higher compared with that of a sodium salt of MTX in both water and simulated body fluids. An assessment of the *in vitro* antitumor activity of the MTX-ILs in a mammalian cell line (HeLa cells) was used to evaluate their cytotoxicity. The amino acid ethyl ester-MTX IL ([ProEt][MTX] and [AspEt][MTX]) showed similar solubility as the MTX sodium salt but it provided improved *in vitro* antitumor activity. In view of practical application, in vivo biocompatibility, pharmacokinetics and antitumor efficacy of methotrexate ionic liquid moieties were investigated for envisaging their therapeutic application as a biocompatible component of a drug delivery system. In pharmacokinetic study through oral admiration, the MTX-ILs showed significantly higher pharmacokinetic parameters than that of sodium salt of

MTX especially amino acid ethyl esters based ILs (AAEt-MTX). The bioavailability of AAEt-MTXs showed at least six times higher than that of sodium MTX. Even though, AAEt-MTXs also orally biocompatible in mutli-doses of every after days at 15 mg/kg. The antitumor efficacy of MTX-ILs and sodium MTX are presently under investigation.

In the **fourth chapter**, we focused our attention for introducing a potent biocompatible cation to ionic liquefied the poorly water insoluble crystalline drugs and envisaging their biomedical applications. We chose the N-methyl-2-pyrrolidone (NMP) because of the advantageous properties such as biodegradability, the Food and Drug Administration (FDA)-approved enlisted as generally recognized as a safe solvent with low toxicity and well-known skin enhancer for topically applied drugs. The synthesized NMP cation was liquid at room temperature and showed lower cytotoxicity than that of conventional counter cations in mammalian cell lines (NIH3T3 and L929 cells). The synthesized NMP-based ionic liquid (NMP-IL) was characterized using ^{1}H & ^{13}C-NMR, FT-IR, DSC and TGA. In view of topical application, skin permeation studies were performed using a female Yucatan micro pig skin with temperature controlled Franz diffusion cell and demonstrated that NMP-IL showed enhanced skin penetration, and enriched drug accumulation 2.6 times higher than that of IL [Cho][Ibu] in the target tissue.

In conclusion, the obtained results (**chapter 2, 3 & 4**) suggest that AAEs or NMP could be a potent biocompatible counter ion to eliminate the use of traditional toxic solvents for oral/ topical/ transdermal delivery of poorly water-soluble drugs, since they allow an improved solubility and bioavailability or permeability of the studied APIs.

5.2. Future Work

In the presented studies, the concept of API-IL was focused on acidic APIs. The promising results suggest to expand the applicability of API-IL concept for converting crystalline basic APIs into IL form. Generally, basic APIs are ionized in in the acidic gastric fluids after oral administration and favored their dissolution and apparent solubility. ILs for basic APIs may be enhanced to stabilize these against precipitation in high pH environments.

The applicability of presented API-ILs were mainly in vitro topical/ transdermal applications. These result suggest for in vivo studies for envisaging their commercial biomedical applications. In addition, API-ILs concept may be obviously usable for many drugs and extended their applications in other routes of delivery. The applicability of API-ILs in oral and/ or transdermal delivery may be enhanced by considering appropriate counterions, lipophilic counterions may be the promising candidate for designing the effective drug delivery of API-ILs. However, the newly synthesized NMP cation would be a potential counterion for delivering many acidic drugs, although their molecular IL formation mechanisms are yet explored. The applicability of this cation would be generalized for envisaging their biomedical applications.

The studies presented here may be regarded as a starting point for this novel formulation platform, leading to a better insight of ILs as a formulation strategy and promising new IL based drug delivery systems.

ABBREVIATIONS

API	Active pharmaceutical ingredient
IL	Ionic liquid
API-IL	Active pharmaceutical ingredient ionic liquid
FDA	Food and drug administration
GRAS	Generally regarded as safe
GIT	Gastrointestinal tract
PBS	Dulbecco's phosphate buffered saline
SIF	Simulated intestinal fluid
SFG	Simulated gastric fluid
MEM	Minimum essential media
TDD	Topical or transdermal drug delivery
SC	Stratum corneum
MEs	Microemulsions
AAE	Amino acid ester
AspEt	L-Aspartic acid diethyl ester
ProEt	L-Proline ethyl ester
Cho	Cholinium
TMA	Tetramethylammonium
TBP	Tetrabutylphosphonium
EMI	Trimethylimidazolium
IC50	Half maximal inhibitory concentration
LD50	Half maximal lethal dose
Sal	Salicylic acid
MTX	Methotrexate
Ibu	Ibuprofen
Sal-IL	Salicylate ionic liquid
MTX-IL	Methotrexate ionic liquid
TGA	Thermogravimetric analysis
DSC	Differential scanning calorimetric
NMR	Nuclear magnetic resonance spectroscopy
FT-IR	Fourier transform infrared
XRD	X-ray diffractometer

LIST OF SCHEMES

LIST OF TABLES

LIST OF FIGURES

CHAPTER 1

CHAPTER 2

CHAPTER 3

CHAPTER 4

ACKNOWLEDGEMENTS

I would like to express my heartfelt gratitude to Prof. Masahiro Goto for your kind support, guidance, and giving me an opportunity to work independently in your research groups. Your cordial cooperation, insightful ideas and constant enthusiasm toward research, perseverance for learning new things, and indispensable scientific intuition significantly influenced me to learn and become a skillful researcher during my PhD education. Without yours guidance, encouragement and constant feedback this PhD would not have been achievable. I am indebted to you for accepting me as a PhD student at a critical stage of research career. I would also like to sincerely thank to Prof. Noriho Kamiya for your thoughtful guidance, inspiration and continuous support throughout PhD course and for valuable advice and profound suggestion during the lab meetings and on my PhD thesis. I am really honored and fortunate to become a member of the Goto-Kamiya Lab. I would like to express my sincere gratitude to Prof. Hiroyuki Ijima for agreeing to be one of my PhD thesis committee. I really appreciate for his constructive comments and invaluable advice.

I would like to express my sincere thanks to Associate Prof. Muhammad Moniruzzaman at Universiti of Teknologi Petronans, Malaysia for your great cooperation, exchange of ideas and inspiring conversations, encouragement and constant support in my research and for the contributions to the manuscripts. I also would like to express my gratitude to Assistant Prof. Rie Wakabayashi and Yoshiro Tahara for their contributions to the manuscripts and providing me the guidance from the initial stage of my research. I am very grateful to Assistant Profs. Fukiko Kubota and Kosuke Minamihata for their support, conversations and valuable suggestions in many aspects of my research. I would also like to thank Dr. Momoko Kitaoka and staffs for their kind cooperation throughout my study in Kyushu University.

I am very happy to acknowledge all the members of Goto-Kamiya Lab, past and present for their help, support, and friendship. I am especially grateful to Mr. Kozaka Shuto, Mr. Genki Kagawa and Mr. Araki shota for helping and teaching me doing some experiments, and supporting in many occasions during my stay in Japan. I am very grateful to Bangladesh GK lab members (Raihan, Rafiq, Ali and Shihab) for their constant help and moral support. I also would like to thank for all Japanese labmates (Mr. Ryuichiro Hashimoto, Mr. Wataru Yoshida, Mr. Naoki Fujimoto, Mr. Hiroki Obayashi, Ms. Morita Kaho, Ms. Ayaka Kashima, Ms. Imatani Rino, and others) and international labmates (Dr. Muhamad Alif Razi, Dr. D.Tyas, Dr. Maha M. Sharaf, Ms. Nguyen Minh Thi Hong, Mr. Qingliang Kong, Mr. Firmansyah M. Lutfi, Ms. Patmawati Wahyudin, Mr. Dani Permana, Mr. Ramadhan Wahyu, Mr. Faiar T. N. Adroit, and others) for their help, support, friendship, and supportive research environment in the lab.

I would like to express my gratitude to the Government of Japan for providing a scholarship. I greatly appreciate the support from the Support Center of Faculty of Engineering, especially Mrs. Yasura Oiwa. I also thank Mr. Y. Hirano for help with elemental analysis and Dr. M. Watanabe for facility support for NMR, p-XRD, DSC and TGA.

I would like to thank my family - I am deeply grateful for their constant and immeasurable support. Finally but most importantly, all praise be to almighty God Allah and a heartfelt thanks to Allah for every things that happens for me. Without his blessings, this work would never have been possible.